

**Ministry of Higher Education
and Scientific Research
University of Diyala
College of Science**



**Inhibition of carbon steel corrosion in acid
medium using Citrus aurantium leaves extract**

**A Thesis Submitted to The Council of the College of Sciences,
University of Diyala in Partial Fulfillment of the Requirements
for the Degree of Master of Science in Chemistry**

By

NOOR HATEM KHORSHEED

B.Sc.in Chemistry 2014

College of Science - University of Diyala

Supervised by

Prof. Dr. Karim H. Hassan

Prof. Dr. Anees A. Khadom

2016 AD

IRAQ

1438 AH

بِسْمِ اللَّهِ الرَّحْمَنِ الرَّحِيمِ

يَأْتِيهَا الَّذِينَ ءَامَنُوا إِذَا قِيلَ لَكُمْ تَفَسَّحُوا فِي الْمَجَالِسِ فَافْسَحُوا يَفْسَحِ
اللَّهُ لَكُمْ وَإِذَا قِيلَ انشُرُوا فَانشُرُوا يَرْفَعُ اللَّهُ الَّذِينَ ءَامَنُوا
مِنْكُمْ وَالَّذِينَ أُوتُوا الْعِلْمَ دَرَجَاتٍ وَاللَّهُ بِمَا تَعْمَلُونَ خَبِيرٌ ﴿١١﴾

صدق الله العظيم

CERTIFICATION

We certify that this thesis was prepared under our supervision at the University of Diyala /College of Science / Department of Chemistry as a partial requirement for the Degree Master of Science in Chemistry.

Signature:

Name: Professor. Dr

Karim H. Hassan

Date:

Head of the Chemistry Department

In view of the available recommendation, I forward this thesis for debate by the examining committee.

Signature:

Name: Professor. Dr

Anees A. Khadom

Date:

Signature:

Name: Dr. Wassan B. Ali

Title: Lecturer

Date: / /



**In the name of Allah, the Beneficent, the
Merciful**

All praise is due to Allah, the Lord of the Worlds

DEDICATION

**I DEDICATED THIS THESIS
TO MY FATHER,
TO MY MOTHER.**

Noor.H.K

ACKNOWLEDGEMENT

All the praise and thanks be to God, the Most Beneficent, the Most Merciful for allowing me to finish this work.

I would like to thank the head of the Chemistry Sciences Department **Dr. Wassan B. Ali**, and the staff of the Department of Chemistry Sciences for providing electrochemical equipment facilities.

I would like to express my thanks and appreciation to my supervisor **Prof. Dr. Karim H. Hassan** and Co – supervisor **Prof. Dr. Anees A. Khadom**, for their support and guidance in each step of my research.

I would like to thank **Mr. Mustafa S. Mahdi** the coordinator of chemical engineering department / University of Diyala for his help during experimental work.

I am very thankful as well to my family (specially my mother) for their support and encouragement throughout my study.

Abstract

In this work the corrosion rates of low carbon steel in 0.5, 1 and 1.5 M H_2SO_4 at a temperature of 30-60 °C in the presence and absence of *Citrus aurantium leaves* extract as an organic inhibitor in the range of 2-10 ml/L at a time of 3h at static condition has been investigated. Weight loss technique is employed in this investigation. The results showed that the corrosion rate in the presence and absence of (*Citrus aurantium leaves* extract) as inhibitor is increased with temperature for a given inhibitor concentration. The corrosion rate decreased with increasing inhibitor concentration for a given temperature. The maximum value of inhibitor efficiency obtained in 0.5 M was 88.6% at 50 °C in presence of 10 ml/L inhibitor concentration and a time of 3h, in 1 M was 89% at 40 °C in presence of 10 ml/L inhibitor concentration and a time of 3h, and in 1.5 M was 83.3% at 30 °C in presence of 10 ml/L inhibitor concentration and a time of 3h. The fraction of surface covered calculated from corrosion rates followed the Langmuir adsorption isotherm. Arrhenius plot was obtained from which the activation energies were calculated. The values of the free energy of adsorption ($\Delta G_{\text{ads}}^{\circ}$) of -20 kJ/mol, is indicative of the physical adsorption between charge molecules and a charge metal. Kinetic study shows that zero order is best fitting because the values of correlation coefficient is high. The fourier transform infrared spectroscopy (**FTIR**) and scanning electron microscope (**SEM**) were evaluated to examine molecular structure of inhibitor and surface morphdogy respectably. Quantum chemical calculations were also used as a theoretical tool to support the experimental results. Several mathematical models were suggested and the Logarithmic – Linear model was the best one with a higher correlation coefficient and a lowest standard error.

TABLE OF CONTENTS

Subject		Page
Dedication		
Acknowledgement		
Abstract		I
Table of Contents		II
List of Terminology		IV
List of Symbols		V
List of Tables		VI
List of Figures		VIII
Chapter One: Introduction		
1.1	Introduction	1-3
1.2	Importance of Corrosion Studies	3
1.3	Classification of Corrosion	4
1.3.1	Temperature of corrosion	4
1.3.1.1	Low temperature corrosion	4
1.3.1.2	High temperature corrosion	4
1.3.2	Reaction of corrosion	5
1.3.2.1	Electrochemical corrosion	5
1.3.2.2	Chemical corrosion	6
1.3.3	Medium of corrosion	6
1.3.3.1	Dry corrosion	6
1.3.3.2	Wet corrosion	6
1.3.3.2.a	General (Uniform) corrosion	6-7
1.3.3.2.b	Pitting corrosion	7
1.3.3.2.c	Crevice corrosion	7-8
1.3.3.2.d	Intergranular corrosion	8
1.3.3.2.e	Selective corrosion (Selective Leaching)	8
1.3.3.2.f	Erosion corrosion	8
1.3.3.2.g	Cavitation corrosion	9
1.3.3.2.h	Stress corrosion cracking	9
1.4	Thermodynamics of the corrosion	9-10
1.5	Corrosion control	10
1.6	Studies of green inhibitors	10-11
1.7	General characteristics of green Inhibitors	11
1.8	Types of corrosion inhibitors	12

1.8.1	Inorganic inhibitors	12
1.8.2	Organic inhibitors	12-13
1.9	Mechanism of Inhibitor	13
1.10	Theoretical and Quantum Chemical Background	14-15
1.11	Parameters Effect on Wet Corrosion	16
1.11.1	Effect of temperature	16-17
1.11.2	Effect of acid concentration	17-18
1.11.3	Effect of reaction time	18-19
1.11.4	Effect of inhibitor concentration	19
1.12	Mechanism of adsorption	19-20
1.12.1	Adsorption of inhibitor and isotherm	20
1.12.1.a	Langmuir adsorption isotherm	20-21
1.12.1.b	Freundlich adsorption isother	21
1.12.1.c	Kinetic-thermodynamic adsorption isotherm	22
1.13	Previous Studies	23-29
1.14	Objectives (aims of study)	29
Chapter Two : Materials and Methods		
2.1	Used Materials	30
2.1.1	Chemical	30
2.1.2	Used Electrode	30
2.2	Used Instrument	31
2.3	Corrosion Specimen Preparation	32-33
2.4	Preparation of Corrosion Solution	34
2.5	Preparation of Citrus aurantium Leaves Extract	34
2.6	Weight Loss Measurement	35
2.7	Kinetic Measurement	35
Chapter Three : Results & Discussion		
3.1	Weight Loss Measurements	37
3.2	Corrosion Rate Evaluation	41
3.2.1	Uninhibited acid	41
3.2.2	Inhibitor Concentration Interpretation	42
3.3	Inhibitor Performance and Adsorption Interpretation	49-56
3.4	Thermodynamic Interpretation	59-63
3.5	Kinetics Interpretation	66-67
3.6	Inhibitor Compositions and FTIR Interpretation	72-73
3.7	Scanning Electron Microscope (SEM) Interpretation	75
3.8	Quantum Chemical Interpretation	78-79

3.9	Mathematical Modeling and Theoretical Studies	81-83
3.10	Conclusions	86-87
3.11	Recommendation for Further Work	88
References		89-95

TERMINOLOGY

Symbol	Definition
CAL	Citrus aurantium leaves extract
AAS	Atomic Absorption Spectrometry
CC	Crevice Corrosion
CRTs	Cathode ray tubes
FTIR	Fourier transform infrared spectroscopy
SCC	Stress corrosion cracking
SEM	Scanning electron microscope
EDX	Energy dispersive X-ray
XRD	X-ray diffraction
EIS	Electrochemical impedance spectroscopy
DRFTIR	Diffuse reflectance Fourier transform infrared spectroscopy
GCMS	Gas chromatography mass spectroscopy

LIST OF SYMBOLS

Symbol	Definition	Units
A	Frequency factor	-
CR	Corrosion rate	gm /m ² d
CR _{inhib}	Corrosion rate of inhibited	gm /m ² d
CR _{uninhib}	Corrosion rate of uninhibited acid	gm /m ² d
d	Density	g/m ³
E _a	Activation energy	kJ/mole
ΔG ^o _{ads}	Standard adsorption free energy	kJ mol ⁻¹
ΔH [*]	Enthalpy change	kJ/mole
ΔS [*]	Entropy change	kJ/mol K
h	Plank constant	J.s
IE	Inhibition efficiency	-
N	Avogadro number	mole

MW	Molecular weight	g/mole
R	Gas constant	J/mole.K
T	Absolute temperature	K
β	Constant	-
α	Constant	-
ε	Standard error	-
n	number of variables	-
ΔN	Electron transferred	-
ΔE	Energy gap	ev
IP	Ionization potential	ev
EA	Electron affinity	ev
μ	Dipole moment	ev
η	Global hardness	ev
σ	Global softness	ev
ω	Global electrophilicity index	ev
X	Electronegativity	ev
χ_{Fe}	Denote the absolute electronegativity of iron	ev
χ_{inh}	Denote the absolute electronegativity of inhibitor	ev
k_0	Rate constant in zero order	g/m^2h
k_1	Rate constant in first order	1/h
k_2	Rate constant in second order	$m^2/g h$
$t_{1/2}$	Half –life	h
K^{\wedge}	Kinetic-thermodynamic adsorption constant	(L/ml)
y^{\wedge}	Slope	-
C_i	Inhibitor concentration	ml/L
θ	Surface coverage	-
K_F	Freundlich adsorption constant	(L/ml)
n^{\wedge}	Slope	-
K_L	Equilibrium adsorption constant	(L/ml)
W_t	Carbon steel consumption	g
W_i	Initial carbon steel consumption	g
n^{\wedge}	Order of reaction	-
R^2	Correlation coefficient	-

LIST OF TABLES

Table Number	Title	Page
2.1	Used chemical materials.	30
2.2	Carbon steel compositions.	30
2.3	Used Instrument.	31
3.1	Effect of temperature on the corrosion rate of carbon steel in 0.5 M H ₂ SO ₄ in absence and presence of Citrus aurantium leaves extract as corrosion inhibitor.	38
3.2	Effect of temperature on the corrosion rate of carbon steel in 1 M H ₂ SO ₄ in absence and presence of Citrus aurantium leaves extract as corrosion inhibitor.	39
3.3	Effect of temperature on the corrosion rate of carbon steel in 1.5 M H ₂ SO ₄ in absence and presence of Citrus aurantium leaves extract as corrosion inhibitor.	40
3.4	Equilibrium constant , standard adsorption free energy (ΔG_{ads}^0) and correlation coefficient (R^2) for Langmuir type adsorption isotherm of the inhibitor on carbon steel in 0.5 M H ₂ SO ₄ at different temperature.	52
3.5	Equilibrium constant , standard adsorption free energy (ΔG_{ads}^0) and correlation coefficient (R^2) for Langmuir type adsorption isotherm of the inhibitor on carbon steel in 1 M H ₂ SO ₄ at different temperature.	52
3.6	Equilibrium constant , standard adsorption free energy (ΔG_{ads}^0) and correlation coefficient (R^2) for Langmuir type adsorption isotherm of the inhibitor on carbon steel in 1.5 M H ₂ SO ₄ at different temperature.	52
3.7	Equilibrium constant , slope (n'') and correlation coefficient (R^2) for Freundlich type adsorption isotherm of the inhibitor on carbon steel in 0.5 M H ₂ SO ₄ at different temperature.	55
3.8	Equilibrium constant , slope (n'') and correlation coefficient (R^2) for Freundlich type adsorption isotherm of the inhibitor on carbon steel in 1 M H ₂ SO ₄ at different temperature.	55
3.9	Equilibrium constant , slope (n'') and correlation coefficient (R^2) for Freundlich type adsorption isotherm of the inhibitor on carbon steel in 1.5 M H ₂ SO ₄ at different temperature.	55
3.10	Equilibrium constant , slope (y') and correlation coefficient (R^2) for Kinetic-thermodynamic adsorption of the inhibitor on carbon steel in 0.5 M H ₂ SO ₄ at different temperature.	58
3.11	Equilibrium constant , slope (y') and correlation coefficient (R^2) for Kinetic-thermodynamic adsorption of the inhibitor on carbon steel in 1 M H ₂ SO ₄ at different temperature.	58
3.12	Equilibrium constant , slope (y') and correlation coefficient (R^2)	58

	for Kinetic-thermodynamic adsorption of the inhibitor on carbon steel in 1.5 M H ₂ SO ₄ at different temperature.	
3.13	Values of activation energies for the corrosion of carbon steel in 0.5 M H ₂ SO ₄ in presence and absence Citrus aurantium leaves extract as the corrosion inhibitor.	61
3.14	Values of activation energies for the corrosion of carbon steel in 1 M H ₂ SO ₄ in presence and absence Citrus aurantium leaves extract as the corrosion inhibitor.	62
3.15	Values of activation energies for the corrosion of carbon steel in 1.5 M H ₂ SO ₄ in presence and absence Citrus aurantium leaves extract as the corrosion inhibitor.	62
3.16	Enthalpy and Entropy of activation values of the corrosion reaction with various concentration of Citrus aurantium leaves extract in 0.5 M H ₂ SO ₄ .	65
3.17	Enthalpy and Entropy of activation values of the corrosion reaction with various concentration of Citrus aurantium leaves extract in 1 M H ₂ SO ₄ .	65
3.18	Enthalpy and Entropy of activation values of the corrosion reaction with various concentration of Citrus aurantium leaves extract in 1.5 M H ₂ SO ₄ .	66
3.19	Rate constant values, half-life and correlation coefficient (R ²) at different temperatures in presence and absence of inhibitor in 0.5 M H ₂ SO ₄ .	69
3.20	Rate constant values, half-life and correlation coefficient (R ²) at different temperatures in presence and absence of inhibitor in 1 M H ₂ SO ₄ .	69
3.21	Rate constant values, half-life and correlation coefficient (R ²) at different temperatures in presence and absence of inhibitor in 1.5 M H ₂ SO ₄ .	69
3.22	Rate constant values, half-life and correlation coefficient (R ²) at different temperatures in presence and absence of inhibitor in 0.5 M H ₂ SO ₄ .	71
3.23	Rate constant values, half-life and correlation coefficient (R ²) at different temperatures in presence and absence of inhibitor in 1 M H ₂ SO ₄ .	71
3.24	Rate constant values, half-life and correlation coefficient (R ²) at different temperatures in presence and absence of inhibitor in 1.5 M H ₂ SO ₄ .	72
3.25	Groups active values stretching frequency in alcohol.	73
3.26	Quantum chemical parameters for most important components of CAL.	79
3.27	Linear models analysis.	83
3.28	Polynomial models analysis.	84

LIST OF FIGURES

Figure Number	Title	Page
2.1. a, b, c, d, e, f, g and i	Carbon steel preparation steps.	33
2.2. a, b, c, d and e	Citrus aurantium leaves extract preparation steps.	34
2.3	Algorithm of experimental work.	36
3.1	Effect of temperature on the corrosion rate of carbon steel exposed to H ₂ SO ₄ acid.	41
3.2	Effect of inhibitor concentration on the corrosion rate of carbon steel exposed to 0.5 M H ₂ SO ₄ .	43
3.3	Effect of inhibitor concentration on the corrosion rate of carbon steel exposed to 1 M H ₂ SO ₄ .	43
3.4	Effect of inhibitor concentration on the corrosion rate of carbon steel exposed to 1.5 M H ₂ SO ₄ .	44
3.5	Effect of temperature on the corrosion rate of carbon steel in 0.5 M H ₂ SO ₄ at different inhibitor concentration.	44
3.6	Effect of temperature on the corrosion rate of carbon steel in 1 M H ₂ SO ₄ at different inhibitor concentration.	45
3.7	Effect of temperature on the corrosion rate of carbon steel in 1.5 M H ₂ SO ₄ at different inhibitor concentration.	45
3.8	Effect of concentration of Citrus aurantium leaves extract on inhibitive efficiency of carbon steel corrosion in 0.5 M H ₂ SO ₄ .	46
3.9	Effect of concentration of Citrus aurantium leaves extract on inhibitive efficiency of carbon steel corrosion in 1 M H ₂ SO ₄ .	46
3.10	Effect of concentration of Citrus aurantium leaves extract on inhibitive efficiency of carbon steel corrosion in 1.5 M H ₂ SO ₄ .	47
3.11	Effect of temperature on inhibitive efficiency of Citrus aurantium leaves extract for carbon steel corrosion in 0.5 M H ₂ SO ₄ .	47
3.12	Effect of temperature on inhibitive efficiency of Citrus aurantium leaves extract for carbon steel corrosion in 1 M H ₂ SO ₄ .	48
3.13	Effect of temperature on inhibitive efficiency of Citrus aurantium leaves extract for carbon steel corrosion in 1.5 M H ₂ SO ₄ .	48
3.14	Langmuir adsorption isotherm of Citrus aurantium leaves extract on carbon steel in 0.5 M H ₂ SO ₄ .	50
3.15	Langmuir adsorption isotherm of Citrus aurantium leaves extract on carbon steel in 1 M H ₂ SO ₄ .	51
3.16	Langmuir adsorption isotherm of Citrus aurantium leaves	51

	extract on carbon steel in 1.5 M H ₂ SO ₄ .	
3.17	Freundlich adsorption isotherm of Citrus aurantium leaves extract on carbon steel in 0.5 M H ₂ SO ₄ .	53
3.18	Freundlich adsorption isotherm of Citrus aurantium leaves extract on carbon steel in 1 M H ₂ SO ₄ .	54
3.19	Freundlich adsorption isotherm of Citrus aurantium leaves extract on carbon steel in 1.5 M H ₂ SO ₄ .	54
3.20	Kinetic-thermodynamic adsorption isotherm of Citrus aurantium leaves extract on carbon steel in 0.5 M H ₂ SO ₄ .	56
3.21	Kinetic-thermodynamic adsorption isotherm of Citrus aurantium leaves extract on carbon steel in 1 M H ₂ SO ₄ .	57
3.22	Kinetic-thermodynamic adsorption isotherm of Citrus aurantium leaves extract on carbon steel in 1.5 M H ₂ SO ₄ .	57
3.23	Arrhenius plot of carbon steel corrosion in 0.5 M H ₂ SO ₄ containing various concentration of Citrus aurantium leaves extract at a temperature range of (30-60 °C).	60
3.24	Arrhenius plot of carbon steel corrosion in 1 M H ₂ SO ₄ containing various concentration of Citrus aurantium leaves extract at a temperature range of (30-60 °C).	60
3.25	Arrhenius plot of carbon steel corrosion in 1.5 M H ₂ SO ₄ containing various concentration of Citrus aurantium leaves extract at a temperature range of (30-60 °C).	61
3.26	Transition state plot for carbon steel corrosion in 0.5 M H ₂ SO ₄ in absence and presence of different concentrations of Citrus aurantium leaves extract	63
3.27	Transition state plot for carbon steel corrosion in 1 M H ₂ SO ₄ in absence and presence of different concentrations of Citrus aurantium leaves extract	64
3.28	Transition state plot for carbon steel corrosion in 1.5 M H ₂ SO ₄ in absence and presence of different concentrations of Citrus aurantium leaves extract.	64
2.29	Weight loss against time for carbon steel corrosion in 0.5 M H ₂ SO ₄ in presence and absence of Citrus aurantium leaves extract at (40-60 °C).	67
3.30	Weight loss against time for carbon steel corrosion in 1 M H ₂ SO ₄ in presence and absence of Citrus aurantium leaves extract at (40-60 °C).	68
3.31	Weight loss against time for carbon steel corrosion in 1.5 M H ₂ SO ₄ in presence and absence of Citrus aurantium leaves extract at (40-60 °C).	68
3.32	Plot of ln(W ₁ /W ₂) against time for carbon steel corrosion in 0.5 M H ₂ SO ₄ in presence and absence of Citrus aurantium leaves extract at (40-60 °C).	70
3.33	Plot of ln(W ₁ /W ₂) against time for carbon steel corrosion in	70

	1 M H₂SO₄ in presence and absence of Citrus aurantium leaves extract at (40-60 °C).	
3.34	Plot of ln(W₁/W₂) against time for carbon steel corrosion in 1.5 M H₂SO₄ in presence and absence of Citrus aurantium leaves extract at (40-60 °C).	71
3.35. a	FTIR spectrum of Citrus aurantium leaves extracted with 0.5 M H₂SO₄.	73
3.35. b	FTIR spectrum of protective film formed on the surface of the metal after immersion in 0.5 M H₂SO₄.	74
3.36	FTIR spectrum of Citrus aurantium leaves extracted with 1 M H₂SO₄.	74
3.37	FTIR spectrum of Citrus aurantium leaves extracted with 1.5 M H₂SO₄.	75
3.38	SEM images of carbon steel surface (a) before immersion in 1 M H₂SO₄ at 30 °C for 3h (b) after immersion in 1 M H₂SO₄ at 30 °C for 3h (c) after immersion in 1 M H₂SO₄ at 30 °C for 3h and in presence of CAL.	76
3.39	SEM images of carbon steel surface (a) before immersion in 1 M H₂SO₄ at 60 °C for 3h (b) after immersion in 1 M H₂SO₄ at 60 °C for 3h (c) after immersion in 1 M H₂SO₄ at 60 °C for 3h and in presence of CAL.	77
3.40. a, b, and c	A: Optimized geometry of linalool, B: HOMO distribution, C: LUMO distribution.	80
3.41	3D diagram of experimental corrosion rate against temperature and inhibitor concentration.	84
3.42	3D diagram of experimental corrosion rate against acid concentration and inhibitor concentration.	85
3.43	Experimental corrosion rate against predicated corrosion rate for linear models.	85
3.44	Experimental corrosion rate against predicated corrosion rate for polynomials models.	86

1.1 Introduction

Corrosion specifically refers to any process involving the deterioration or degradation of metal components, it is the primary means by which metals deteriorate. Most metals corrode on contact with water (and moisture in the air), acids, bases, salts, oils, aggressive metal polishes and other solid and liquid chemicals. Metals will also corrode when exposed to gaseous materials like acid vapours, formaldehyde gas, ammonia gas and sulfur containing gases [1]. In other words corrosion is the destructive attack on a metal by chemical or electrochemical reaction with its environment, or it is the extractive metallurgy in reverse.

All metals have a characteristic, inherent tendency to corrode and react in aqueous environments to produce metal ions and release electrons. This inherent reactivity can be shown in terms of either free-energy, ΔG . The inherent reactivity of a metal can be expressed by the magnitude of the free energy change on the metal suffering a corrosion process. The corrosion process of the metal dissolving as ions generates some electrons that are consumed by a secondary reaction; the two processes must balance their charges. The sites hosting these two processes may be located close to each other on the metals surface, or far apart depending on local circumstances. When a metal (Fe) is placed in pure water, some ions will immediately pass into solution:



Build-up of negative charge on the metal and the existence of metal ions in solution makes it possible for a back-reaction to proceed:



and ultimately the equilibrium is established:



Now, a steady potential difference exists between the metal and the solution. The magnitude of this potential difference depends on the metal type and composition of the solution [1]. The three main reasons for the importance of corrosion prevention are economics, safety and environmental damage. To reduce the economic impact of corrosion, corrosion engineers, with the support of corrosion scientists, aim to reduce material losses, as well as the accompanying economic losses, that result from the corrosion of piping, tanks, metal components of machines, ships, bridges, marine structures, and so on.

Loss of metal by corrosion is a waste not only of the metal, but also of the energy, and the human effort that was used to produce and fabricate the metal structures in the first place.

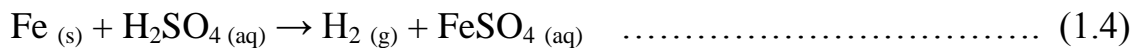
The economic factor is a very important motivation for much of the current research in corrosion. Losses sustained by industry and by governments amount to many billions of dollars annually.

However, corrosion has a tremendous effect on the environment in the sense corrosion-related failure of oil pipelines or gas pipelines or oil tankers can have very detrimental effect on the environment in the form of water and air pollution, leading to the demise of aquatic life . Industries depend heavily on the use of metals and alloys. One of the most challenging and difficult tasks for industries are the protection of metals from corrosion. Corrosion is a ubiquitous problem that continues to be of great relevance in a wide range of industrial applications and product [2].

Carbon steel alloys are widely used in most industries for the fabrication of various reaction vessels, such as heat exchangers, cooling towers, and

pipes, for its low cost and availability. However, carbon steel is highly susceptible to corrosion and the corrosion of carbon steel has been a matter of great concern to various industries [1].

Particularly sulfuric acid is frequently used in industrial processes such as acid cleaning, acid pickling, acid descaling, and oil well acidizing [3]. The acid constitutes strong corrosive environments for carbon steel and as a result, the study of the prevention of steel corrosion is always a subject of high theoretical and practical interest [1]. Dilute sulfuric acid reacts with metals via a single displacement reaction as with other typical acids, producing hydrogen gas and salts (the metal sulfate). It attacks reactive metals (metals at positions above copper in the reactivity series) such as iron, aluminum, zinc, manganese, magnesium and nickel.



1.2 Importance of Corrosion Studies

The importance of corrosion studies is two folds. The first is economic, including the reduction of material losses resulting from wasting away or sudden failure of piping, tanks, metal components of machines, ships, hulls, marine, structures...etc. The second is conservation, applied primarily to metal resources, the world's supply of which is limited, and the wastage of which includes corresponding losses of energy and water resources accompanying the production and fabrication of metal structures. Losses sustained by industry, by the military, by municipalities amount to many billions of dollars annually [4].

1.3 Classification of Corrosion

Corrosion can be classified in many ways as:

1.3.1. Temperature of corrosion

1.3.1.1 Low temperature corrosion

In the low - temperature region, the oxidation rate of iron is sensitive to crystal face, decreasing in the order $(100) > (111) > (110)$. The oxide nuclei, apparently consisting of Fe_3O_4 , grow to form a uniform film of oxide. Oxidation of iron in the parabolic range is complicated by the formation of as many as three distinct layers of iron oxide, and the proportions of these layers change as the temperature or oxygen partial pressure changes. Data reported by various investigators are not in good agreement, probably because of variations in the purity of iron used for oxidation tests — particularly its carbon content [5].

1.3.1.2 High temperature corrosion

High-temperature corrosion is considered to be electrochemical in nature, with the high-temperature scale formed acting as an electrolyte. Corrosion is usually uniform in nature. The predominant effects are oxidation and carburization /decarburization. Changes in mechanical properties, specifically a loss of ductility due to phase changes, also take place. Most high-temperature reactions involve oxidation because oxides are common products in the many applications where air or oxygen-rich environments are present. In clean atmospheres, a thick oxide film forms that develops into a thicker scale. Oxidation phenomena are controlled by thermodynamic and kinetic factors, notably gas composition and temperature [5].

1.3.2. Reaction of corrosion:

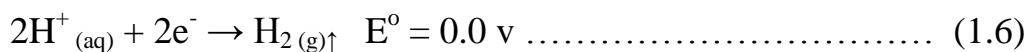
1.3.2.1 Electrochemical corrosion

Corrosion can be separated into two or more partial reactions. These partial reactions are divided into two classes: oxidation and reduction [6]. These two separated reactions are taking place at different areas on the metal surface. One of the reactions (oxidation and reduction) being the anodic reaction consists of an oxidation type chemical change in which the metal changes from the metallic state to an ionic state, i.e. the valance of metal is increased by giving off electrons.



At different sites from the anodic one will occur the cathodic reaction. There are different cathodic reactions which are frequently encountered in metallic corrosion. The most widespread cathodic reactions are:

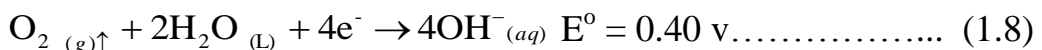
1. Hydrogen formation:



2. Oxygen reduction (acid solution):



3. Oxygen reduction (neutral or basic solutions):



4. Metal ion reduction:



5. Metal deposition:



1.3.2.2 Chemical corrosion

Direct chemical attack, or pure chemical corrosion, is an attack resulting from a direct exposure of a bare metal surface to caustic liquid or gaseous agents. Unlike electrochemical attack where the anodic and cathodic changes may be taking place a measurable distance apart, the changes in direct chemical attack are occurring simultaneously at the same point. The most common agents causing direct chemical attack on aircraft are: (1) spilled battery acid or fumes from batteries; (2) residual flux deposits resulting from inadequately cleaned, welded, brazed, or soldered joints; and (3) entrapped caustic cleaning solutions.

1.3.3 Medium of corrosion:**1.3.3.1 Dry corrosion:**

It's occurs with gases as the corrosive agent and in the absence of aqueous phases on the metal surface such as Cl_2 ; HF ; fumes H_2SO_4 .

1.3.3.2 Wet corrosion:

It's occurs when aqueous phases are present on the surface of the metal [7]. The wet corrosion proceeds faster than dry corrosion since the dipolar water molecule stabilizes the free metal ions in solution, in addition, the metallic structure and water in contact with it are both electric current conducting. Various forms of wet corrosion have therefore been identified and classified such as uniform, pitting, crevice, erosion, intergranular, selective leaching and stress corrosion cracking, as shown below [8]:

a. General (uniform) corrosion

It's an even rate of metal loss over the exposed surface, which is characterized by corrosive attack proceeding evenly over the entire surface area, or a large fraction of the total area.

Uniform corrosion is the simplest form of corrosion, it is one of the most easily measured and predictable forms of corrosion, making disastrous failures relatively rare therefore it is not always the most important in terms of cost or safety. But if surface corrosion is permitted to continue, the surface may become rough and surface corrosion can lead to more serious types of corrosion [8, 7].

b. Pitting corrosion

Pitting corrosion is characterized by a highly localized loss of metal. It appears as a deep, tiny hole on the metal. The width of the pit may increase with time but not to the extent to which the depth increases. Most often, the pit opening remains covered with the corrosion product, making it difficult to detect during inspection [8, 7].

Pitting may occur in most metal with protective film. Therefore initiation of a pit is associated with the breakdown of the protective film on the metal surface. Many metals and their alloys are subject to pitting in different environments such as alloys of carbon steels, stainless steels, titanium, nickel, copper, and aluminum [7].

c. Crevice corrosion (CC)

This is localized corrosion concentrated in crevices in which the gap is sufficiently wide for liquid to penetrate into the crevice and sufficiently narrow for the liquid in the crevice to be stagnant.

Various metals, e.g. Al, Fe, Cr and Ni, may suffer from crevice corrosion. CC which is affected by several factors; of a metallurgical, environmental, electrochemical, surface physical and last but not least, a geometrical nature. CC occurs beneath flange gaskets nail and screw heads and paint coating edges in overlap joints between tubes and tube plates in heat exchangers etc. The same form of corrosion develops beneath deposits of,

e.g. corrosion products, dirt, sand, leaves and marine organisms, hence it is called deposit corrosion in such cases. It comprises mechanisms, modelling, test methods and results, practical experience, protective measures and monitoring. A review of the mechanisms of CC has recently been published [7].

d. Intergranular corrosion

Intergranular corrosion is a localized attack on or at grain boundaries with insignificant corrosion on other parts of the surface. The attacks propagate into the material. This is a dangerous form of corrosion because the cohesive forces between the grains may be too small to withstand tensile stresses; the toughness of the material is seriously reduced at a relatively early stage, and fracture can occur without warning [8].

e. Selective corrosion (Selective leaching)

This form of corrosion is observed in alloys in which one element is clearly less noble than the other (s). The corrosion mechanism implies that the less noble element is removed from the material. The most common example of selective corrosion is dezincification of brass, in which is the term used to describe the leaching of zinc from brass [8].

f. Erosion corrosion

The term "erosion" applies to deterioration due to mechanical force. Erosion corrosion is usually caused by a gaseous or corrosive liquid flowing over the metal. It is affected by velocity, turbulence, impingement, the presence of suspended solids and temperature.

Turbulence phenomena can destroy protective films and cause very high corrosion rates in materials, therefore all equipment exposed to flowing fluid is subject to erosion corrosion [8].

g. Cavitation corrosion

This corrosion form is closely related to erosion corrosion, but the appearance of the attack differs from the erosion corrosion attacks described in the last section. While the latter has a pattern reflecting the flow direction, cavitation attacks are deep pits grown perpendicularly to the surface. Both high corrosion resistance and high hardness improve the resistance to cavitation attacks. Relative resistance of various steels, stainless steels, irons, copper alloys and nickel alloys are reported in references [7].

h. Stress corrosion cracking

Stress corrosion cracking (SCC) is a process involving the initiation of cracks and their propagation, possibly up to complete failure of a component, due to the combined action of tensile mechanical loading and a corrosive medium. This stress can either be applied (external load), or can be residual stress in the metal (e.g., due to production process or heat treatment) [7].

1.4 Thermodynamics of The Corrosion

Thermodynamics could suggest which reactions are possible and whether a particular reaction is likely will occur. This helps in the understanding of corrosion phenomena and is essential to the study of corrosion cells. Chemical thermodynamics studies investigate the role of entropy in chemical reactions [1]. Thermodynamics defines equilibrium as a function of the elements and compounds present and the environmental conditions, such as pressure, temperature, and chemical composition. Thermodynamics is used to determine whether corrosion can occur and to predict which stable corrosion products will be formed. A law of nature postulates that the most stable state for a set of reactants is that state which has the lowest free energy. Consequently, metal surfaces in contact with a

solution tend toward the lowest free-energy state possible. When the system reaches at this state, there is no further change. Ultimately this final, unique, lowest-energy state is the equilibrium state. At equilibrium, the system is stable, no driving forces are available for any change from that state.

1.5 Corrosion Control

Corrosion control is a process focuses mainly on (i) materials and (ii) environments. Corrosion management focuses on “people” and aims at improving the performance of engineering systems. So, effective corrosion control requires a complete management strategy involving people as much as equipment. And it's aimed to reduce the corrosion rate to a tolerable level (or predictable limits).

Sheir, et al [9], presented an outline scheme of ‘Methods of Preventing Corrosion’ in which five categories were defined, Design, Materials selection, Coating, Modification of the environment (adding inhibitors), Electrochemical methods,

- Cathodic protection

- Anodic protection

1.6 Studies of Green Inhibitors

An inhibitor is a substance added in a very low concentration to protecting the surface of a metal that is exposed to a corrosive environment that terminates or diminishes the corrosion of a metal [1]. The use of inhibitors has been well documented as an effective method of protecting metallic materials from corrosion. Many industrial processes have been put to use. Most inhibitors have been developed by empirical experimentation, to be used effectively, the inhibitor must be:-

1. Compatible with expected environment.
2. Economical for operation.
3. Amenable to protecting .
4. Contribute the greatest desired effect.

Many factors including cost, amount, easy availability and most important safety to environment need to be considered when choosing an inhibitor.

1.7 General Characteristics of Green Inhibitors

Green inhibitors possess adsorption properties that are similar to the 'non-green' inhibitors. Most of the green inhibitors adsorb on the metal surface by means of both physical and chemical adsorption at room temperature. In general, at elevated temperatures, inhibition occurs mainly through chemisorption. On prolonged exposure of the green inhibitor towards the corrosive environment, inhibitor gains or losses its effectiveness during the process of corrosion inhibition. The evaluation of the effect of increased time on the inhibition efficiency provide information about the stability of inhibitive behavior of the green inhibitor on time scale. In general, the effectiveness of the inhibitor decreases upon increasing the time, Which means that the adsorption of the inhibitor molecules on the metal surface occurs predominantly via physical interactions [10,11].

1.8 Types of Corrosion Inhibitors

Inhibitors are classified in to two types:

1.8.1 Inorganic inhibitors

It's used for corrosion protection but as a result of cost and toxicity, attention is currently shifted towards the use of more eco-friendly inhibitors. Inorganic inhibitors like chromate, phosphates, molybdates etc.

1.8.2 Organic inhibitors

It's used for corrosion protection containing functional groups with oxygen, nitrogen and /or sulfur atoms in a conjugate system have been reported to exhibit good inhibiting properties. This has made plant extracts an important choice for environmentally friendly, readily available and renewable source for a wide range of inhibitors referred to as green inhibitors. Some of the advantages of green inhibitors are low cost of processing, biodegradability, and absence of heavy metals or other toxic compounds which pose great hazard to the environment [12]. Some investigations in recent time have been made into the focused on corrosion inhibiting properties of natural products of plant origin, which showed good inhibition efficiencies. Each inhibitor must be tailored to the specific corrosion problem that needs solution [6]. While the use of inhibitors for some types of corrosion can be similar to other, this similarity must be treated as coincidence. Organic inhibitors generally contain heteroatoms such as O, N, and S which are found to have higher basicity and electron density suitable to act as corrosion inhibitor. O, N, and S are the active centers for the process of adsorption on the metal surface. The inhibition efficiency follows the sequence $O < N < S < P$ [1].

Using organic inhibitors containing oxygen, sulfur, and especially nitrogen to reduce corrosion attack on steel has been studied in some detail

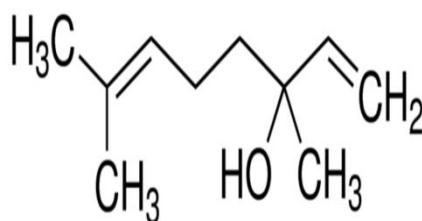
[1]. The use of inhibitor (*Citrus aurantium leaves extract*) (*CALE*), (*Rutaceae family*), also known as *sour orange* or *bitter orange*, is generally used as a rootstock and has a number of advantages, including resistance to several viral diseases, tolerance to cold, improvement in the fruit quality of the grafted plants, and it can be used as an ornamental tree [13].

1.9 Mechanism of Inhibitor

The inhibitors influence the kinetics of the electrochemical reactions which constitute the corrosion process, corrosion inhibitors adsorb on the metal surface and thereby change the structure of electrical double layer. Most of the efficient inhibitors used in industry are organic compounds that contain oxygen, sulfur, nitrogen atoms, which lead to the adsorption of the compounds on the metal surface [14]. Green or safe corrosion inhibitors are biodegradable and do not contain heavy metals or other toxic compounds. Corrosion inhibitors generally control corrosion by forming various types of films. Inhibitors form films in several ways: by adsorption, the formation of bulky precipitates, and /or the formation of a passive layer on the metal surface. Most of organic inhibitors retard corrosion by adsorption to form a thin, invisible film only a few molecules thick [15]. The existing data reveals that most organic inhibitors are adsorbed on the metal surface by displacing water molecules on the surface and forming a compact protecting barrier. Availability of no bonded (lone pair) and π -electrons in inhibitor molecules facilitate electron transfer from the inhibitor to the metal. A coordinate covalent bond involving transfer of electrons from inhibitor to the metal surface may be established.

1.10 Theoretical and Quantum Chemical Backgrounds

Quantum chemical calculations were used as a theoretical tool to support the experimental results and to explain the interaction between the inhibitor molecules and the steel surface, as well as the properties of this inhibitor concerning their reactivity. Linalool is the most important component which consists of than 58 % of *CAL* components [16, 17]. The chemical structure of these component were shown below



Linalool

According to PM3 theorem [18], the HOMO energy is related to the ionization potential (IP) whereas the LUMO energy is linked to the electron affinity (EA), as follows:

$$IP = -E_{\text{HOMO}} \quad E^\circ = -9.37 \quad \dots\dots\dots (1.11)$$

$$EA = -E_{\text{LUMO}} \quad E^\circ = -0.38 \quad \dots\dots\dots (1.12)$$

So, the electronegativity (χ), the chemical potential (μ) and the global hardness (η) were evaluated, based on the finite difference approximation, as linear combinations of the calculated IP and EA :

$$\chi = -\mu = \frac{IP + EA}{2} \quad \dots\dots\dots (1.13)$$

$$\eta = \frac{IP - EA}{2} \quad \dots\dots\dots (1.14)$$

The softness (σ) is the inverse of the global hardness.

$$\sigma = \frac{1}{\eta} \dots\dots\dots (1.15)$$

The chemical hardness fundamentally signifies the resistance towards the deformation or polarization of the electron cloud of the atoms, ions or molecules under small perturbation of chemical reaction. A hard molecule has a large energy gap and a soft molecule has a small energy gap. The global electrophilicity (ω) index was introduced as a measure of energy lowering due to maximal electron flow between donor and acceptor and is given by

$$\omega = \frac{\mu^2}{2} \sigma \dots\dots\dots (1.16)$$

The fraction of transferred electrons (ΔN), evaluating the electronic flow in a reaction of two systems with different electro negativities, in particular case; a metallic surface and an inhibitor molecule was calculated according to Pearson theory [19] as:

$$\Delta N = \frac{\chi_{\text{Fe}} - \chi_{\text{inh}}}{2 (\eta_{\text{Fe}} + \eta_{\text{inh}})} \dots\dots\dots (1.17)$$

Where; χ_{Fe} and χ_{inh} denote the absolute electronegativity of iron and inhibitor molecule respectively, η_{Fe} and η_{inh} denote the absolute hardness of iron and the inhibitor molecule respectively. In this study, we use the theoretical value of $\chi_{\text{Fe}} = 7.0\text{eV}$ and $\eta_{\text{Fe}} = 0.0\text{eV}$ for the computation of number of transferred electrons. The difference in electronegativity drives the electron transfer, and the sum of the hardness parameters acts as a resistance.

1.11 Parameters Effect on Wet Corrosion

1.11.1 Effect of temperature

Temperature increases the rate of almost all chemical reactions, lead to increase in corrosion rate but inhibitor efficiency decreases with increase it. Like most chemical reactions, the rate of corrosion of iron and steel in aqueous acid solutions increases with increasing temperature [6]. This effect can be expressed by Arrhenius equation in which the rate of corrosion reaction in correlated with temperature [20].

$$\text{Corrosion rate (CR)} = A \exp \left[-\frac{E_a}{RT} \right] \dots\dots\dots (1.18)$$

Where; A is Frequency factor, E_a is Activation energy (kJ/mole), R is Gas constant (8.314 J/mole.K), T is Absolute temperature (K). From Arrhenius equation activation energy and frequency factor can be calculated by taking the natural (ln) of the previous equation lead to:

$$\ln(\text{CR}) = \ln A \left[-\frac{E_a}{RT} \right] \dots\dots\dots (1.19)$$

So ln (CR) can be plotted against (1/T) with a slope of ($-E_a / R$) and intercept of ln A. Temperature changes have the greatest effect when the rate determining step is the activation process. It is therefore not surprising that the activation energy of inhibited reactions at high coverages can be either larger or smaller than that of uninhibited reactions. Information contained in the literature shows that the relationship $\ln(\text{CR}) = f(1/T)$ is quite frequently, although not always linear in the presence of inhibitor. While equation of transition state can be used to calculate enthalpy and entropy of activation as [21].

$$\text{CR} = \frac{RT}{Nh} \exp \left(\frac{\Delta S_{\text{act}}}{R} \right) \exp \left(-\frac{\Delta H_{\text{act}}}{RT} \right) \dots\dots\dots (1.20)$$

$$\frac{CR}{T} = \frac{R}{Nh} \exp\left(\frac{\Delta S_{act}}{R}\right) \exp\left(-\frac{\Delta H_{act}}{RT}\right) \dots\dots\dots (1.21)$$

$$\ln\left[\frac{CR}{T}\right] = \ln\left[\frac{R}{Nh} \exp\left(\frac{\Delta S_{act}}{R}\right) \exp\left(-\frac{\Delta H_{act}}{RT}\right)\right] \dots\dots\dots (1.22)$$

$$\ln\left[\frac{CR}{T}\right] = \ln\left(\frac{R}{Nh}\right) + \ln \exp\left(\frac{\Delta S_{act}}{R}\right) + \ln \exp\left(-\frac{\Delta H_{act}}{RT}\right) \dots\dots\dots (1.23)$$

$$\ln\left[\frac{CR}{T}\right] = \ln \frac{R}{Nh} + \left(\frac{\Delta S_{act}}{R}\right) - \left(\frac{\Delta H_{act}}{RT}\right) \dots\dots\dots (1.24)$$

Where; h is the Planck's constant (J.s), N is the Avogadro's number (mol), ΔS^* is the apparent entropy of activation ($\text{kJmol}^{-1} \text{K}^{-1}$), ΔH^* is the enthalpy of activation (kJmol^{-1}).

From equation (1.24) we can be plot $\ln (CR /T)$ against $1/T$ and the slope of the straight line show a value $(- \Delta H_{act} /R)$ and intercept show a value of $(\Delta S_{act}/R + \ln R /Nh)$ from which ΔH_{act} and ΔS_{act} can be calculated.

1.11.2 Effect of acid concentration

As the concentration of a corrosive acid media is increased, the corrosion rate is likewise increased and this is primarily due to the fact that the amounts of hydrogen ions, which are the active species, are increased, as acid concentration is increased. Hydrogen ion activity is commonly expressed, for convenience in term of pH. At low pH values, hydrogen evolution usually predominate both in presence and absence of oxygen. Kinetic study of corrosion reactions of iron in H_2SO_4 by measuring the reaction rates in different molarity (0.5-1.5 M) at (30-60 °C). Development the kinetic observed that sulfuric acid because corrosive in (0.5M) lower than (1.5M). The dissolution rate and the amount of hydrogen absorbed by carbon steel in H_2SO_4 , at different molarity (0.5-1.5 M) and different temperatures (30-60 °C). It was concluded that the dissolution rate of steel

in (1.5 M) of H₂SO₄ at 30 °C was much faster than the corresponding concentrations of the other [6].

1.11.3 Effect of reaction time

The rate of reaction can be obtained by plotting the concentration of carbon steel consumption against time and measuring the slope of the curve dW/dt (W is carbon steel consumption and t is time) at the required time. The rate of reaction obtained from such a method is known as instantaneous rate. For the determination of the instantaneous rate at any point, the slope of the curve is determined. The rate of reaction can be expressed by the following equation [22]:

$$\frac{dW}{dt} = k W^{n'} \dots\dots\dots (1.25)$$

$$\ln\left(\frac{dW}{dt}\right) = \ln k + n' \ln W \dots\dots\dots (1.26)$$

Where; k is rate constant and n` is order of reaction. Equation (1.26) can be drawn as ln(dw/dt) versus lnW and the values of slope and intercept can be obtained. However, the average rates calculated by concentration versus time plots are not accurate. This could be achieved by integrating the differential rate equation as below :

$$\int \frac{dW}{W^{n'}} = k \int dt \dots\dots\dots (1.27)$$

Equation (1.27) can be integrated for different values of n`. Equations (1.28, 1.29 and 1.30) represent the rate equation for zero, first and second order, in order:

$$x = k_0 t \dots\dots\dots (1.28)$$

$$W_i = W_t \exp(k_1 t) \dots\dots\dots (1.29)$$

$$k_2 t = \frac{1}{a-x} - \frac{1}{a} \dots\dots\dots (1.30)$$

Where; W_i is the initial carbon steel consumption at $t = 0$ (gram), W_t is carbon steel consumption at any time (gram), a is the initial carbon steel consumption at $t = 0$ (gram), $(\Delta W = x)$, x is the reaction concentration and $t_{1/2}$ is half-life (h). The half-life period is defined as the time necessary for the concentration of a reactant to decrease to half of its initial value. Half-life indicates the stability of reactants, the longer half-life the greater the stability of reactants.

1.11.4 Effect of inhibitor concentration

Investigators of acid corrosion soon learn that there is a characteristic relation between inhibitor concentration and loss in weight of the metal specimen. As the concentration of inhibitor increases, the weight loss decreases and tends to approach a low constant value, which depends on the properties of particular inhibitor [6].

1.12 Mechanism of Adsorption

Fundamentally, for solid–liquid adsorption system, adsorption largely depends on the charge and nature of the metal surface, electronic characteristics of the metal surface, properties of solvent and other ionic species, temperature of corrosion reaction and finally on the electrochemical potential at solution-interface. Adsorption of inhibitor involves the formation of two types of interaction. The physical adsorption is weak interaction and is due to electrostatic attraction between inhibiting organic ions or dipoles and the electrically charged surface of metal. The zero charge potential plays a key role in the electrostatic adsorption process. The second type of adsorption occurs when the directed forces

govern the interaction between the adsorbate and adsorbent. Chemical adsorption involves charge sharing or charge transfer from adsorbates to the metal surface atoms in order to establish a coordinate type of bond. Chemical adsorption has a free energy of adsorption and activation energy higher than physical adsorption and, hence, usually it is irreversible [23]. Adsorption isotherms are usually used to describe the adsorption process.

1.12.1 Adsorption of inhibitor and isotherm

The most frequently used isotherms are: Langmuir, Freundlich , Kinetic-thermodynamic models [24].

To obtain the adsorption isotherm, the degree of surface coverage (θ) for various concentrations of the inhibitor must be calculated and the various models must be tested to show the compatibility of the model with data through equations follows.

$$\theta = \frac{IE}{100} \dots\dots\dots (1.31)$$

Where; θ is the Surface coverage, IE is the inhibitor efficiency.

a. Langmuir adsorption isotherm

The model for the Langmuir isotherm is a set of uniform adsorption sites and many cases of strong adsorption do not fit this isotherm.

Mathematically, this isotherm is given as:

$$\theta = \frac{K_L C_i}{1 + K_L C_i} \dots\dots\dots (1.32)$$

Where; K_L is the equilibrium constant (L/ml) for the Langmuir adsorption isotherm representing the degree of adsorption (i.e., the higher the value of K_L indicates that the inhibitor is strongly adsorbed on the metal surface,

C_i is the inhibitor concentration (ml/L), and θ is the surface coverage [6].
Rearranging equation (1.32) will give:

$$\frac{C_i}{\theta} = \frac{1}{K_L} + C_i \dots\dots\dots (1.33)$$

$$K_L = \frac{1}{55.55} \exp\left(-\frac{\Delta G_{ads}^{\circ}}{RT}\right) \dots\dots\dots (1.34)$$

Where; ΔG_{ads}° is standard adsorption free energy (kJ mol^{-1}), The value of (55.5) is the water concentration in solution expressed in M. Equation (1.33) can be plotted as C_i/θ against C_i . From intercept the values of K_L . Can be calculated behavior of equilibrium constant of adsorption (K_L) was noticed decreased with increase in temperature as the same behavior was reported by Umoren et al [25].

b. Freundlich adsorption isotherm

This isotherm can be represented by the equation (1.35).

$$\theta = K_F C_i^{n''} \dots\dots\dots (1.35)$$

Where; K_F and n'' are constant for a given system at a given temperature [25]. This isotherm can be written as:

$$\ln \theta = \ln (K_F C_i^{n''}) \dots\dots\dots (1.36)$$

$$\ln \theta = \ln K_F + n'' \ln C_i \dots\dots\dots (1.37)$$

Where; θ is surface coverage, K_F is the equilibrium constant for the Freundlich adsorption constant (L/ml), n'' is slope. Equation (1.37) can be plotted as $\ln \theta$ against $\ln C_i$, where slope and intercept yield the values of n'' and K_F respectively.

c. Kinetic-thermodynamic adsorption isotherm:

Recent researches have looked in to the action of adsorptive inhibitors from purely mechanistic kinetic point of view [26]. A kinetic-thermodynamic model for adsorption process at metal-solution interface has been suggested. In this model, (y') is the number of inhibitor molecules occupying one active site. This model can be given by the following equation;

$$\left(\frac{\theta}{1-\theta} \right) = K' (C_i)^{y'} \dots\dots\dots (1.38)$$

Where; θ is surface coverage, K' is the equilibrium constant for the kinetic-thermodynamic adsorption (L/ml), C_i is inhibitor concentration (ml/L), y' is slope.

$$K_{ads} = K' \left(\frac{1}{y'} \right) \dots\dots\dots (1.39)$$

Rearranging equation (1.38) will give:

$$\ln \left(\frac{\theta}{1-\theta} \right) = \ln K' + y' \ln C_i \dots\dots\dots (1.40)$$

Equation (1.40) can be plotted as $\ln \left(\frac{\theta}{1-\theta} \right)$ against $\ln C_i$, where slope and intercept yield the values of y' and K' respectively.

1.13 Previous Studies

(Saratha et al. 2009) Observed the effect of acid extracted from *Citrus aurantiifolia leaves* plant which exhibited 97.51% inhibition efficiency on the corrosion of mild steel in 1 M HCl studied by weight loss technique. The nature of adsorption were proved by theoretical fitting of different isotherms, Frumkin , Freundlich, Temkin , Langmuir, Flory-Huggins and the kinetic thermodynamic model [27].

(Adnan and Hanan. 2009) Used economical and environmentally safe substances as inhibitor, the fresh leaves extract of *Zizyphus Spina – Chritis* were utilized as corrosion inhibitors by using weight loss procedure, The corrosion inhibition of carbon steel in HCl acid in the presence *Zizyphus Spina – Chritis leaves extract* showed the optimum inhibition efficiency for carbon steel be 99.5%, 75% and 66% at 1%, 1% and 2% concentration of the inhibitor at the temperatures 25 °C, 35 °C and 45 °C respectively [28].

(Dahmani et al. 2010) Corrosion inhibition effect of *black pepper extract* and its *piperine* isolated by ethanol from ground *black pepper* were investigated by weight loss technique on corrosion of C38 steel in 1 M HCl solution. The value attained showed higher efficiency reached above 95% at 2g/L inhibitor concentration which is tested for the natural compounds by weight loss measurements. It is observed that the corrosion rate decreases massively in the presence of *piperine*, and with increases of inhibitor concentration caused to increase the value of inhibition efficiency. Langmuir adsorption isotherm entrusted the mechanistic of adsorption process for *piperanine* on metal surface [29].

(Yaro et al. 2011) *Peach juice* were utilized as inhibitor of mild steel in 1 M of hydrochloric solution in the concentration range of 5-50 cm³ /L and at temperature range of 30-60 °C by using both polarization and weight loss

procedure, the extreme inhibition efficiency reached about 91% at 50°C, when the concentration of inhibitor is 50 cm³/L. Adsorption characteristics, the inhibition effect, mathematical and electrochemical modeling of *peach juice* were explained. The inhibitor adsorbed physically on metal surface through Langmuir isotherm [30].

(**Iloamaeke et al. 2012**) *Pterocarpus soyauxi*, extract were employed as the inhibitor substance of mild steel using weight loss technique at the temperature 30 °C and 60 °C, observed the inhibition efficiency increased with increase in inhibitor concentration but decreased with a raising temperature. The inhibition of corrosion of mild steel obey Freundlich and Tempkin adsorption isotherms and correspond into first order reaction kinetics. By calculating thermodynamics parameters; ΔH , E_a , and ΔG , inferred that inhibition of corrosion of mild steel occurred by physical adsorption mechanism in the presences of ethanol extract of *Pterocarpus soyauxi*, extract [31].

(**Cang et al. 2013**) *Aloes leaves extract* were utilized to prevent the corrosion of mild steel in 1.0 M Hydrochloric acid using weight loss procedures. Ones illustrated that the inhibition efficiency increases with the increase of the extract concentration. The influence of temperature on the corrosion actions of mild steel in 1M HCl as well varying the extract concentration was also investigated. The adsorption of the *Aloes leaves extract* molecules occurs spontaneously and conform Langmuir isotherm. The thermodynamic parameters and activation energy for the inhibition progression was calculated, for interaction between inhibitor and mild steel surface [32].

(**Abdulkhaleq. 2013**) Tried *Eucalyptus camaldulenis leaves extract* functioned as the inhibitor corrosion for low carbon steel in 3M

Hydrochloric acid using the gravimetric method. Different concentrations of (2, 4, 6, 8 and 10) g/L of extract were verified. Ones illustrated that inhibition efficiency increased rapidly with increasing the extract concentration at 25°C and increased with a raising temperature but progressively at 35 °C, 45 °C and less than other at 55 °C .the results which obtained from the experimental data showed that adsorption of *Eucalyptus camaldulenis leaves extract* molecules occurs spontaneously and conform Langmuir isotherm [33].

(Yaro et al. 2013) Studied the corrosion inhibition of mild steel in 1M H₃PO₄ solution by using *apricot juice* at various temperatures by weight loss procedure. Activation, adsorption and statistical investigated in this search had manifested that inhibitor adsorbed on metal surface correspond Langmuir isotherm. From the value of heat of adsorption of -14.93 kJ/mol inferred that inhibition of corrosion of mild steel occurred by physical adsorption, furthermore the inhibition efficiency reached 75 % at 30 °C where the concentration of the extract were 40 g/L [34].

(Hamdy and El-Gendy. 2013) Used aqueous extract from *henna leaves* with different concentration to restrain corrosion of carbon steel in 1M Hydrochloric acid by two methods; weight loss and potentiodynamic polarization. The influence of temperature on the corrosion actions of carbon steel was performed within temperature range of 293-333 K. The study showed that the inhibition efficiency increases with increased inhibitor concentration but is reduced with increasing temperature. The activation and free energies for the inhibition progression indicted the mechanism of physical adsorption. The adsorption of extract on carbon steel surface is endothermic, spontaneous and corresponded with the Langmuir isotherm. Surface of C-steel and protective layer analysis have been tested using; EDX (energy dispersive X-ray), SEM (scanning electron

microscopy), FT-IR spectroscopy (Fourier transforms infrared) and X-ray diffraction analysis [35].

(Aejitha et al. 2014) Explored the demonstration of inhibitor from extract *Antigonon leptopus* on the corrosion of mild steel in 1M H₂SO₄ by using weight loss procedure. Results explained that the extract of *Antigonon leptopus* behave as an efficient corrosion inhibitor in 1M H₂SO₄ acid medium. The inhibitor concentration of 0.7 % v/v at 6 hours inundation showed maximum inhibition efficiency reached to 92.6% [36].

(Anbarasi and Vasudha. 2014) Were functioned *peel of Cucurbita maxima extract* as a disincentive for mild steel corrosion in 1M HCl using weight loss and FTIR procedures. The calculated results of corrosion rates of mild steel and the inhibition efficiency of *peel of Cucurbita maxima extract* show that the extract utilized as a good corrosion inhibitor with inhibition efficiency increased with extract concentration. Extreme inhibition efficiency reached of 93 % at 2 % v/v concentration of the *peel of Cucurbita maxima extract* [37].

(Fouda et al. 2014) Utilized *Anise extract* had been used by to discouragement corrosion of carbon steel in 1 M HCl solution using weight loss procedure. Protecting film and surface morphology were verified using scanning electron microscope (SEM). The adsorption mechanism of the inhibitors on carbon steel surface corresponded with the Langmuir isotherm [38].

(Thilagavathy et al. 2015) Utilized different concentrations of the extract of *mirabilis jalapa flowers* to restrained the corrosion of mild steel in 1M HCl using weight loss technique, various immersion periods at certain elevated temperatures. The adsorption of the extract of *mirabilis jalapa flowers* molecules conform Langmuir and Temkin isotherms. The

result showed extreme maximum inhibition efficiency at 5 % v/v concentration of the extract and at 323 K [39].

(Olasehinde et al. 2015) Utilized *Alchornea laxiflora leaves extract* to prevent the corrosion of mild steel in acidic medium by using gravimetric technique. Research was conducted by varying the concentration of extract, immersion time and temperature. The extract exhibited a potential inhibitor for the corrosion of mild steel in the presence of 1M HCl, as the corrosion rate decreases with increase in the concentration of the extract. The inhibition efficiency increases gradually as the concentration of the extract increased but decreases with elevation in temperature and exposure time. The extreme inhibition efficiency reached to 96 % in the presence of the extract. Activation energy was found to be 21.81 kJ mol⁻¹ for the blank and increases to 82.57 kJ mol⁻¹ in the presence of the extract. Thermodynamic parameters such as, entropy change, enthalpy change and Gibb's free energy were calculated. Kinetics of the reaction in the presence of the extracts indicated to match a first order reaction and the half-life increase as the concentration of the extract increases, furthermore the adsorption showed that Langmuir isotherm is the perfect adsorption form to conform the adsorption of the extract on mild steel surface [40].

(Kulandai and Vasudha. 2015) Studied the adsorption and inhibitive efficiency of *Millingtonia hortensis leaves extract* on mild steel in 1M HCl and 1M H₂SO₄ at a temperature range of (303 to 343K) by mass loss measurements. The value of inhibition efficiency increased with the increase of inhibitor concentration and decreased at 333K. The value of inhibition efficiency in H₂SO₄ at 323K was (97.10 %) and the value of inhibition efficiency in HCl at 333K was (97.41%). ΔG_{ads} adsorption value of 12 – 24 KJ/ mol is suggestive of physisorption process. Adsorption of inhibitor on the metal surface was found to obey Langmuir and Temkin

isotherm. The values of activation energy (ΔE_a), enthalpy of adsorption (ΔH) and entropy of adsorption (ΔS) were calculated [41].

(Muthukrishnan et al. 2015) Prevent corrosion by *Ficus hispida leaf extract* were in 1M HCl by using weight loss, electrochemical impedance spectroscopy (EIS) and potentiodynamic polarization techniques. The extreme Inhibition efficiency reached 90 % in 250 ppm of extract at 308 K. in the presence of the extract, an increase in inhibition efficiency was observed with decrease in temperature and the value of activation energies increased. The adsorption of *Ficus hispida leaf* on mild steel surface conforms to Langmuir isotherm. The morphology overlay coating which is formed on the mild steel surface tested by SEM and the surface synthesis verified by using EDX, diffuse reflectance fourier transform infrared spectroscopy (DRFT-IR) and X-ray diffraction (XRD) tests. [21].

(Abdulrahman et al. 2015) Utilized *Africa parquetina leaves extract* to prevent the corrosion of mild steel in sulphuric acid solution using gasometric, gravimetric and thermometric techniques. The chemical characterizations of the leaves extract were also performed using gas chromatography mass spectroscopy (GCMS) and fourier transformation Infra-Red (FTIR) analysis. Experiments showed the maximum inhibition efficiency 87.78 % at 0.5 g/L concentration of extract, and it was increased with the increases in concentration of extract but reduced with the increase in temperature. The adsorption of inhibitor conformed Langmuir isotherm and the thermodynamic parameters calculations indicated that it was physisorption [42].

(Noor et al. 2016) Were investigated the inhibitor action of red onion seeds and peels extracts (ROSE & ROPE) and comparing on the corrosion of steel in 0.75 M H_3PO_4 using chemical measurements, (hydrogen

evolution and mass loss) and SEM technique. The effect of temperature on the corrosion of steel in 0.75 M H_3PO_4 without and with certain concentration of each extract was studied in the temperature range of 303–333 K. The inhibition efficiency of both extracts increases with increasing concentration and gives powerful fitting to the Langmuir adsorption isotherm with the highest adsorption affinity for ROSE. The values of E_a without and with inhibitor revealed chemisorption and physical adsorption behavior for ROSE and ROPE, respectively, on the steel surface [43].

1.14 Objectives (aims of study)

1. Studying the corrosion rates of carbon steel in different concentrations of sulfuric acid and temperatures.
2. Extraction and evaluating a natural and environmental friendly corrosion inhibitor.
3. Studying the kinetics of reaction of carbon steel in H_2SO_4 solutions at different operating conditions.
4. Studying the steel surface morphology by scanning electron microscope.
5. Studying the active group in the inhibitor by fourier transform infrared spectroscopy.
6. Correlating of dependent variable (corrosion rate) and independent variables (temperature, inhibitor and acid concentration) in a mathematical models.

2.1 Used Materials**2.1.1 Chemical****Table (2.1) Used chemical materials**

	Materials	Origin	Function	Purity
1	Sulfuric acid	India	Corrosion medium	98.0 %
2	Benzene	Europe	Grease removal	99.7 %
3	Acetone	Europe	Cleaning and drying	99.9 %

2.1.2 Used Electrode

The used electrode was carbon steel having the following composition as determined by atomic absorption spectrometry, (table 2.2) in College of Science Ibn Al-Haitham.

Table (2.2) Carbon steel compositions

Element	Wt %
Fe	(99.5%)
Mn	(0.4%)
C	(0.09%)
Cu	(0.01%)
Cr	(0.01%)
Ni	(0.01%)
Pb	(0.004%)

2.2 Used Instruments

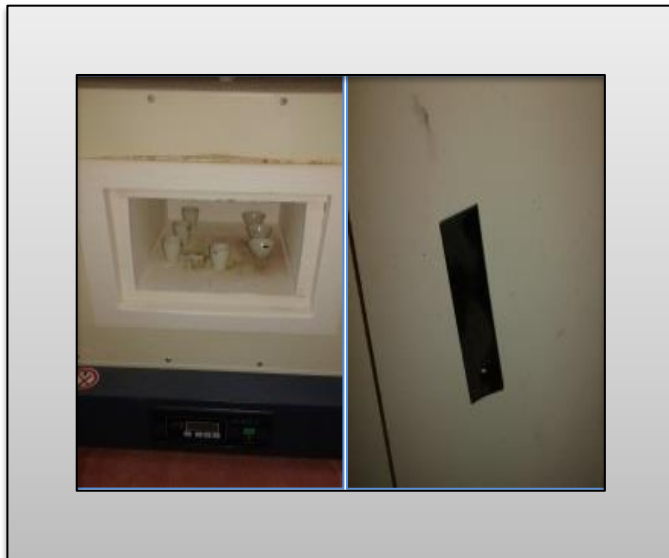
The used instruments are given in (table 2.3) with their origins and specifications. (1 to 6 in College of Science, Diyala University) while (7, 8 and 9) in (College of Science Ibn Al-Haitham)

Table (2.3) Used instruments

Instrument Name		The Company and Model
1	Electrical Furnace	Type-KR170E,Max temp, 1150 °C, 220 V, 13.8A, 50/60 Hz, Japan origin
2	Oven	BINDER Hotline International
3	Water Bath	YCW-O1
4	Heating Magnetic Stirrer	AREC
5	Electronic Balance	KERN & Sohn GmbH, Type ACS 120-4, NO. WB12AE0308,CAPACITY 120g, READABILITY 0.1mg.
6	Distillation Device	LUZ DE AVISO AGUA INSUFICIENTE
7	SEM	(AIS2300C model) made in Korea
8	FTIR	(UK) AC:220V/50Hz DATE:2014.10 S/N: 14500039
9	AAS	(AI 7000 model) made in Canada

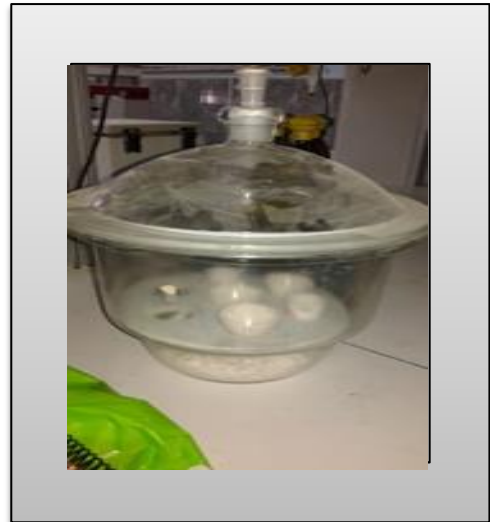
2.3 Corrosion Specimen Preparation

Specimens of dimensions 3 x 1 x 0.1cm, with exposing surface area of about 7 cm² to the aggressive solution. The specimens were first annealed in furnace at 600 °C for 1 h, and then cooled down to room temperature, as shown in (figure 2.1.a) [44]. The samples were abraded with emery paper of grade number, 150, 600 and 850, (figure 2.1.b), then washed with flow tap water followed by distilled water. It is dried with cleaning tissue, immersed in benzene and acetone, dried again (figure 2.1.c), then kept in a desiccator over silica gel (figure 2.1.d). The samples were weighted by 4-digits electronic balance, and the dimensions were measured by an electronic vernier, as shown in (figure 2.1.e and 2.1.f) respectively, then were completely immersed corrosion solution and transferred to water bath as in (figure 2.1.g and 2.1.i) respectively.

**a****b**



c



d



e



f



g



i

Fig. (2.1 a, b, c, d, e, f, g and i) Carbon steel preparation steps

2.4 Preparation of Corrosion Solution

Corrosion solution was prepared from the concentrated H_2SO_4 with the molarity of 0.5, 1 and 1.5 M by dilution method.

2.5 Preparation of Citrus aurantium Leaves Extract:

Citrus aurantium leaves which is very common, available and cheap plants in Diyala governorate /Iraq, were collected from gardens, shade dried, grind and converted to powder. The extract was prepared by refluxing 10 g of powder in 100 ml of 0.5, 1 and 1.5 M H_2SO_4 acid for 3h and kept overnight, then filtered and the filtrate was made up to 50 ml using the same acid and this was taken as stock solution [45]. (Figure 2.2.a) show *Citrus aurantium powder dry leaves* 10 gm. (Figure 2.2.b) show *Citrus aurantium* powder with H_2SO_4 acid. (Figure 2.2.c) show the extract prepared by refluxing. (Figure 2.2.d) show the extract before filtering and the (figure 2.2.e) show the extract after filtering.

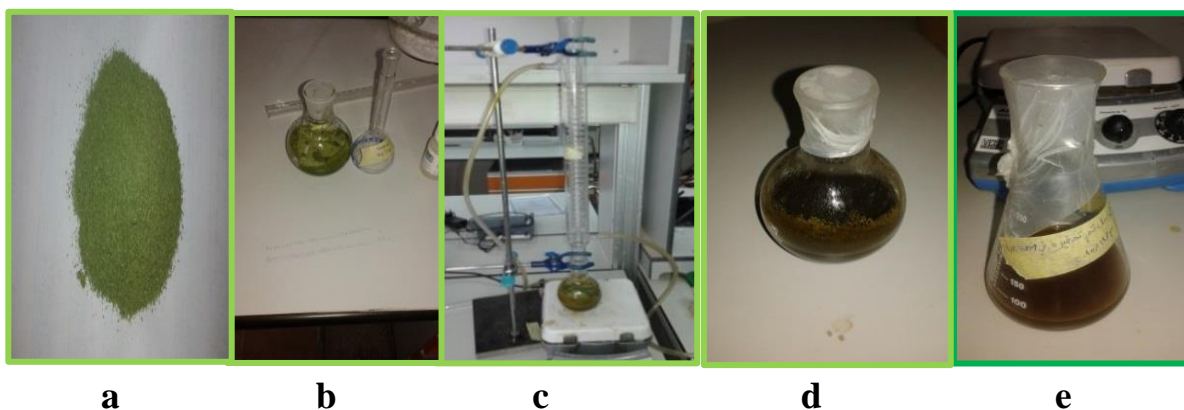


Fig.(2.2.a, b, c, d and e) Citrus aurantium leaves extract preparation steps.

2.6 Weight Loss Measurement

For weight loss measurements, the metal samples were completely immersed in 200 cm³ corrosion solution of 0.5, 1, and 1.5 M H₂SO₄ in conical flask then transferred to water bath, as in (figure 2.1.f) and (figure 2.1.g). They were exposed for a period of 3h at the desired temperature, molarity and inhibitor concentration. Then the metal samples were cleaned, washed with flow tap water followed by distilled water dried with clean tissue, immersed in benzene and acetone and dried again. Weight losses were determined in the presence and absence of inhibitor at 30, 40, 50, and 60 °C, (2, 4, 6, 8, and 10 ml/L) inhibitor concentration.

2.7 Kinetic Measurement

Kinetics studies were carried out at different four times (1, 2, 3,4h), two temperature (40 and 60 °C) in absence and presence of inhibitor concentration (0ml/L and 6ml/L). Using know reaction order from through know values equilibrium constant and half-life.

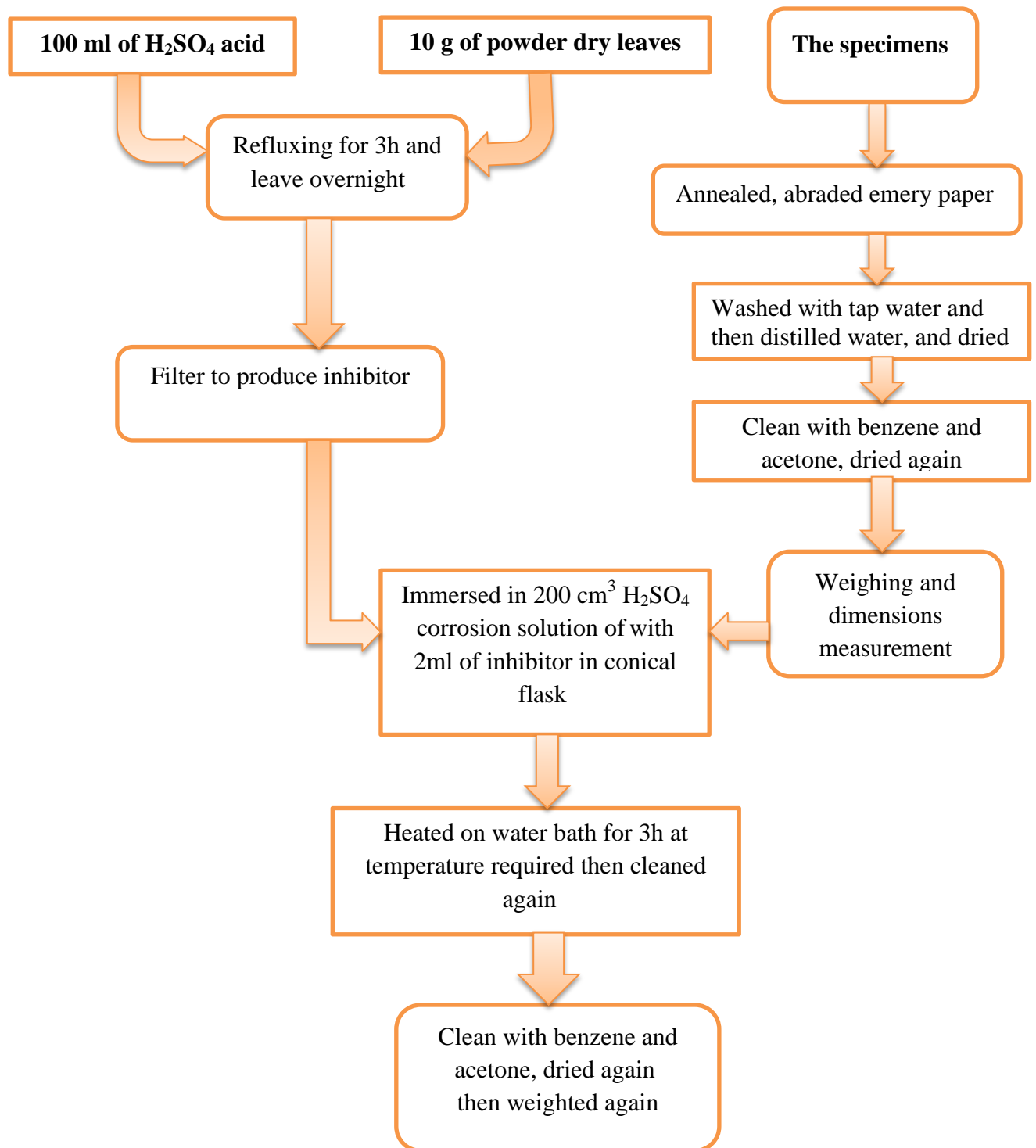


Fig (2.3) Algorithm of experimental work

3.1. Weight Loss Measurements

Corrosion rates (CR) were determined in presence and absence of inhibitor using the following formula [6]:

$$CR = \frac{\Delta W}{A \times T} \dots\dots\dots (3.1)$$

Where; ΔW is weight loss in grams, A is area of specimen in m^2 , T is exposure time in days. Corrosion rates were obtained in term of g/m^2 day (gmd).

Inhibition efficiency was calculated using the equation:-

$$IE = \frac{CR_o - CR_i}{CR_o} \times 100 \dots\dots\dots (3.2)$$

Where; CR_o and CR_i are the corrosion rates in the absence and presence of various concentrations of inhibitor respectively. Corrosion rate and inhibitor efficiency were evaluated at different operating conditions and the results were collected in tables (3.1), (3.2) and (3.3). It is clear that corrosion rate increased with temperature, and H_2SO_4 acid concentration, and decreased with inhibitor concentration.

Table (3. 1) Effect of temperature on the corrosion rate of carbon steel in 0.5 M H₂SO₄ in absence and presence of Citrus aurantium leaves extract as corrosion inhibitor.

Exp	C _i ml/L	T, °C	Corrosion rate (gmd)	% IE
1	0	30	900	0
2		40	1440	0
3		50	2650	0
4		60	4700	0
5	2	30	270	70
6		40	520	63.8
7		50	1050	60.3
8		60	1800	61.7
9	4	30	200	77.7
10		40	450	68.7
11		50	999	62.3
12		60	1400	70.2
13	6	30	180	80
14		40	393	72.7
15		50	760	71.3
16		60	1200	74.4
17	8	30	150	83.3
18		40	250	82.6
19		50	555	79
20		60	800	82.9
21	10	30	120	86.6
22		40	170	88.1
23		50	300	88.6
24		60	770	83.6

Table (3. 2) Effect of temperature on the corrosion rate of carbon steel in 1 M H_2SO_4 in absence and presence of Citrus aurantium leaves extract as corrosion inhibitor.

Exp	C_i ml/L	T, °C	Corrosion rate (gmd)	% IE
1	0	30	1440	0
2		40	2640	0
3		50	4800	0
4		60	8640	0
5	2	30	384	73.3
6		40	720	72.7
7		50	2000	58.3
8		60	4500	47.9
9	4	30	336	76.6
10		40	528	80
11		50	1104	77
12		60	2640	69.4
13	6	30	240	83.3
14		40	408	84.5
15		50	984	79.5
16		60	2160	75
17	8	30	216	85
18		40	312	88.1
19		50	888	81.5
20		60	1920	77.7
21	10	30	160	88.8
22		40	288	89
23		50	600	87.5
24		60	1200	86.1

Table (3. 3) Effect of temperature on the corrosion rate of carbon steel in 1.5 M H₂SO₄ in absence and presence of Citrus aurantium leaves extract as corrosion inhibitor.

Exp	C _i ml/L	T, °C	Corrosion rate (gmd)	% IE
1	0	30	1680	0
2		40	3120	0
3		50	6240	0
4		60	12960	0
5	2	30	480	71.4
6		40	960	69.2
7		50	2880	53.8
8		60	7440	42.5
9	4	30	456	72.8
10		40	936	70
11		50	1920	69.2
12		60	5520	57.4
13	6	30	408	75.7
14		40	758.4	70
15		50	1680	73
16		60	3840	70.3
17	8	30	360	78.5
18		40	744	76.1
19		50	1392	77.6
20		60	3312	74.4
21	10	30	280	83.3
22		40	600	80.7
23		50	1320	78.8
24		60	3264	74.8

3.2 Corrosion Rate Evaluation:

3.2.1 Uninhibited Acid:

Weight loss measurements were used to calculate the corrosion rates in uninhibited acid solutions at different temperatures after 3 h exposure time. It was found that the corrosion rate in (0.5, 1 and 1.5 M) sulfuric acid increased from 900 to 4700 gmd in 0.5 M, 1440 to 8640 gmd in 1M and 1680 to 12960 in 1.5 M as the temperature increased from 30 to 60 °C. Figure (3.1) show the variation in corrosion rate with temperature. The corrosion rate increases with increasing temperature [46]. The relationship between the temperature as a variable and the corrosion rate is exponential one shall be discussed later according to the Arrhenius equation.

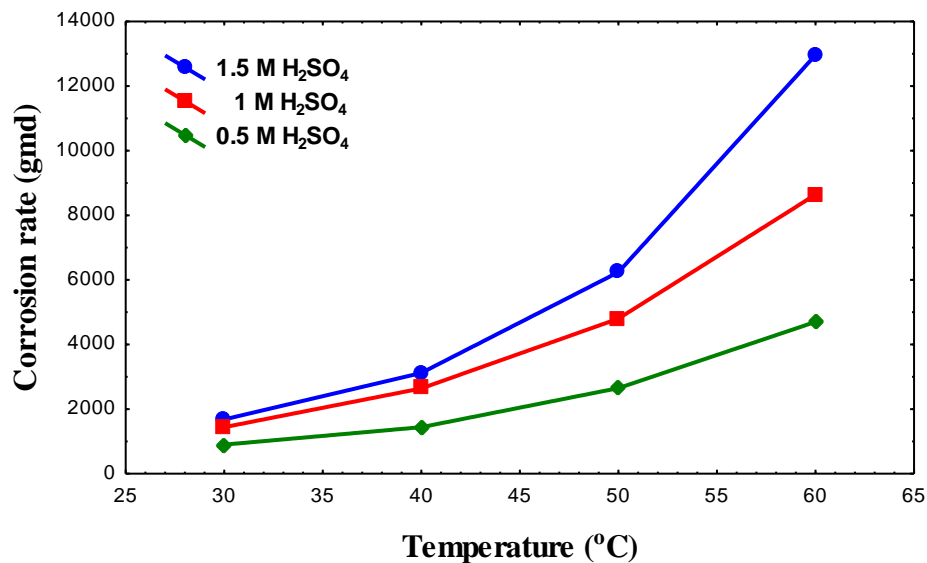


Fig.(3.1) Effect of temperature on the corrosion rate of carbon steel exposed to H₂SO₄ acid.

3.2.2 Inhibitor Concentration Interpretation :

Generally the addition of *Citrus aurantium leaves* extract reduces the corrosion rate markedly. Tables (3.1), (3.2) and (3.3) and figures (3.2), (3.3) and (3.4) show the variation of corrosion rate with the inhibitor concentration at various temperatures. It is clear that the corrosion rate decreases with increasing the concentration of inhibitor at any used temperature [47].

The effect of temperature on corrosion rate for different inhibitor concentration is expressed in figures (3.5), (3.6) and (3.7). This figures shows that the corrosion rate increases with increasing temperature at all studied inhibitor concentration. At inhibitor concentration of 2 ml/L, the corrosion rate increases significantly when the temperature increased from 30 to 60 °C. The effect of 4 ml/L inhibitor concentration is less than 2 ml/L. While at inhibitor concentration of 6, 8 and 10 ml/L the temperature increases corrosion rate slightly. Values of inhibitor efficiency increases with increasing the inhibitor concentration [48].

Figures (3.8), (3.9) and (3.10) show the variation of inhibitor efficiency with inhibitor concentration. It varies, from 70 to 83.6 % at 2 to 10 ml/L inhibitor concentration in 0.5 M H₂SO₄, and from 73.3 to 86.1 % at 2 to 10 ml/L in 1M H₂SO₄, and from 71.4 to 74.8 % at 2 to 10 ml/L in 1.5 M H₂SO₄, as temperature increased from 30 to 60 °C.

Figures (3.11), (3.12) and (3.13) show the effect of temperature on inhibitor efficiency.

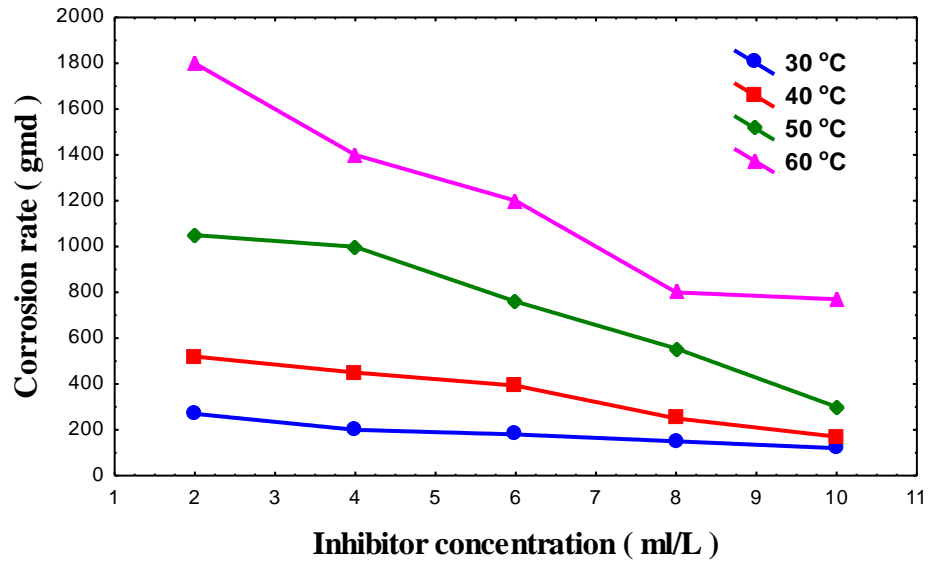


Fig.(3.2) Effect of inhibitor concentration on the corrosion rate of carbon steel exposed to 0.5 M H₂SO₄.

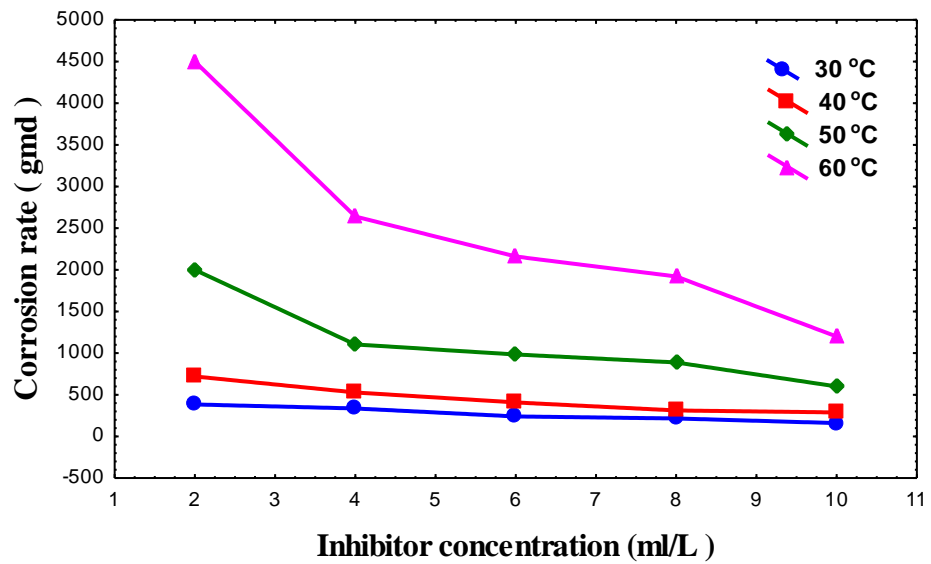


Fig.(3.3) Effect of inhibitor concentration on the corrosion rate of carbon steel exposed to 1 M H₂SO₄.

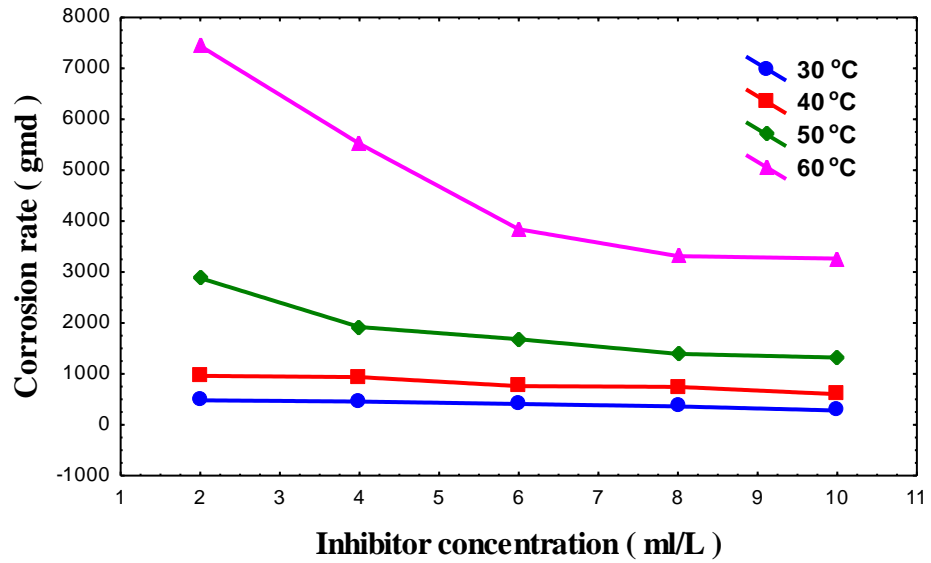


Fig.(3.4) Effect of inhibitor concentration on the corrosion rate of carbon steel exposed to 1.5 M H₂SO₄.

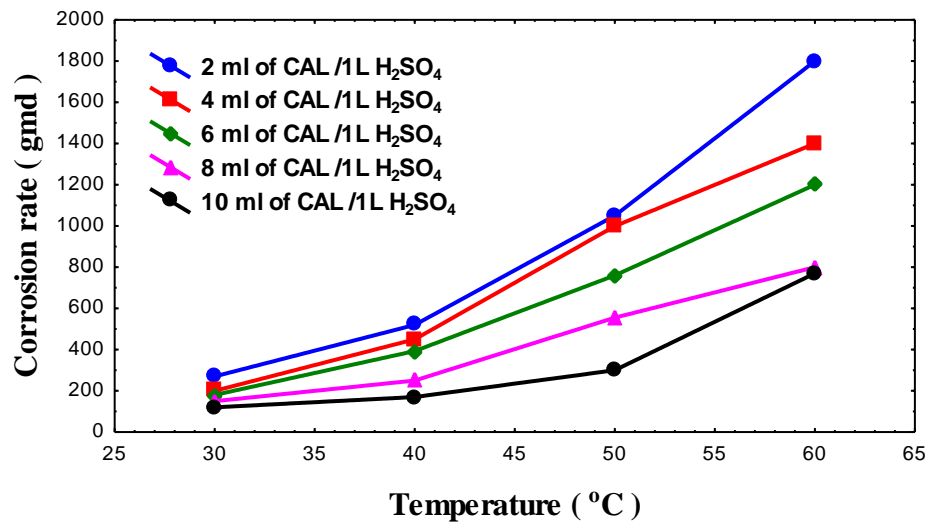


Fig.(3.5) Effect of temperature on the corrosion rate of carbon steel in 0.5 M H₂SO₄ at different inhibitor concentration.

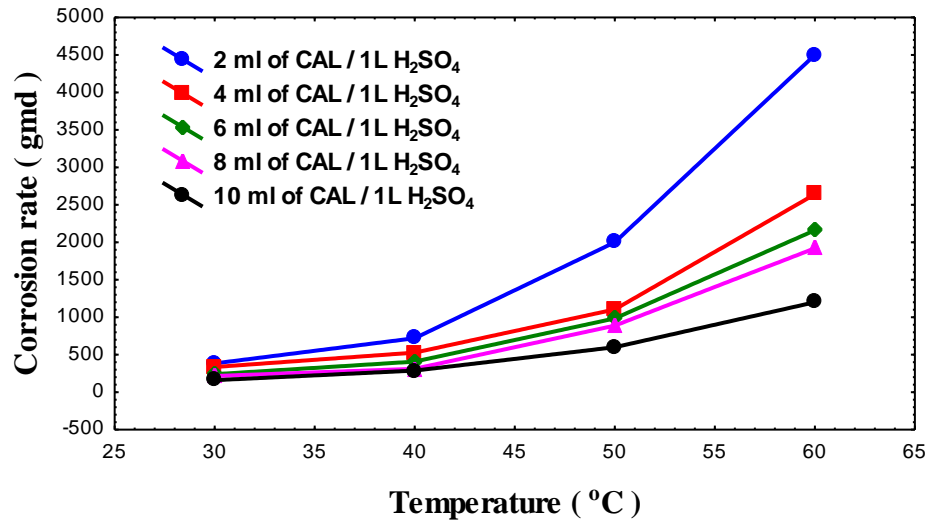


Fig.(3.6) Effect of temperature on the corrosion rate of carbon steel in 1 M H₂SO₄ at different inhibitor concentration.

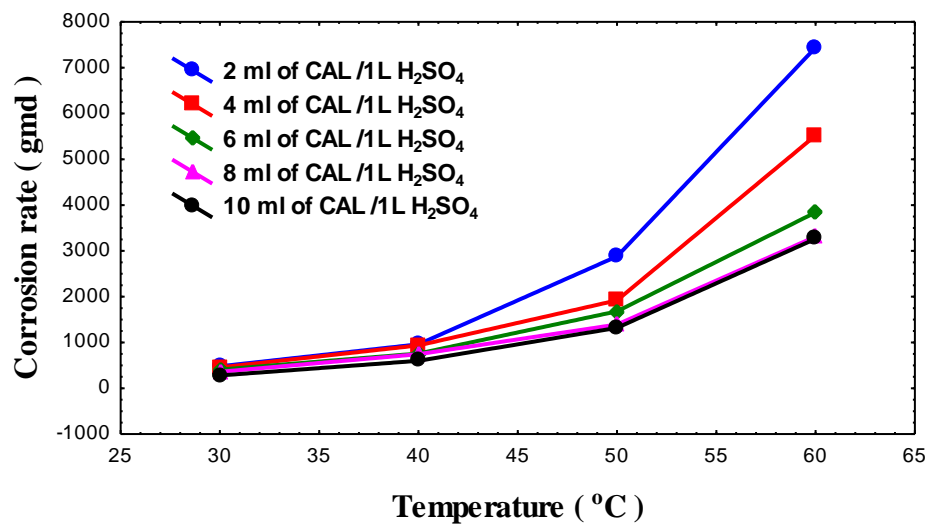


Fig.(3.7) Effect of temperature on the corrosion rate of carbon steel in 1.5 M H₂SO₄ at different inhibitor concentration.

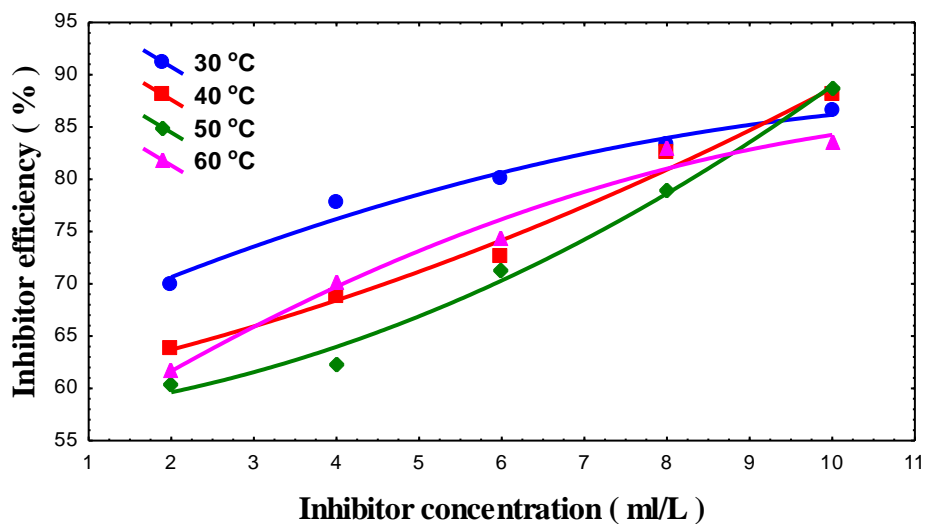


Fig.(3.8) Effect of concentration of Citrus aurantium leaves extract on inhibitive efficiency of carbon steel corrosion in 0.5 M H₂SO₄.

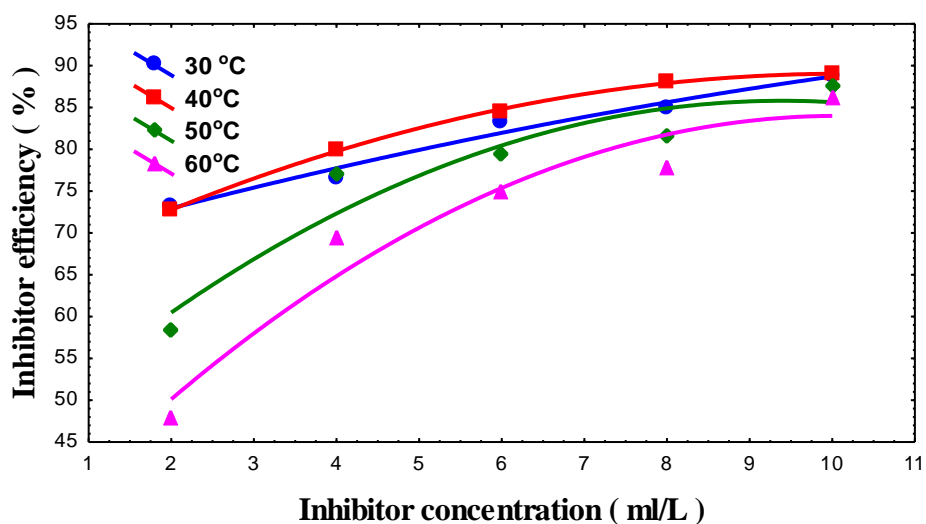


Fig.(3.9) Effect of concentration Citrus aurantium leaves extract on inhibitive efficiency of carbon steel corrosion in 1 M H₂SO₄.

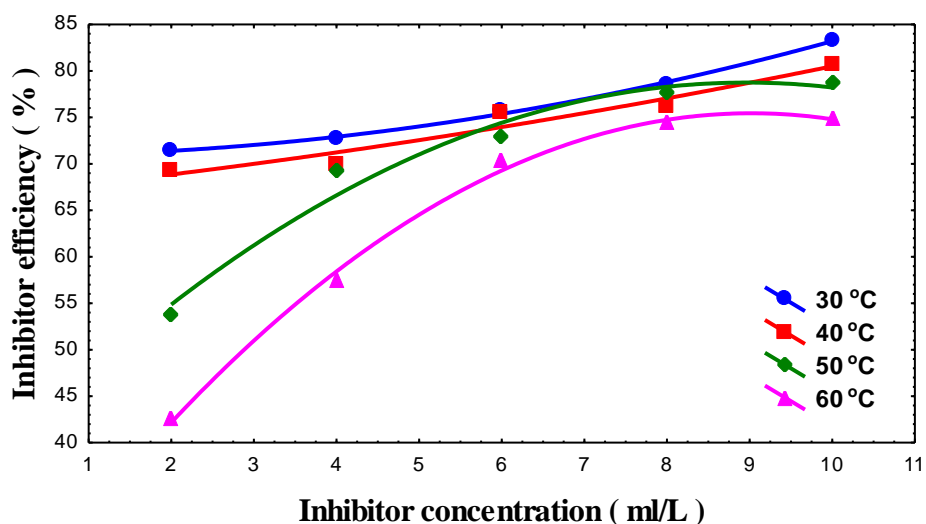


Fig.(3.10) Effect of concentration of Citrus aurantium leaves extract on inhibitive efficiency of carbon steel corrosion in 1.5 M H₂SO₄.

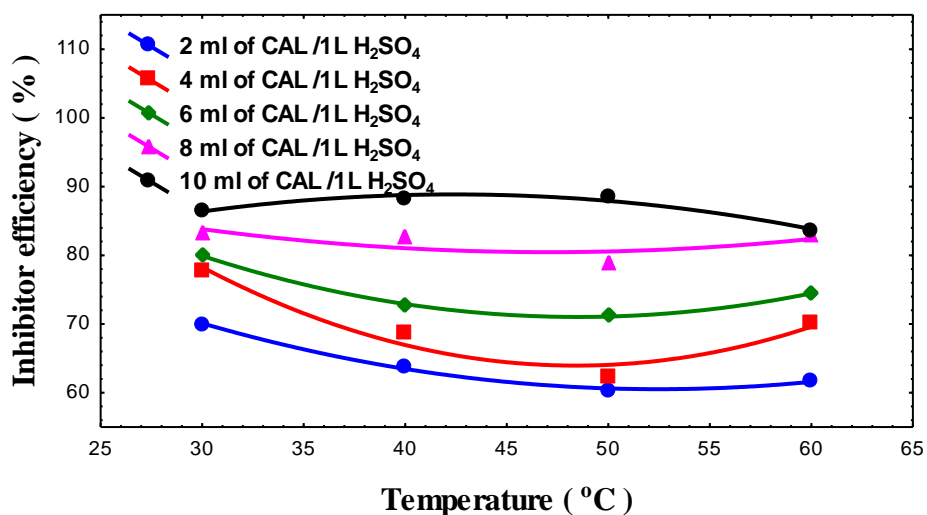


Fig.(3.11) Effect of temperature on inhibitive efficiency of Citrus aurantium leaves extract for carbon steel corrosion in 0.5 M H₂SO₄.

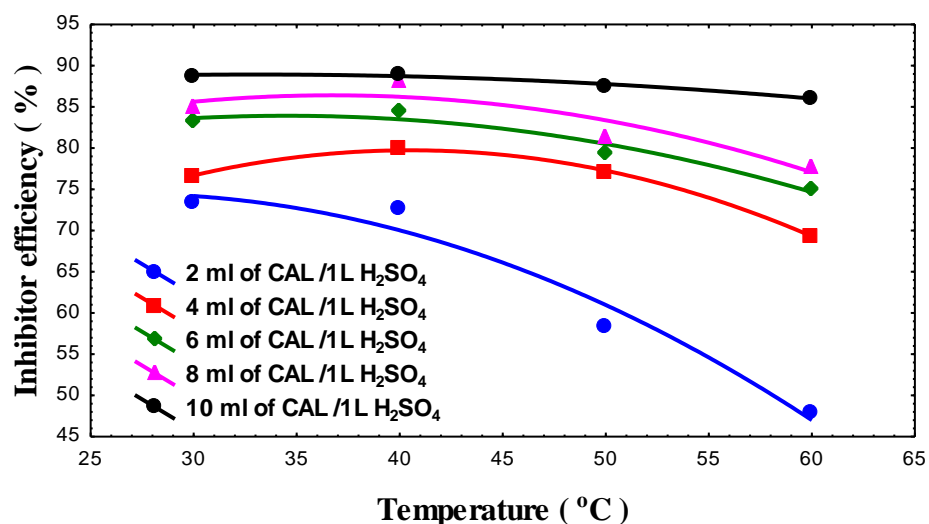


Fig.(3.12) Effect of temperature on inhibitive efficiency of Citrus aurantium leaves extract for carbon steel corrosion in 1 M H₂SO₄.

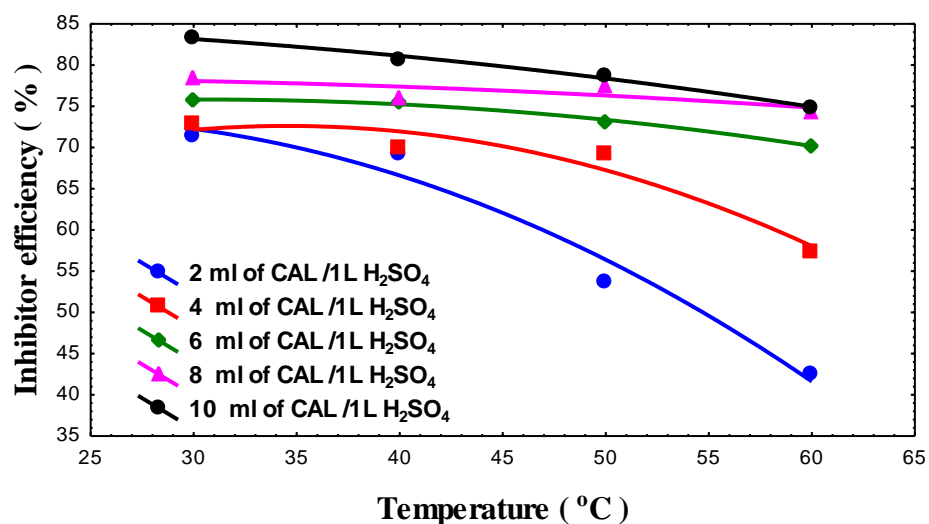


Fig.(3.13) Effect of temperature on inhibitive efficiency of Citrus aurantium leaves extract for carbon steel corrosion in 1.5 M H₂SO₄.

3.3 Inhibitor Performance and Adsorption Interpretation

It was shown that increasing the inhibitor concentration from 2 to 10 ml/L decreases the corrosion rate to very low values. Figures (3.2), (3.3) and (3.4) show this situation clearly. It is clear from those figures that the corrosion rate approaches its minimum value when the inhibitor concentration is 10 ml/L. This might be due to that 10ml/L this inhibitor concentration is enough to cover the metal surface at the temperature range of 30-60 °C. The 8 ml/L inhibitor concentration, the effect of inhibitor concentration will be less than in 10 ml/L. The increase of temperature from (30 to 40 °C) does not lead to significant change in the corrosion rate values as (only 5 % increasing in corrosion rate value, when temperature increased from 30 to 40 °C, but when the temperature increased to 50 and 60 °C, the corrosion rate values changed markedly. At inhibitor concentration of 6 and 2ml/L shown in figures (3.2), (3.3), (3.4) and tables (3.1), (3.2) and (3.3) the reduction in corrosion rate is small and it decreases with temperature increase.

The surface coverage (θ) data are very useful while discussing the adsorption characteristics. The surface coverage of inhibitor at a given concentration is calculated using equation (1.31). The corrosion rate data can be used to analyze the adsorption mechanism. The Langmuir isotherm [6] it is calculated using equation (1.33). Figures (3.14), (3.15) and (3.16) shows plots of $\frac{C_i}{\theta}$ vs. C_i for *Citrus aurantium leaves* extract inhibitor in (0.5,1 and 1.5 M) H_2SO_4 at 30, 40, 50 and 60 °C according to equation (1.33). The data fit straight lines indicating that *Citrus aurantium leaves* extract is adsorbed according to the Langmuir adsorption isotherm. From the intercept of the straight line on the $\frac{C_i}{\theta}$ axis, K_L values can be evaluated which can be substituted in equation (1.34) to calculate ΔG°_{ads} . Tables (3.4), (3.5) and (3.6) shows values of K_L and ΔG°_{ads} . Behavior of

equilibrium constant of adsorption K_L was noticed and indicate decrease with increase in temperature with same behavior reported by Umoren et al [25]. The type of adsorption is physical adsorption because value $\Delta G^\circ_{\text{ads}}$ up of -20 kJ mol^{-1} . For free energy of adsorption ($\Delta G^\circ_{\text{ads}}$) for studied inhibitor lie between (-11.305) and $(-13.426) \text{ kJ mol}^{-1}$ in table (3.4), (-10.720) and $(-14.255) \text{ kJ mol}^{-1}$ in table (3.5), (-10.837) and $(-14.858) \text{ kJ mol}^{-1}$ in table (3.6). The negative values of $\Delta G^\circ_{\text{ads}}$ mean that the adsorption of *Citrus aurantium leaves* extract on carbon steel surface is a spontaneous process and furthermore the negative values of $\Delta G^\circ_{\text{ads}}$ also show the week interaction of the inhibitor molecule on to the carbon steel surface [38].

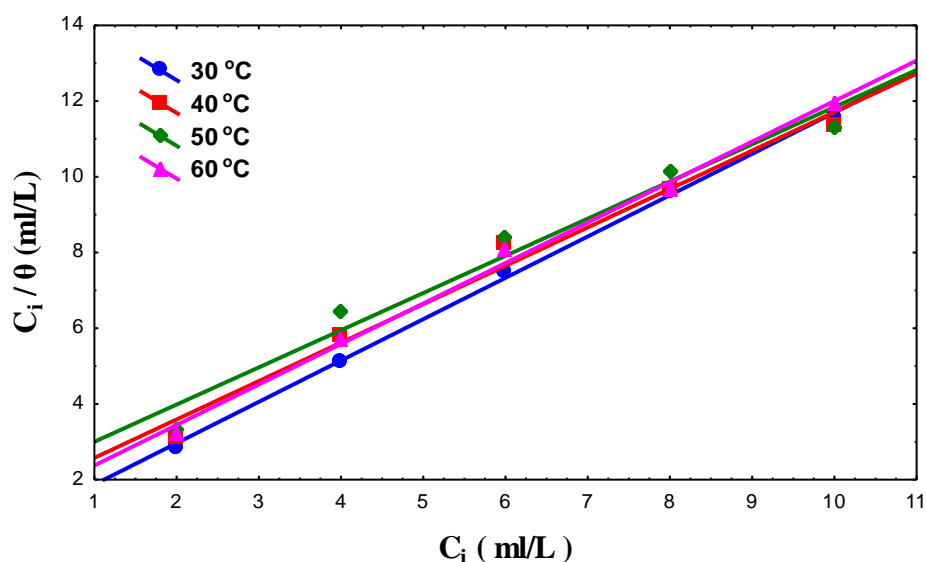


Fig.(3.14) Langmuir adsorption isotherm of Citrus aurantium leaves extract on carbon steel in 0.5 M H₂SO₄.

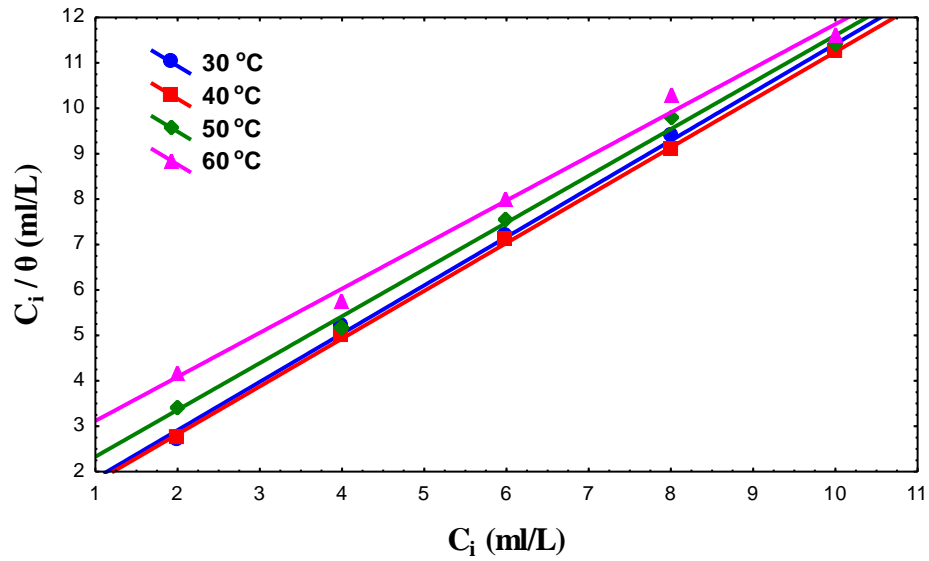


Fig.(3.15) Langmuir adsorption isotherm of Citrus aurantium leaves extract on carbon steel in 1 M H_2SO_4 .

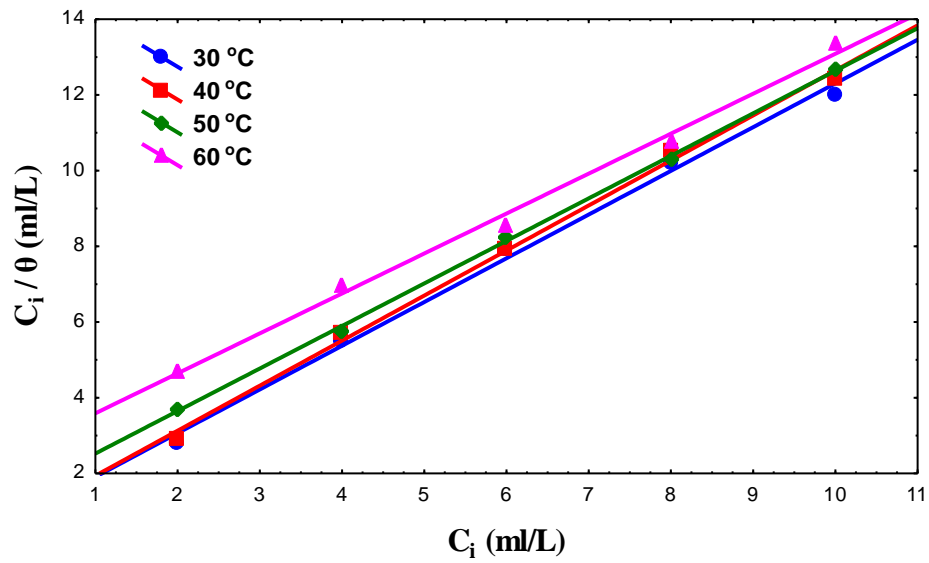


Fig.(3.16) Langmuir adsorption isotherm of Citrus aurantium leaves extract on carbon steel in 1.5 M H_2SO_4 .

Table (3.4) Equilibrium constant, standard adsorption free energy ($\Delta G^{\circ}_{\text{ads}}$), and correlation coefficient (R^2) for Langmuir type adsorption isotherm of the inhibitor on carbon steel in 0.5 M H_2SO_4 at different temperatures.

Temperature (K)	K_L (L/ml)	$\Delta G^{\circ}_{\text{ads}}$ kJ mol ⁻¹	R^2
303	1.6007	-11.305	0.9985
313	2.3809	-12.711	0.9823
323	2.5490	-13.300	0.9676
333	2.2988	-13.426	0.9953

Table (3.5) Equilibrium constant, standard adsorption free energy ($\Delta G^{\circ}_{\text{ads}}$), and correlation coefficient (R^2) for Langmuir type Adsorption isotherm of the inhibitor on carbon steel in 1 M H_2SO_4 at different temperatures.

Temperature (K)	K_L (L/ml)	$\Delta G^{\circ}_{\text{ads}}$ kJ mol ⁻¹	R^2
303	1.2693	-10.720	0.9976
313	1.3912	-11.313	0.9996
323	2.2433	-12.957	0.9961
333	3.1010	-14.255	0.9925

Table (3.6) Equilibrium constant, standard adsorption free energy ($\Delta G^{\circ}_{\text{ads}}$), and correlation coefficient (R^2) for Langmuir type adsorption isotherm of the inhibitor on carbon steel in 1.5 M H_2SO_4 at different temperatures.

Temperature (K)	K_L (L/ml)	$\Delta G^{\circ}_{\text{ads}}$ kJ mol ⁻¹	R^2
303	1.3292	-10.837	0.9949
313	1.3358	-11.207	0.9960
323	2.5334	-13.284	0.9993
333	3.8554	-14.858	0.9936

The corrosion rate data can be used to analyze the adsorption mechanism. The Freundlich isotherm [37] is calculated using equation (1.37).

Figures (3.17), (3.18) and (3.19) show equation (1.37) were produced by plotting $\ln \theta$ against $\ln C$ with slope and intercept yield the values of n'' and K_F respectively as in tables (3.7), (3.8) and (3.9).

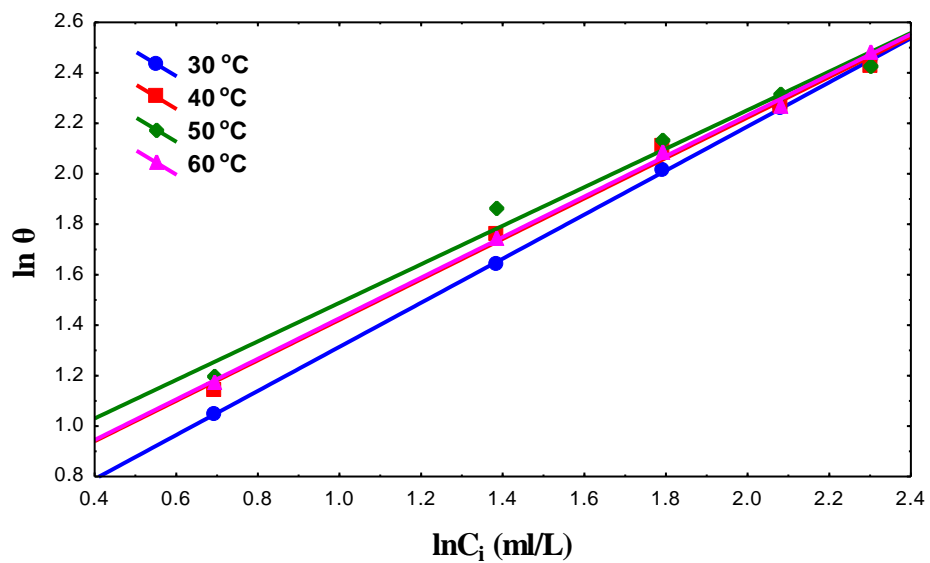


Fig.(3.17) Freundlich adsorption isotherm of Citrus aurantium leaves extract on carbon steel in 0.5 M H₂SO₄.

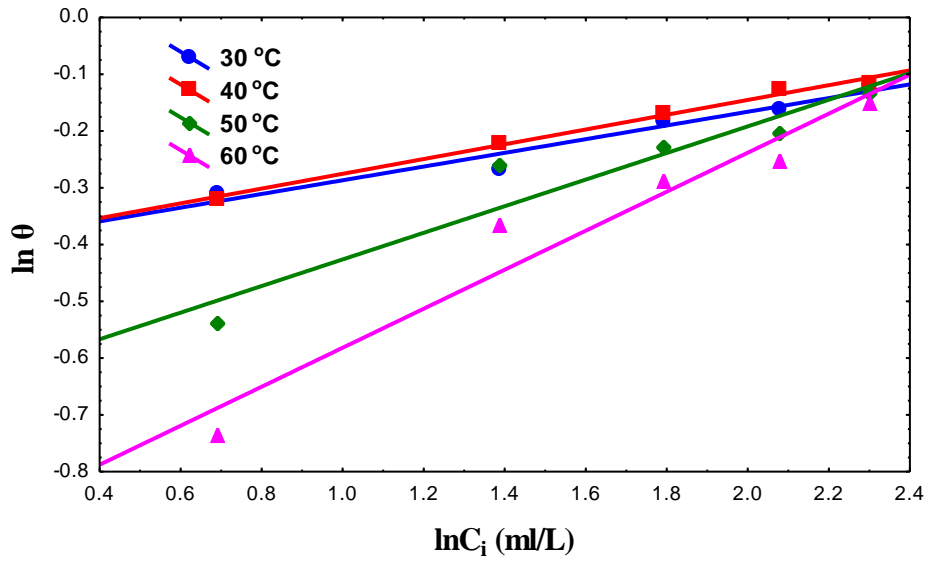


Fig.(3.18) Freundlich adsorption isotherm of Citrus aurantium leaves extract on carbon steel in 1 M H₂SO₄.

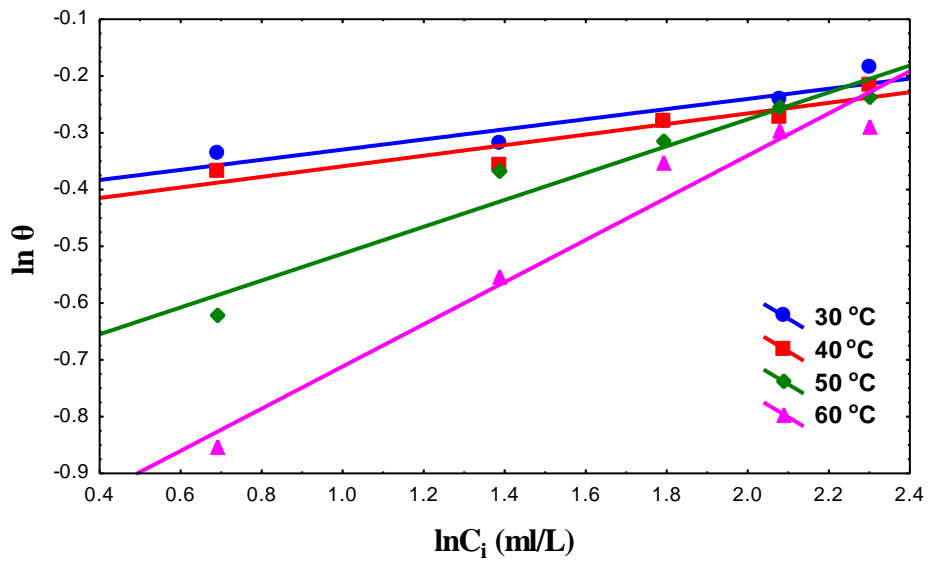


Fig.(3.19) Freundlich adsorption isotherm of Citrus aurantium leaves extract on carbon steel in 1.5 M H₂SO₄.

Table (3.7) Equilibrium constant, slope (n''), and correlation coefficient (R^2) for Freundlich type adsorption isotherm of the inhibitor on carbon steel in 0.5 M H_2SO_4 at different temperatures.

Temperature ($^{\circ}C$)	K_F (L/ml)	n''	R^2
30	1.5539	1.1449	0.9997
40	1.8576	1.2470	0.9937
50	2.0643	1.3094	0.9856
60	1.8658	1.2440	0.9986

Table (3.8) Equilibrium constant, slope (n''), and correlation coefficient (R^2) for Freundlich type adsorption isotherm of the inhibitor on carbon steel in 1 M H_2SO_4 at different temperatures.

Temperature ($^{\circ}C$)	K_F (L/ml)	n''	R^2
30	0.6653	0.1207	0.9555
40	0.6666	0.1301	0.9923
50	0.5165	0.2343	0.9125
60	0.3964	0.3435	0.9415

Table (3.9) Equilibrium constant, slope (n''), and correlation coefficient (R^2) for Freundlich type adsorption isotherm of the inhibitor on carbon steel in 1.5 M H_2SO_4 at different temperatures.

Temperature ($^{\circ}C$)	K_F (L/ml)	n''	R^2
30	0.6577	0.0893	0.8487
40	0.6362	0.0931	0.8592
50	0.4725	0.2367	0.9448
60	0.3385	0.3715	0.9593

It seem that the Freundlich isotherm does not apply well on this system because values correlation coefficient is low but the Langmuir isotherm applies on system adsorption isotherm because values correlation coefficient is high.

The Kinetic- thermodynamic adsorption isotherm is calculated using equation (1.40).

Figures (3.20), (3.21) and (3.22) were obtained by plotting $\ln \left(\frac{\theta}{1-\theta} \right)$ against $\ln C$ of equation (1.40). Tables (3.10), (3.11) and (3.12) show values of (y' , K_{ads} and R^2) produced from slope and intercept. Values of $y' > 1$ imply the formation of multilayers of inhibitor on the surface of metal. Values of $y' < 1$ mean a given inhibitor molecules will occupy more than one active site.

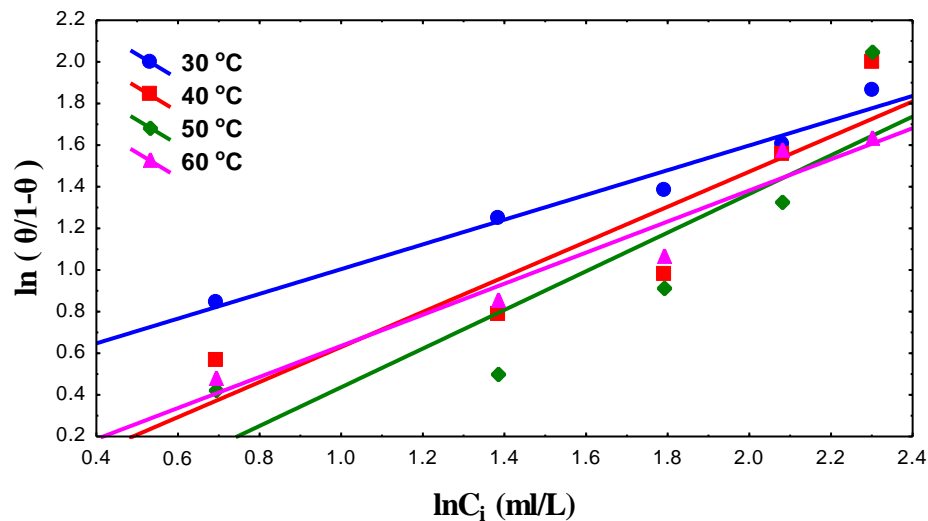


Fig.(3.20) Kinetic-thermodynamic adsorption isotherm of Citrus aurantium leaves extract on carbon steel in 0.5 M H_2SO_4 .

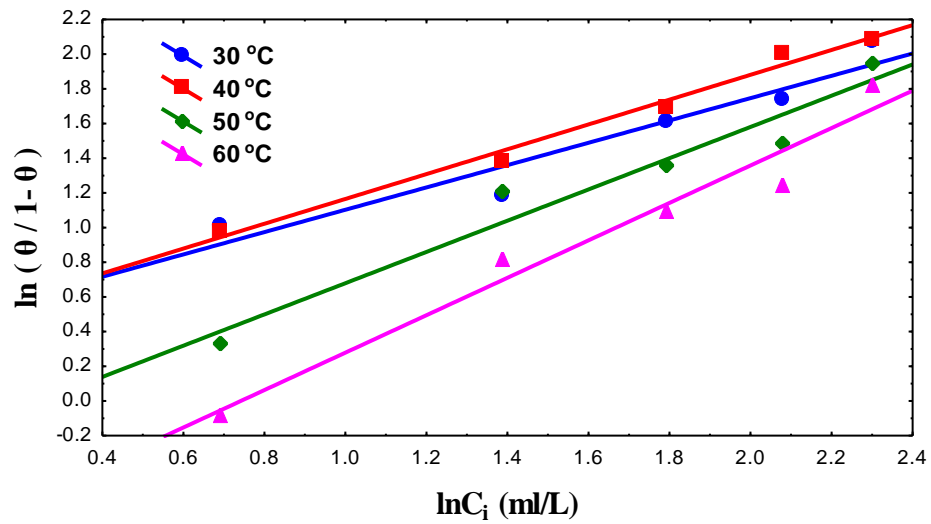


Fig.(3.21) Kinetic-thermodynamic adsorption isotherm of Citrus aurantium leaves extract on carbon steel in 1 M H_2SO_4 .

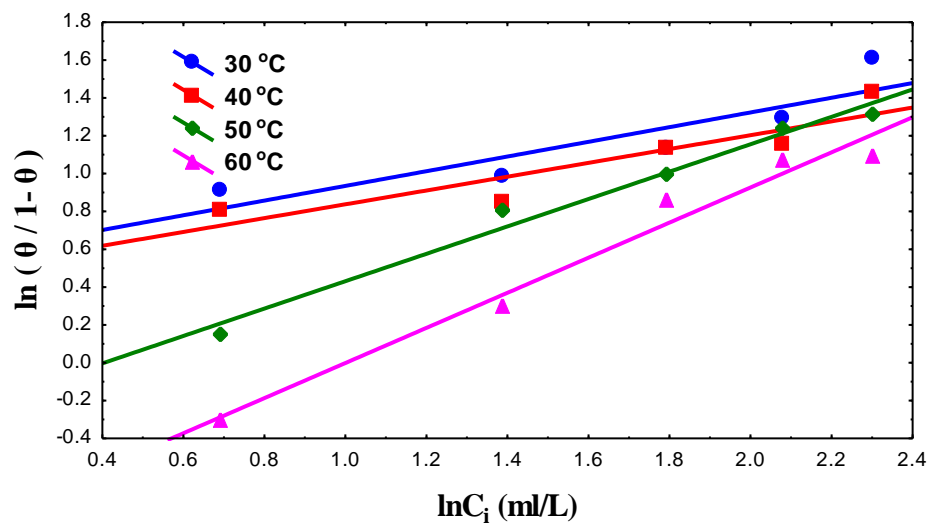


Fig.(3.22) Kinetic-thermodynamic adsorption isotherm of Citrus aurantium leaves extract on carbon steel in 1.5 M H_2SO_4 .

Table (3.10) Equilibrium constant, slope (y'), and correlation coefficient (R^2) for Kinetic-thermodynamic adsorption of the inhibitor on carbon steel in 0.5 M H_2SO_4 at different temperatures.

Temperature ($^{\circ}C$)	K_{ads} (L/ml)	y'	R^2
30	1.993	0.5942	0.9696
40	0.777	0.8424	0.8249
50	0.588	0.9288	0.7762
60	0.861	0.7467	0.9432

Table (3.11) Equilibrium constant, slope (y'), and correlation coefficient (R^2) for Kinetic-thermodynamic adsorption of the inhibitor on carbon steel in 1 M H_2SO_4 at different temperatures.

Temperature ($^{\circ}C$)	K_{ads} (L/ml)	y'	R^2
30	2.039	0.6438	0.9189
40	1.873	0.7158	0.9884
50	0.781	0.9010	0.9453
60	0.476	1.0793	0.9617

Table (3.12) Equilibrium constant, slope (y'), and correlation coefficient (R^2) for Kinetic-thermodynamic adsorption of the inhibitor on carbon steel in 1.5 M H_2SO_4 at different temperatures.

Temperature ($^{\circ}C$)	K_{ads} (L/ml)	y'	R^2
30	4.085	0.3883	0.7963
40	3.642	0.3653	0.8321
50	0.667	0.7239	0.9795
60	0.367	0.9280	0.9728

3.4 Thermodynamic Interpretation

Activation energies of carbon steel corrosion in (0.5, 1 and 1.5 M) H₂SO₄ in presence and absence of *Citrus aurantium leaves* extract are calculated from Arrhenius equation (1.19) by plotting the ln CR versus the reciprocal of absolute temperature data in tables (3.1, 3.2 and 3.3) give straight lines with slopes equal to $-E_a/R$. Figures (3.23), (3.24) and (3.25) show the Arrhenius plots and tables (3.1, 3.2 and 3.3) listing the activation energies. The estimated values of E_a for carbon steel corrosion in the presence of *Citrus aurantium leaves* extract in (0.5, 1 and 1.5 M) H₂SO₄ are listed in the tables (3.13), (3.14) and (3.15). Activation energy was found to be 46.120 kJ mol⁻¹ in the absence of the extract and increases to 53.150 kJ mol⁻¹ in the presence of *Citrus aurantium leaves* extract, and 49.583 kJ mol⁻¹ in the absence of the extract and increases to 69.580 kJ mol⁻¹ in the presence of *Citrus aurantium leaves* extract 56.511 kJ mol⁻¹ in the absence of the extract and increases to 77.135 kJ mol⁻¹ in the presence of *Citrus aurantium leaves* extract in (0.5, 1 and 1.5 M) H₂SO₄ acid respectively.

This shows that the adsorbed organic matter has provided a physical barrier to the charge and mass transfer, leading to a reduction in corrosion rate. It has been reported that the values of $E_a > 80$ kJ/mol indicates chemical adsorption whereas $E_a < 80$ kJ/mol refers to physical one [49,50]. In the present study, a physical adsorption mechanism is proposed since the values of the E_a are less than 80kJ/mol. observed from tables (3.13), (3.14) and (3.15), that the activation energy increased with increasing concentration of *Citrus aurantium leaves* extract and all values of E_a in the range of the studied concentration were higher than those of the uninhibited solution. The increase in E_a in the presence of *Citrus aurantium leaves* extract may be interpreted as due to physical adsorption or weak chemical bonding between the inhibitor species and the carbon steel surface resulted

into a decrease in the corrosion rate of the carbon steel [48]. E_a is in general higher in the presence of the inhibitors than its absence and consequently the rate of corrosion decreases because the presence of inhibitor layer causes the reaction happening constrains.

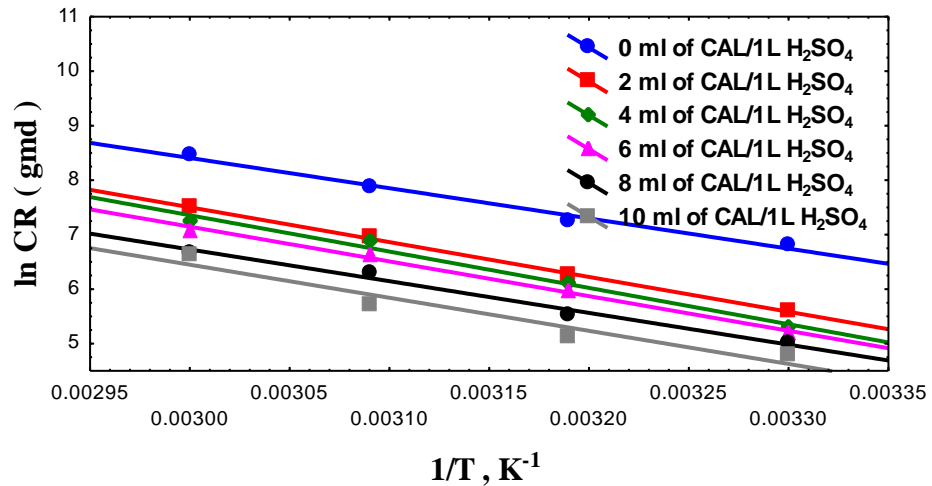


Fig.(3.23) Arrhenius plot of carbon steel corrosion in 0.5 M H_2SO_4 containing various concentrations of Citrus aurantium leaves extract at a temperature range of (30-60 °C).

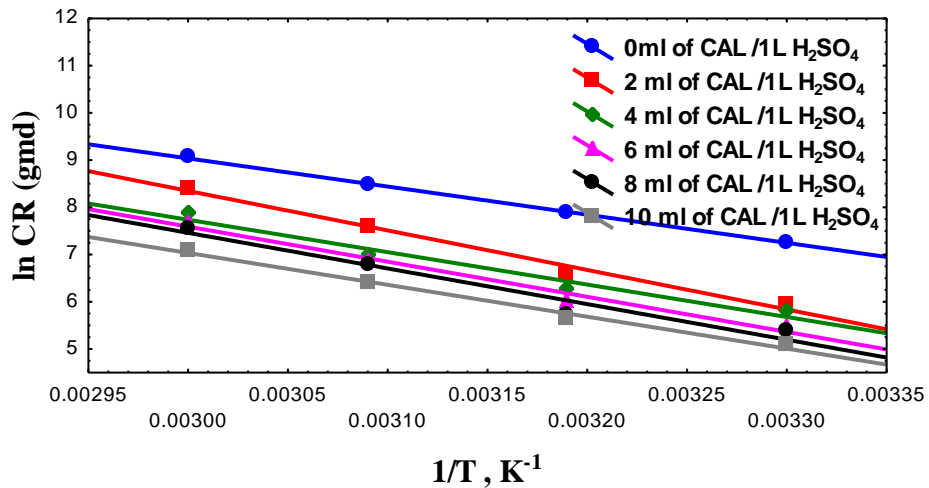


Fig.(3.24) Arrhenius plot of carbon steel corrosion in 1 M H_2SO_4 containing various concentrations of Citrus aurantium leaves extract at a temperature range of (30-60 °C).

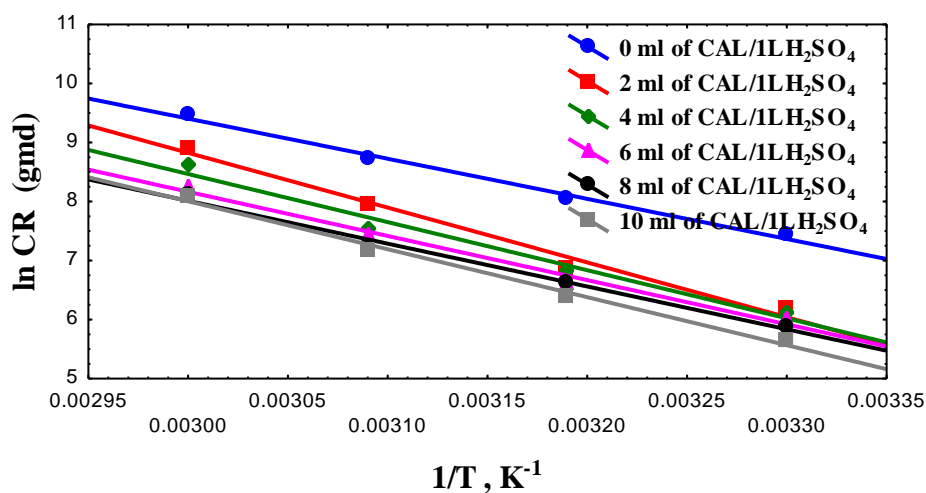


Fig.(3.25) Arrhenius plot of carbon steel corrosion in 1.5 M H_2SO_4 containing various concentrations of Citrus aurantium leaves extract at a temperature range of (30-60 °C).

Table (3.13) Values of activation energies for the corrosion of carbon steel in 0.5 M H_2SO_4 in presence and absence Citrus aurantium leaves extract as the corrosion inhibitor.

C_i (ml/L)	E_a (kJmol ⁻¹)
0	46.120
2	53.150
4	55.448
6	52.964
8	48.406
10	50.491

Table (3.14) Values of activation energies for the corrosion of carbon steel in 1 M H₂SO₄ in presence and absence of Citrus aurantium leaves extract as the corrosion inhibitor.

C_i (ml/L)	E_a (kJmol ⁻¹)
0	49.583
2	69.580
4	57.069
6	61.778
8	62.725
10	56.159

Table (3.15) Values of activation energies for the corrosion of carbon steel in 1.5 M H₂SO₄ in presence and absence of Citrus aurantium leaves extract as the corrosion inhibitor.

C_i (ml/L)	E_a (kJmol ⁻¹)
0	56.511
2	77.135
4	67.767
6	62.233
8	60.313
10	67.563

Experimental corrosion rates from weight loss measurements for carbon steel corrosion in 0.5, 1 and 1.5 M H₂SO₄ in the absence and presence of *Citrus aurantium leaves* extract were used to determine the enthalpy of activation and (ΔH^*) and entropy of activation (ΔS^*) for the formation of the activated complex from the transition state equation [51]. The enthalpy of activation (ΔH^*) and entropy of activation (ΔS^*) were calculated using

equation (1.24). So a Plot of $\ln CR/T$ versus $1/T$ is shown in (figures 3.26, 3.27, and 3.28), where straight lines obtained with slopes of $(-\Delta H^*/R)$ and intercepts of $\{\ln(R/Nh) + (\Delta S^*/R)\}$, from which ΔH^* and ΔS^* were calculated and listed in tables (3.16, 3.17 and 3.18). The results show that the enthalpy of activation values were all positive for *Citrus aurantium leaves* extract which reflects the endothermic nature of the carbon steel dissolution process. Also, the entropies of activation were positive indicating that the activation complex represents association steps and that the reaction was spontaneous and feasible. These results were in excellent agreement with Blaedel and Meloche [52].

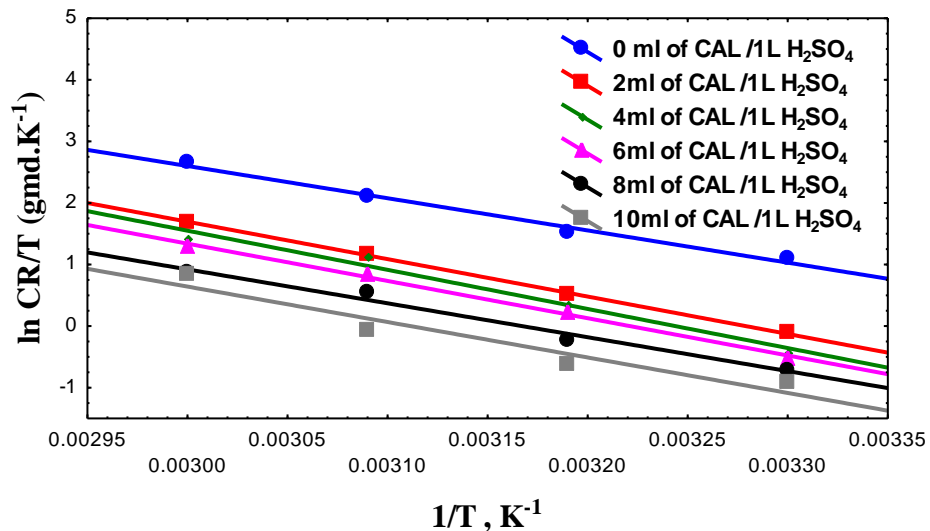


Fig.(3.26) Transition state plot for carbon steel corrosion in 0.5 M H₂SO₄ in absence and presence of different concentrations of Citrus aurantium leaves extract.

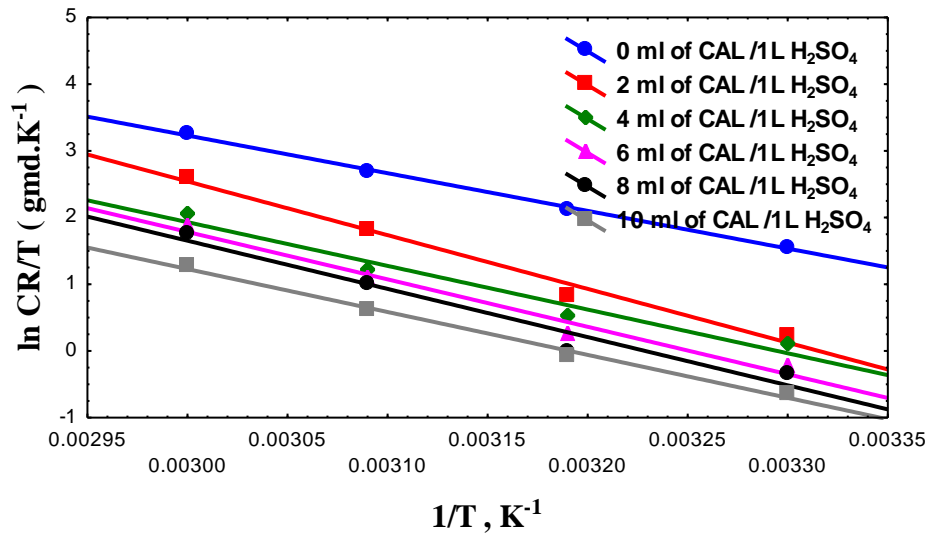


Fig.(3.27) Transition state plot for carbon steel corrosion in 1 M H_2SO_4 in absence and presence of different concentrations of Citrus aurantium leaves extract.

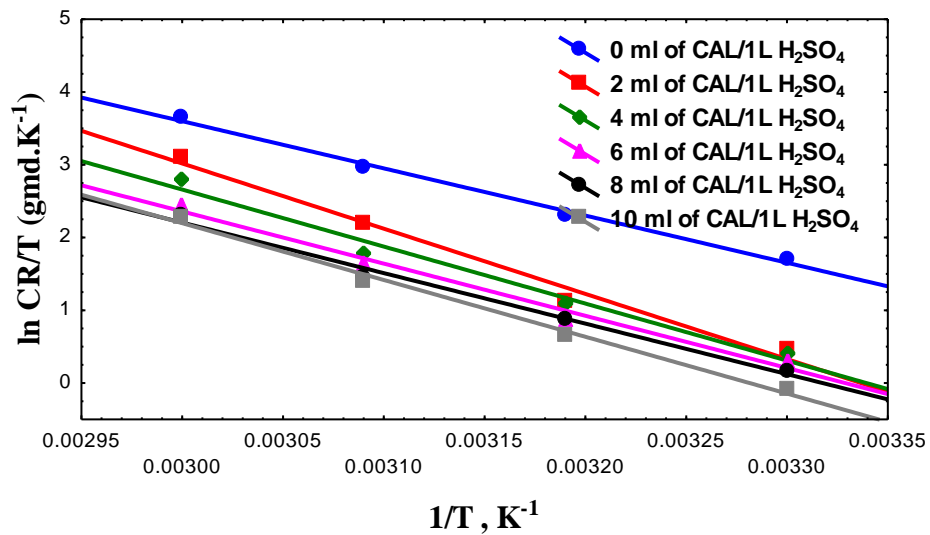


Fig.(3.28) Transition state plot for carbon steel corrosion in 1.5 M H_2SO_4 in absence and presence of different concentrations of Citrus aurantium leaves extract.

Table (3.16) Enthalpy and Entropy of activation values of the corrosion reaction with various concentrations of Citrus aurantium leaves extract in 0.5 M H₂SO₄.

Ci (ml/L)	ΔH^* (kJ mol⁻¹)	ΔS^* (kJ mol⁻¹K⁻¹)
0	43.507	0.134683
2	50.538	0.148256
4	52.835	0.153931
6	50.351	0.144730
8	45.794	0.127580
10	47.879	0.131515

Table (3.17) Enthalpy and Entropy of activation values of the corrosion reaction with various concentrations of Citrus aurantium leaves extract in 1 M H₂SO₄.

Ci (ml/L)	ΔH^* (kJ mol⁻¹)	ΔS^* (kJ mol⁻¹K⁻¹)
0	46.976	0.150327
2	66.982	0.204621
4	54.479	0.162033
6	59.145	0.174817
8	60.077	0.176516
10	53.504	0.153261

Table (3.18) Enthalpy and Entropy of activation values of the corrosion reaction with various concentrations of Citrus aurantium leaves extract in 1.5 M H₂SO₄.

Ci (ml/L)	ΔH^* (kJ mol ⁻¹)	ΔS^* (kJ mol ⁻¹ K ⁻¹)
0	53.914	0.1742
2	74.503	0.231139
4	65.136	0.200056
6	59.625	0.181028
8	57.713	0.174310
10	64.904	0.195522

3.5 Kinetics Interpretation

In order to determine the order of the corrosion reaction of carbon steel in H₂SO₄ equations (3.3 and 3.5) were used for the zero, first model respectively. In addition to that equations (3.4 and 3.6) were used to calculate the half-life of the corrosion reaction for the same models. Tables (3.19), (3.20) and (3.21) shows the results of the zero and first order kinetic at two temperature 40 and 60 °C in presence and absence of inhibitor solution at different times (1, 2, 3, and 4 h).

$$\Delta W = k_0 t \quad \dots\dots\dots (3.3)$$

$$t_{1/2} = \frac{a}{2 k_0} \quad \dots\dots\dots (3.4)$$

$$\ln \left(\frac{W_1}{W_2} \right) = k_1 t \quad \dots\dots\dots (3.5)$$

$$t_{1/2} = \frac{0.693}{k_1} \quad \dots\dots\dots (3.6)$$

Where; ΔW is weight loss in grams, a is initial weight of carbon steel, k_0 and k_1 are rate constant in ($\text{g/m}^2 \text{ h}$ and $1/\text{h}$) respectively, $t_{1/2}$ is half-life in h.

From equation (3.3) a plot of ΔW against (t) is shown in figures (3.29), (3.30) and (3.31) with slope yield the value of k_0 and tables (3.19), (3.20) and (3.21) shows values of k_0 , $t_{1/2}$ and correlation coefficient R^2 in zero order.

From equation (3.5) a plot of $\ln W_1/W_2$ against (t) is shown in figures (3.32), (3.33) and (3.34) with slope yield the value of k_1 and tables (3.22), (3.23) and (3.24) shows values of k_1 , $t_{1/2}$ and correlation coefficient R^2 in first order. The reaction rates can also be expressed in terms of half-life period $t_{1/2}$. Since values of $t_{1/2}$ decreases with increases of temperature and increases with inhibitor concentration, this mean that metal consume its half original weight as temperature of acid increased. Furthermore, the presence of *CAL* raises the values of $t_{1/2}$ [53].

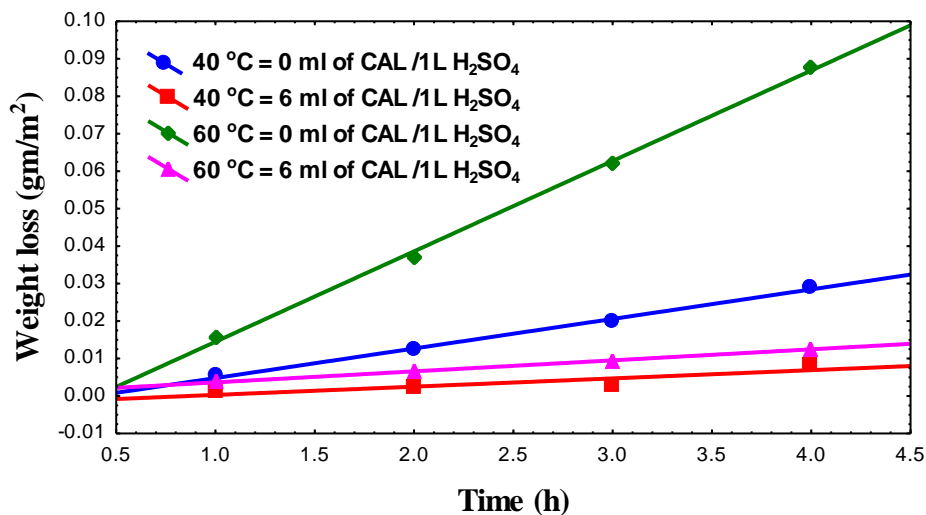


Fig.(3.29) Weight loss against time for carbon steel corrosion in 0.5 M H₂SO₄ in presence and absence of Citrus aurantium leaves extract at (40 and 60 °C).

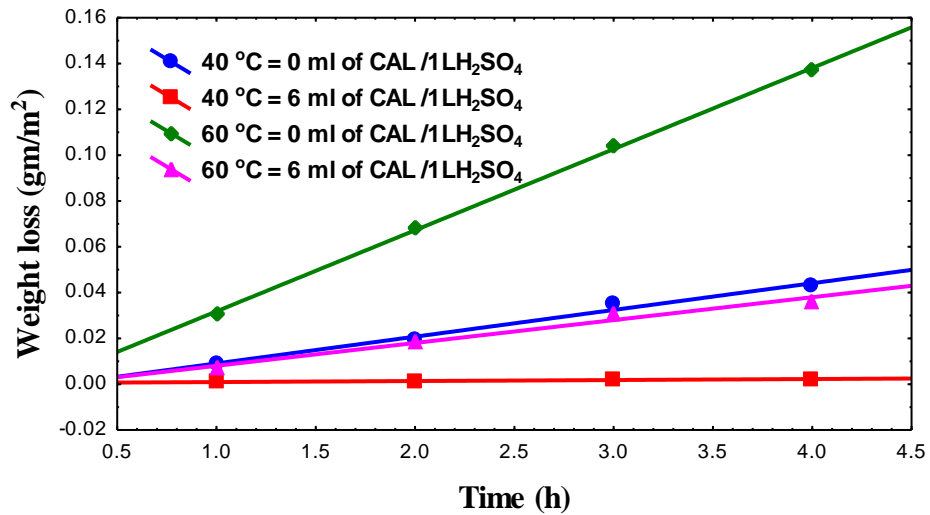


Fig.(3.30) Weight loss against time for carbon steel corrosion in 1 M H₂SO₄ in presence and absence of Citrus aurantium leaves extract at (40 and 60 °C).

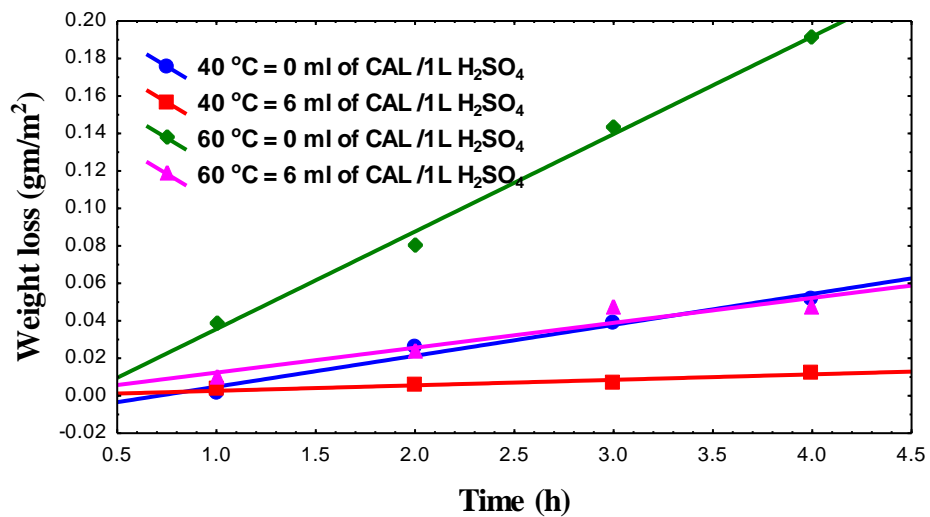


Fig.(3.31) Weight loss against time for carbon steel corrosion in 1.5 M H₂SO₄ in presence and absence of Citrus aurantium leaves extract at (40 and 60 °C).

Table (3.19) Rate constant values, half-life and correlation coefficient (R^2) at different temperatures in presence and absence of inhibitor in 0.5 M H_2SO_4 .

Conditions	k_0 (g/m ² h)	$t_{1/2}$ (h)	R^2
40, °C = 0 ml/L	0.0079	200.9	0.9955
40, °C = 6 ml/L	0.0022	409.5	0.8345
60, °C = 0 ml/L	0.0241	88.435	0.9976
60, °C = 6 ml/L	0.0029	192.758	0.9997

Table (3.20) Rate constant values, half-life and correlation coefficient (R^2) at different temperatures in presence and absence of inhibitor in 1 M H_2SO_4 .

Conditions	k_0 (g/m ² h)	$t_{1/2}$ (h)	R^2
40, °C = 0 ml/L	0.012	202	0.9922
40, °C = 6 ml/L	0.002	435	0.9985
60, °C = 0 ml/L	0.036	42.5	0.9993
60, °C = 6 ml/L	0.011	87.6	0.9932

Table (3.21) Rate constant values, half-life and correlation coefficient (R^2) at different temperatures in presence and absence of inhibitor in 1.5 M H_2SO_4 .

Conditions	k_0 (g/m ² h)	$t_{1/2}$ (h)	R^2
40, °C = 0 ml/L	0.0165	99.5	0.9673
40, °C = 6 ml/L	0.0029	200	0.9265
60, °C = 0 ml/L	0.052	30.10	0.9946
60, °C = 6 ml/L	0.0133	60.22	0.8913

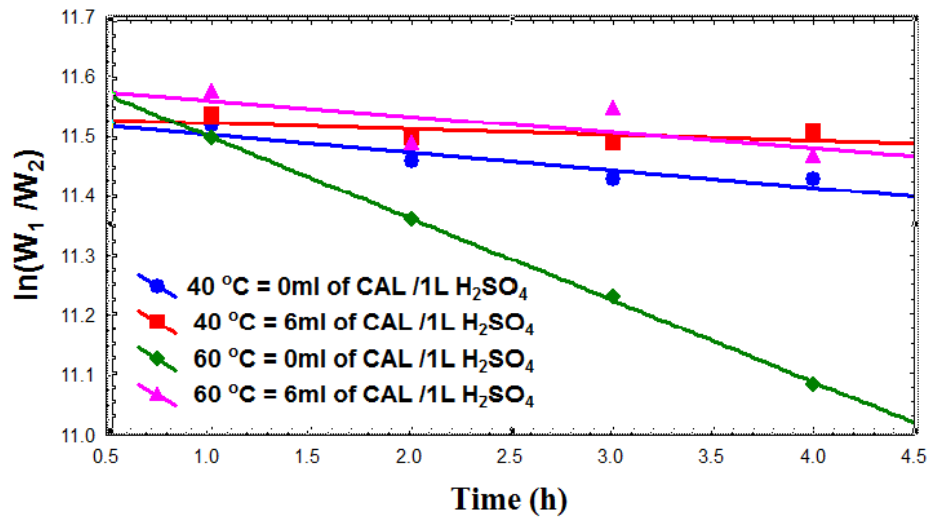


Fig.(3.32) Plot of $\ln(W_1/W_2)$ against time for carbon steel corrosion in 0.5 M H₂SO₄ in presence and absence of Citrus aurantium leaves extract at (40 and 60 °C).

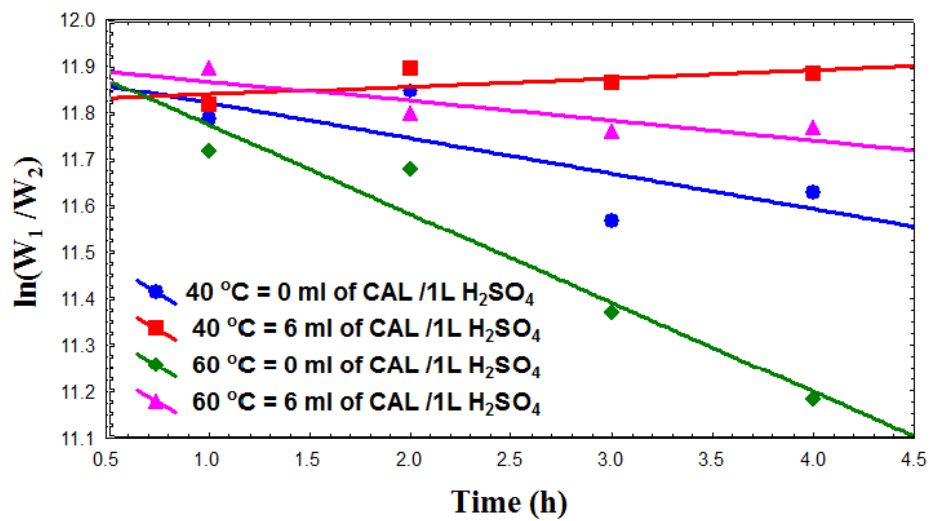


Fig.(3.33) Plot of $\ln(W_1/W_2)$ against time for carbon steel corrosion in 1 M H₂SO₄ in presence and absence of Citrus aurantium leaves extract at (40 and 60 °C).

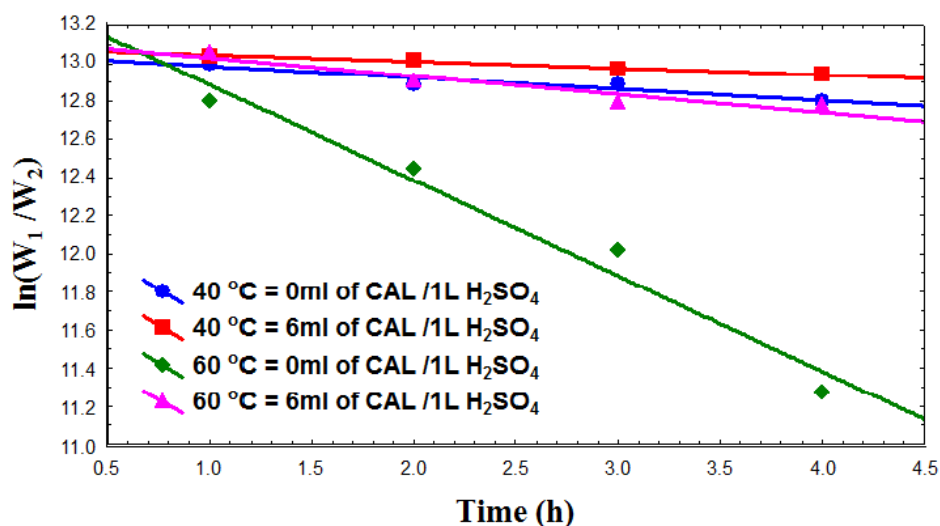


Fig.(3.34) Plot of $\ln(W_1/W_2)$ against time for carbon steel corrosion in 1.5 M H_2SO_4 in absence and presence of Citrus aurantium leaves extract at (40 and 60 °C).

Table (3.22) Rate constant values, half-life and correlation coefficient (R^2) at different temperatures in presence and absence of inhibitor in 0.5 M H_2SO_4 .

Conditions	k_1 (1/h)	$t_{1/2}$ (h)	R^2
40, °C = 0 ml/L	0.03	23.1	0.8333
40, °C = 6 ml/L	0.01	69.3	0.351
60, °C = 0 ml/L	0.139	4.9	0.9993
60, °C = 6 ml/L	0.027	25.6	0.4629

Table (3.23) Rate constant values, half-life and correlation coefficient (R^2) at different temperatures in presence and absence of inhibitor in 1 M H_2SO_4 .

Conditions	k_1 (1/h)	$t_{1/2}$ (h)	R^2
40, °C = 0 ml/L	0.076	9.11	0.5554
40, °C = 6 ml/L	0.018	38.5	0.4263
60, °C = 0 ml/L	0.193	3.59	0.9337
60, °C = 6 ml/L	0.043	16.11	0.7532

Table (3.24) Rate constant values, half-life and correlation coefficient (R^2) at different temperatures in presence and absence of inhibitor in 1.5 M H_2SO_4 .

Conditions	k_1 (1/h)	$t_{1/2}$ (h)	R^2
40, °C = 0 ml/L	0.06	11.55	0.8955
40, °C = 6 ml/L	0.035	19.8	0.9761
60, °C = 0 ml/L	0.502	1.38	0.9671
60, °C = 6 ml/L	0.096	7.21	0.8982

3.6 Inhibitor Compositions and Fourier Transform Infrared Interpretation

Fourier transform infrared analysis have been used to obtain some understanding into the possible interactions between the adsorbed inhibitor and mild steel surface in acidic environment of 0.5 M H_2SO_4 with 10ml/L *Citrus aurantium leaves* extract (Liquid). The strength of the inhibition depends on the molecular structure of the inhibitor. The main constituent of *Citrus aurantium leaves* extract is alcohol groups such as (Linalool, $C_{10}H_{18}O$). The FTIR spectrum of *Citrus aurantium leaves* extract is shown in (figures 3.35.a, 3.36 and 3.37). The alcohol O-H stretching appeared at 3408 cm^{-1} . The peak at 2065 cm^{-1} can be assigned to aliphatic C-H. The aliphatic C=C stretching frequency appeared at 1637 cm^{-1} . The C-O stretching frequency appeared at ($1211, 1101$ and 1051 cm^{-1}). The FTIR spectrum of the protective film formed on the surface of the metal after immersion in 0.5 M H_2SO_4 is shown in (figure 3.35.b). It is found that, almost all the peaks observed for *Citrus aurantium leaves* extract are also noticed for C-steel immersed in 0.5 M H_2SO_4 containing 10 ml/L of *Citrus aurantium leaves* extract. Alcohol O-H stretching has shifted from 3408 to 3402 cm^{-1} . The aliphatic C=C stretching shifted from 1637 to 1630 cm^{-1} . The C-O stretching frequency has been shifted from 1211 to 1203 cm^{-1} .

The aliphatic C-H stretching frequency has been shifted from 2065 to 2054 cm^{-1} orbital to which indicates the formation of Iron extract complex. The band at 592 cm^{-1} probably originates or due to Fe_2O_3 [35]. The alcohol groups would donate electrons to the metal unoccupied molecular achieve its noble state. Which indirectly retard further redox reaction and could resist metal from corrosion attack.

Table (3.25) Groups active values stretching frequency in alcohol.

Groups active	stretching frequency
O-H	3408 to 3402 cm^{-1}
C=C	1637 to 1630 cm^{-1}
C-O	1211 to 1203 cm^{-1}
C-H	2065 to 2054 cm^{-1}

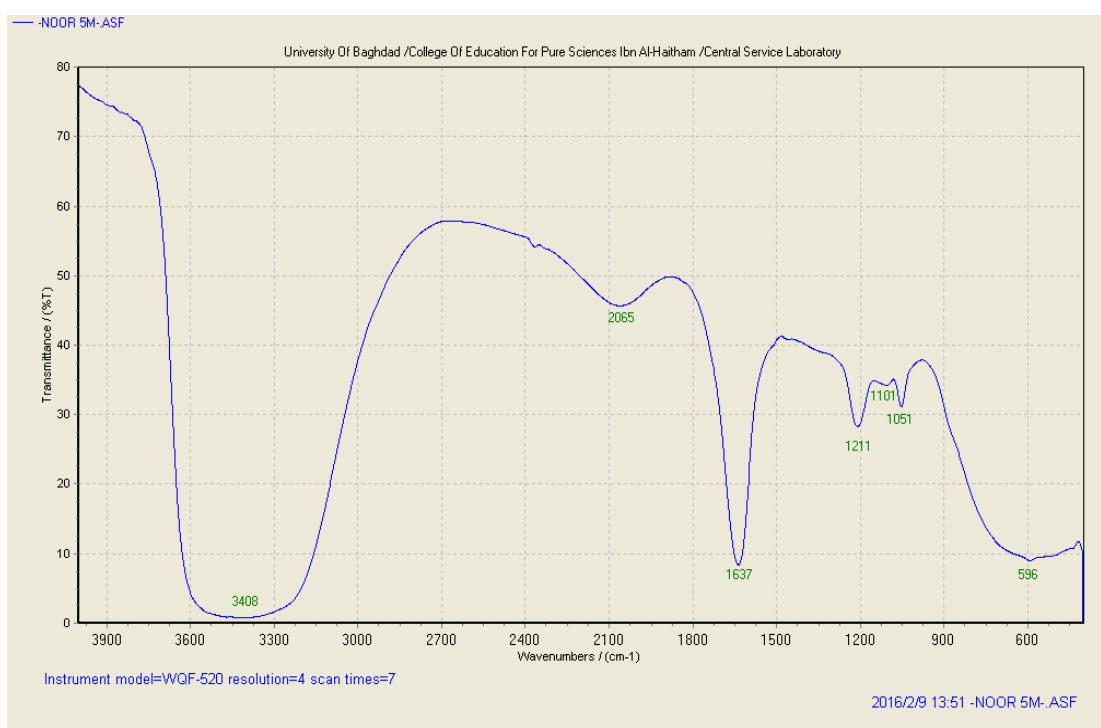


Fig.(3.35.a) FTIR spectrum of Citrus aurantium leaves extracted with 0.5 M H_2SO_4 .

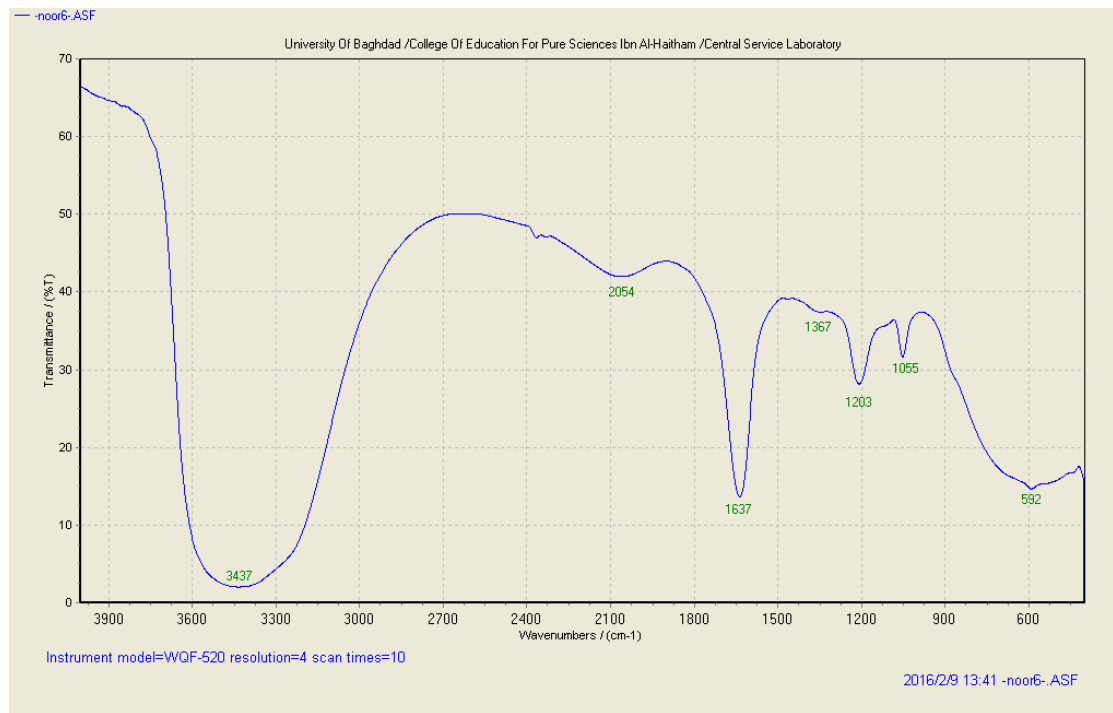


Fig.(3.35.b) FTIR spectrum of the protective film formed on the surface of the metal after immersion in 0.5 M H₂SO₄.

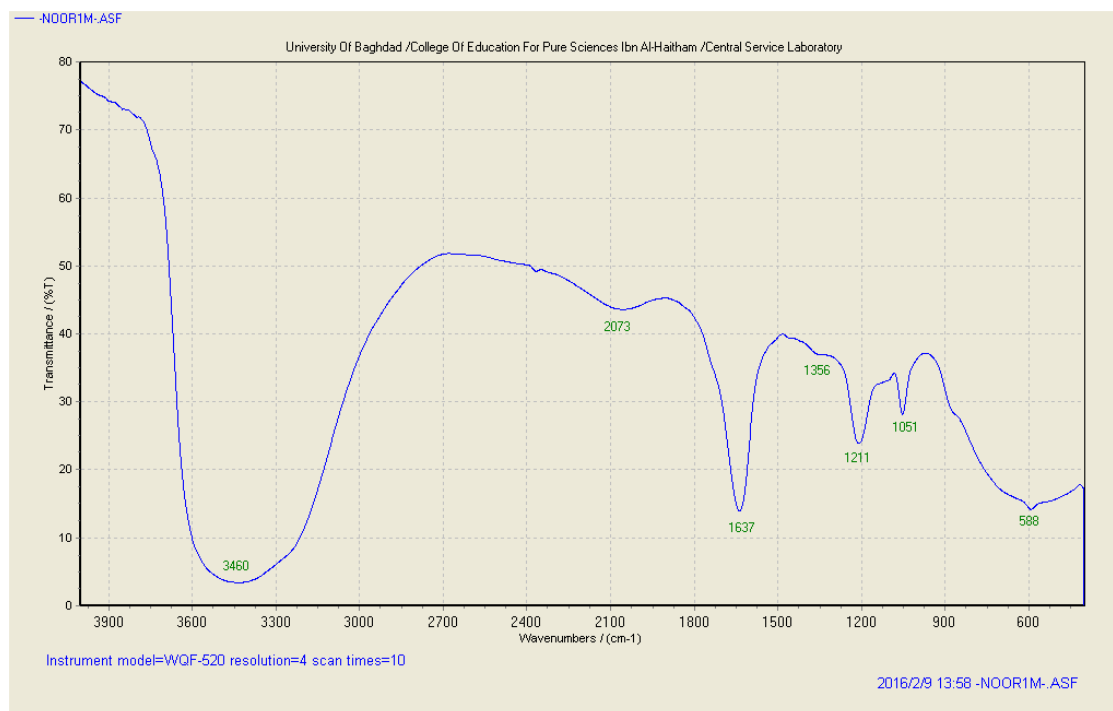


Fig.(3.36) FTIR spectrum of Citrus aurantium leaves extracted with 1 M H₂SO₄.

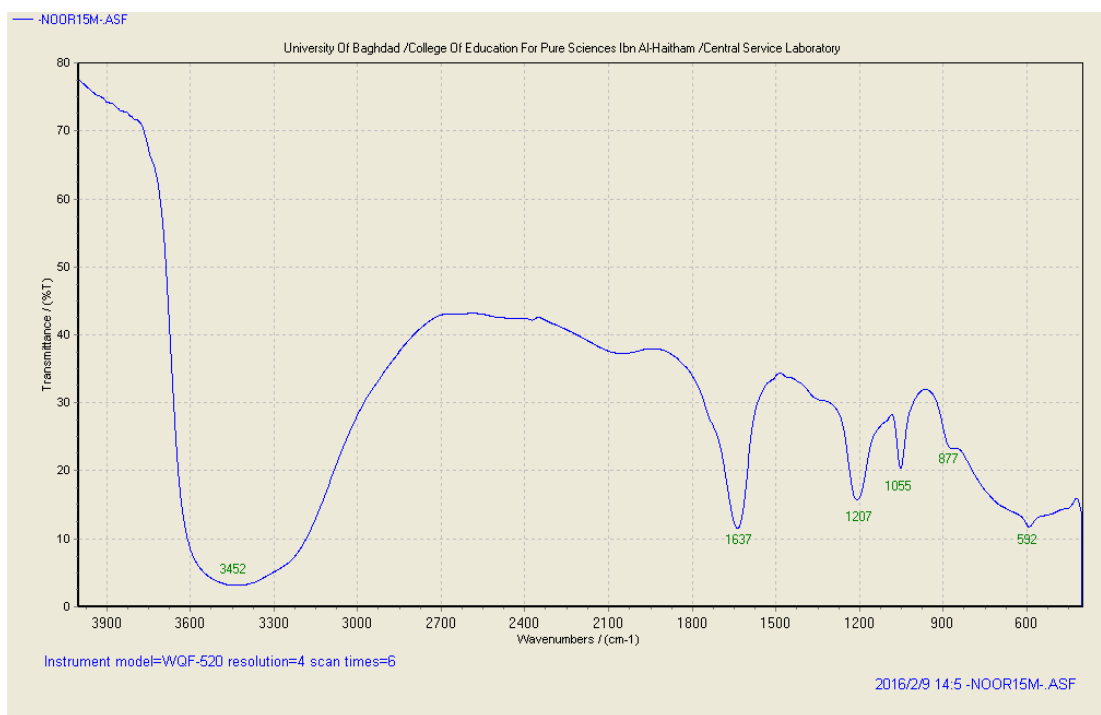


Fig.(3.37) FTIR spectrum of Citrus aurantium leaves extracted with 1.5 M H₂SO₄.

3.7 Scanning Electron Microscope Interpretation

The scanning electron images were taken in order to support the findings of present work. The polished specimens immersed for 3h in the blank 1 M H₂SO₄ and in presence of *CAL* for 3h at 30 °C were observed under a SEM and are images shown in (figure 3.38a, b and c), and (figure 3.39 a, b and c) at a temperature of 60 °C. (Figure 3.38 a) shows the polished mild steel surface before exposure to the corrosion solution, which is associated with the polishing scratches. It is clear from the (figure 3.38 b), that the surface of the carbon steel was heavily corroded in 1 M H₂SO₄, whereas in the presence of inhibitor in 1 M H₂SO₄, the surface condition was comparatively better as in (figure 3.38 c) and this depends on the concentration of the inhibitor solution suggesting that the presence of *CAL* protect the metal surface via formation of adsorbed layer on it [35].

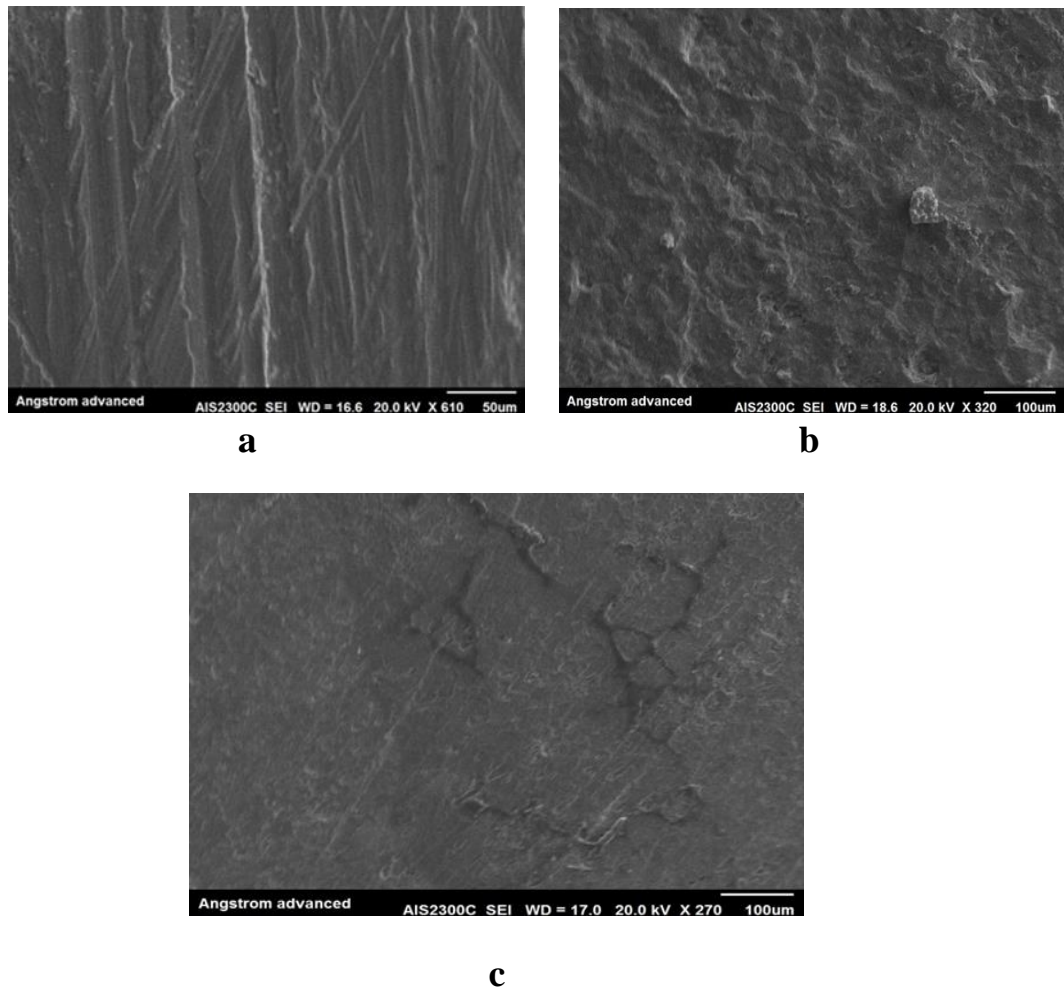


Fig.(3.38) SEM images of carbon steel surface (a) before immersion in 1 M H_2SO_4 at 30 °C for 3h (b) after immersion in 1 M H_2SO_4 at 30 °C for 3h (c) after immersion in 1 M H_2SO_4 at 30 °C for 3h and in presence of CAL.

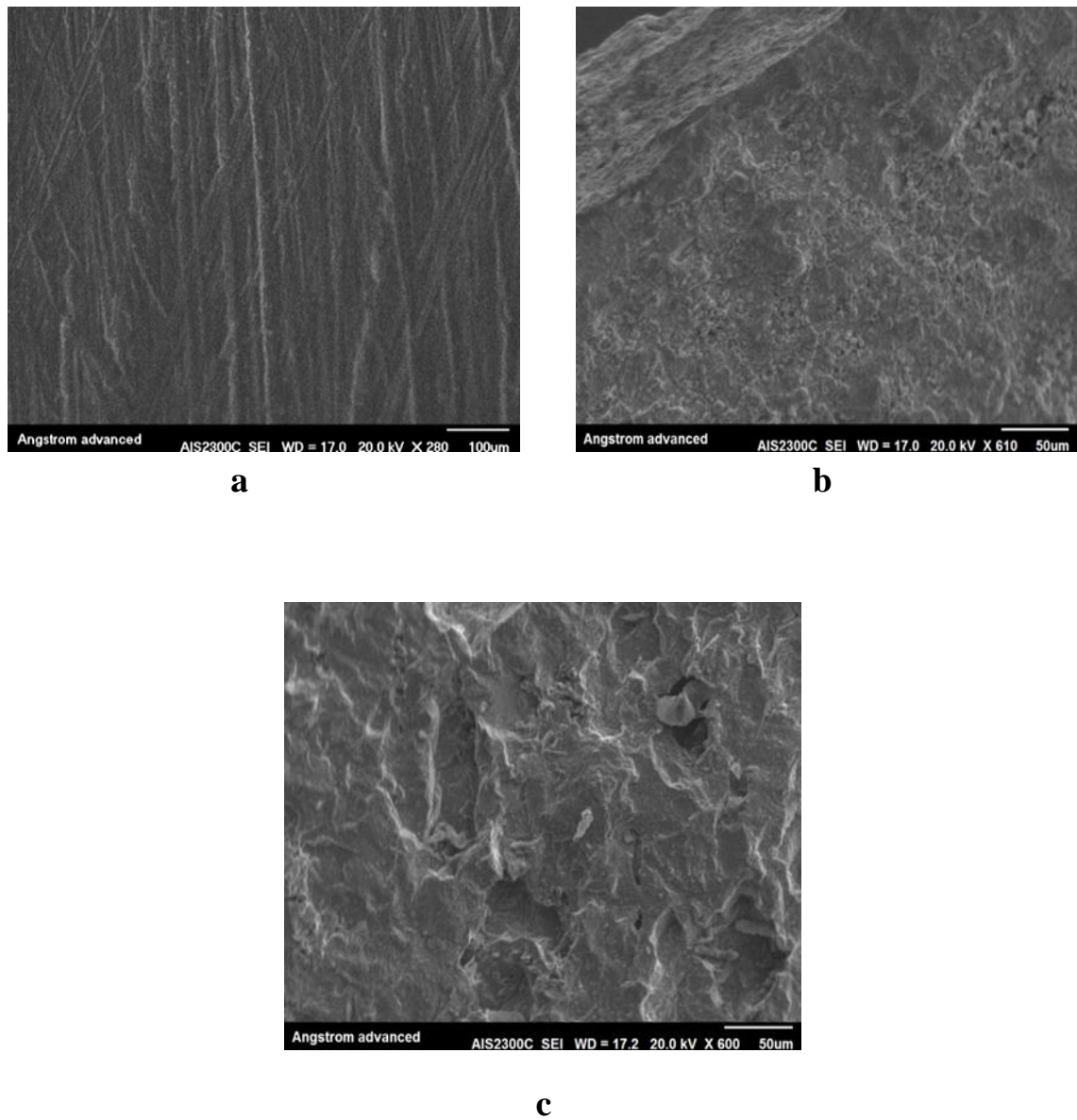


Fig.(3.39) SEM images of carbon steel surface (a) before immersion in 1 M H_2SO_4 at 60 °C for 3h (b) after immersion in 1 M H_2SO_4 at 60 °C for 3h (c) after immersion in 1 M H_2SO_4 at 60 °C for 3h and in presence of CAL.

3.8 Quantum Chemical Interpretation:

Linalool represent the most effective component of *CAL* [16, 17]. Quantum chemical calculations are proven to be a very powerful tool to know the inhibition mechanism and to emphasis the experimental data. Through the method of quantum chemical calculations, the structural parameters, such as the frontier molecular orbital, HOMO (highest occupied molecular orbital) and LUMO (lowest unoccupied molecular orbital), dipole moment (d), the fraction of electrons (ΔN) transfer from inhibitors to metal surface, and other quantum parameters were calculated and correlated. The optimized minimum energy geometrical configurations of test compounds are given in (figure 3.40). The computed quantum chemical parameters are summarized in (table 3.25). It has been well documented in literature that higher the value of E_{HOMO} of the inhibitor, greater is the ease of inhibitor to offer electrons to unoccupied d orbital of metal atom and higher is the inhibition efficiency of the inhibitor. Further lower the E_{LUMO} , easier is the acceptance of electrons from metal atom to form feedback bonds. The gap between HOMO–LUMO energy levels of molecules was another important parameter that needs to be considered. Smaller the value of ΔE of an inhibitor, higher is the inhibition efficiency of that inhibitor. Further higher values of dipole moment will favor the enhancement of corrosion inhibition [54]. The dipole moment values stands in the approximately same order that support our findings. Values of X and η were calculated by using the values of ionization potential (IP) and electron affinity (EA) obtained from quantum chemical calculation in equations (1.13) and (1.14) respectively. The fraction of electrons transferred from inhibitor to the iron molecule (ΔN) was calculated in equation (1.17). According to other reports [18], value of ΔN showed inhibition effect resulted from electrons donation.

In this study, The *CAL* was the donators of electrons while the carbon steel surface was the acceptor. These components were bound to the carbon steel surface, and thus formed a protective inhibition adsorption film.

Table (3.26) Quantum chemical parameters for most important components of CAL.

Component	Linalool (C ₁₀ H ₁₈ O)
E _{HOMO} (ev)	- 9.37
E _{LUMO} (ev)	- 0.38
IP	9.37
EA	0.38
X	4.875
η	4.495
σ	0.22
ω	2.64
ΔN	0.24
ΔE (ev)	8.99
Debye	1.22

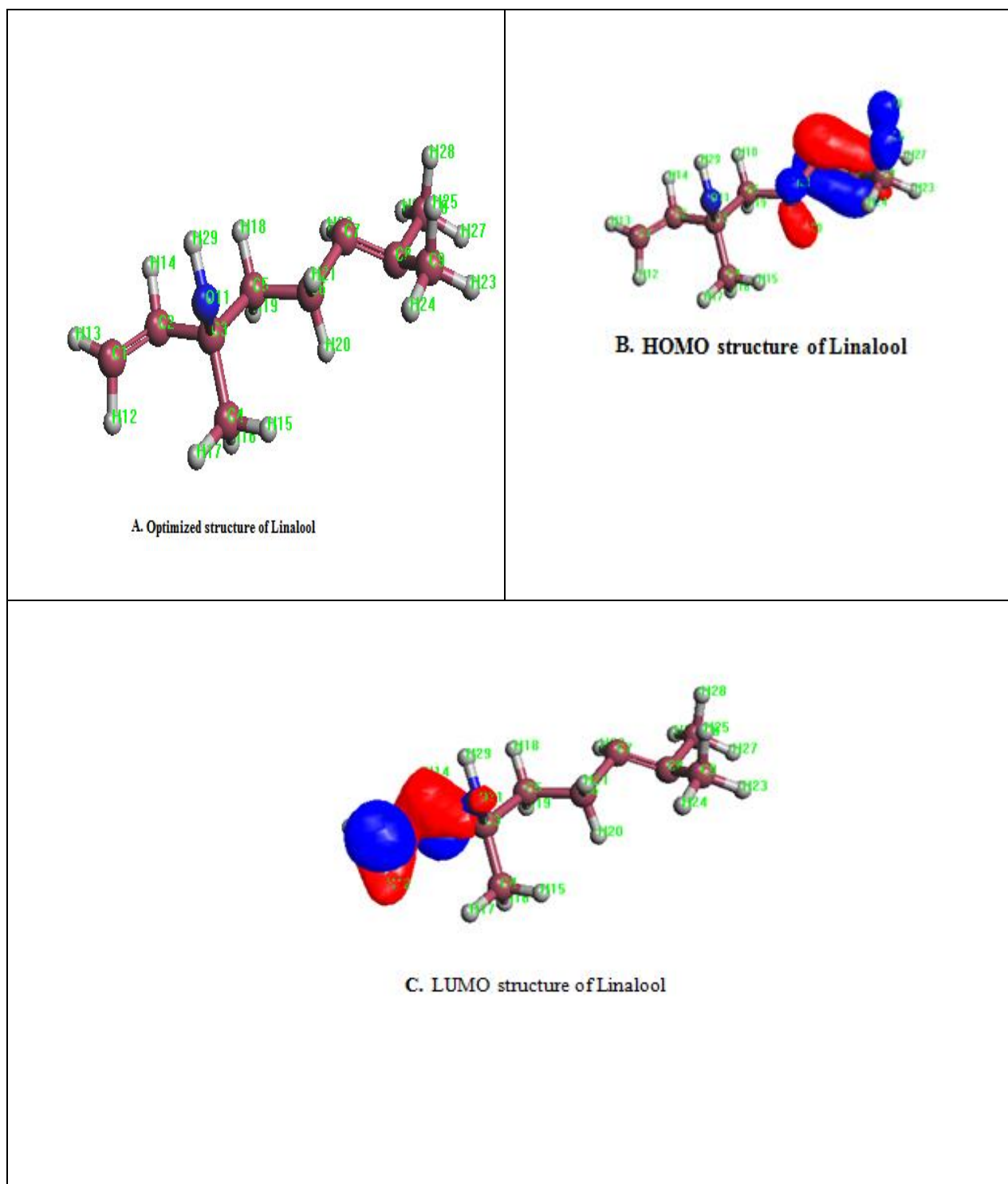


Fig. (3.40) A: Optimized geometry of linalool, B: HOMO distribution, C: LUMO distribution.

3.9 Mathematical and Modelling Studies

Tables (3.1, 3.2 and 3.3) show the results of 72 test runs using weight loss technique of carbon steel corrosion as a function of temperature and acid concentration in the absence and presence of *Citrus aurantium leaves* extract as corrosion inhibitor. (Figures 3.41 and 3.42) show a surface plots for corrosion rate as a function of different variables. Corrosion rate increased with temperature and acid concentration, and decreased with addition of inhibitor. Temperature increases the rate of almost all-chemical reactions. When corrosion is controlled by diffusion of oxygen, the corrosion rate at given oxygen concentration approximately doubles for every 30 °C rise in temperature [55]. When corrosion is attended by hydrogen evolution, which is the case of present work, the rate increasing is more than double for every 30°C rise in temperature [4]. Like most chemical reactions, the rate of corrosion of carbon steel in acids solutions increases with increasing of temperature [56]. The greatest effect of temperature is attained by activation-controlled processes. Molarity as the concentration of corrosive H₂SO₄ solutions is increased, the corrosion rate likewise increased. This is primarily due to the fact that the amounts of hydrogen ions, which are the active species, are increased, as acid concentration increased. Addition of *Citrus aurantium leaves* extract as corrosion inhibitor reduces the corrosion rate. This can be achieved by formation of protective layer on metal surface. The layer can adsorbed on anodic, or cathodic, or both sites on metal surface [57]. Corrosion rates as a function of different variables can be correlated in the formula of mathematical equations. Several mathematical models were suggested to represent the corrosion rate data. The models are divided into two groups. The linear and polynomial models. The linear models are:

$$\text{Linear model } y = \alpha + \sum_{i=1}^{i=n} \beta_i \chi_i + \sum_{i=1}^{i=n} \varepsilon_i \dots\dots\dots(3.7)$$

$$\text{Linear-Logarithmic model } y = \alpha + \sum_{i=1}^{i=n} \beta_i \log \chi_i + \sum_{i=1}^{i=n} \varepsilon_i \dots\dots\dots (3.8)$$

$$\text{Logarithmic - Linear model } \log y = \alpha + \sum_{i=1}^{i=n} \beta_i \chi_i + \sum_{i=1}^{i=n} \varepsilon_i \dots\dots\dots (3.9)$$

The second order polynomial model also suggested. This model takes into account the individual effect of each variables and the interaction between them. Polynomial – individual effect model

$$y = \alpha + \sum_{i=1}^{i=n} \beta_i \chi_i + \sum_{i=1}^{i=n} \beta_i \chi_i^2 + \sum_{i=1}^{i=n} \varepsilon_i \dots\dots\dots (3.10)$$

Polynomial – interaction effect model

$$y = \alpha + \sum_{i=1}^{i=n} \beta_i \chi_i + \sum_{i=1, j=1}^{i=n, j=1} \beta_i \chi_i \chi_j + \sum_{i=1}^{i=n} \beta_i \chi_i^2 + \sum_{i=1}^{i=n} \varepsilon_i \dots\dots\dots (3.11)$$

Where; y is corrosion rate (g.m⁻².day⁻¹, gmd), x₁ is inhibitor concentration (M), x₂ is temperature (°C), x₃ is acid concentration (M), n is number of variables, ε is standard error, α and β are constants.

Mathematical modeling can be used as a tool of predication corrosion rate as a function of different variables surface [58]. Equations (3.7 to 3.11) can be expanded and regression has been carried out to evaluate the coefficients of these equations. STATISTICA 7 software was used to estimate the coefficients. This software was based on Levenberg-Marquardt non-linear estimation least squares method. Maximum number of iteration was 1000, confidence level 95%, and convergence criterion was 1×10⁻⁶. The expanded equations can be rewritten as:

$$y = \alpha + \beta_1 x_1 + \beta_2 x_2 + \beta_3 x_3 + \varepsilon_{total} \dots\dots\dots (3.7a)$$

$$y = \alpha + \beta_1 \log x_1 + \beta_2 \log x_2 + \beta_3 \log x_3 + \varepsilon_{total} \dots\dots\dots (3.8a)$$

$$\log y = \alpha + \beta_1 x_1 + \beta_2 x_2 + \beta_3 x_3 + \varepsilon_{total} \dots\dots\dots (3.9a)$$

$$y = \alpha + \beta_1 \chi_1 + \beta_2 \chi_2 + \beta_3 \chi_3 + \beta_4 \chi_1^2 + \beta_5 \chi_2^2 + \beta_6 \chi_3^2 + \varepsilon_{total} \dots (3.10a)$$

$$y = \alpha + \beta_1 \chi_1 + \beta_2 \chi_2 + \beta_3 \chi_3 + \beta_4 \chi_1^2 + \beta_5 \chi_2^2 + \beta_6 \chi_3^2 + \beta_7 \chi_1 \chi_2 + \beta_8 \chi_1 \chi_3 + \beta_9 \chi_2 \chi_3 + \varepsilon_{total} \dots (3.11a)$$

The numerical values of these coefficients, standard errors, and correlation coefficients were listed in (tables 3.26 and 3.27). These equations represent the corrosion rate data with high correlation coefficients. The best fitting was obtained with Logarithmic – Linear model ($R^2=0.957$, average standard error = 0.0348) and Polynomial – interaction effect model ($R^2=0.954$, average standard error = 481.472) show in figures (3.43) and (3.44). It is clear that the lowest standard error was obtained via regression of Logarithmic – Linear model. The values of correlation coefficient (R^2) were almost the same. Generally, correlation coefficient up to 0.30 indicates a poor relationship and is of uncertain validity; between 0.50 and 0.70 indicates a significant relationship and is of practical importance; while above 0.90 means a strong relationship [58].

Table (3.27) Linear models analysis

Coefficient	Linear model		Linear–Logarithmic model		Logarithmic–Linear model	
	Value	ε	Value	ε	Value	ε
α	- 3404.54	847.01	-9897.10	1719.674	1.39	0.089
β_1	-308.60	49.26	-1627.95	467.377	-0.08	0.005
β_2	107.92	15.05	7526.98	1026.549	0.03	0.002
β_3	1778.72	412.13	3021.73	585.677	0.54	0.043
R^2	0.785		0.789		0.957	

Table (3.28) Polynomial models analysis

Coefficient	Polynomial – individual effect model		Polynomial – interaction effect model	
	Value	ϵ	Value	ϵ
α	5303.116	3057.165	6043.10	2058.416
β_1	-923.876	152.499	109.06	147.500
β_2	-251.884	132.098	-290.60	80.122
β_3	1079.492	2504.331	-3822.97	1713.790
β_4	61.528	14.638	61.53	8.545
β_5	3.998	1.461	4.00	0.853
β_6	349.617	1239.322	349.62	723.440
β_7	-	-	-18.50	2.233
β_8	-	-	-200.44	61.142
β_9	-	-	131.21	18.679
R^2	0.851		0.954	

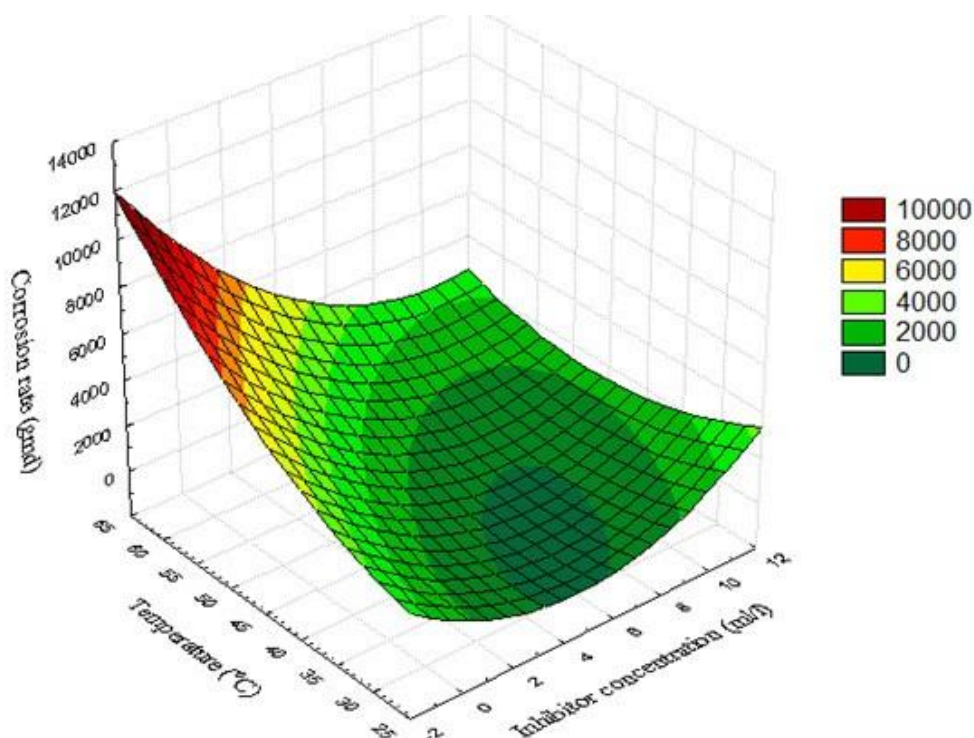


Fig.(3.41) 3D diagram of experimental corrosion rate against temperature and inhibitor concentration.

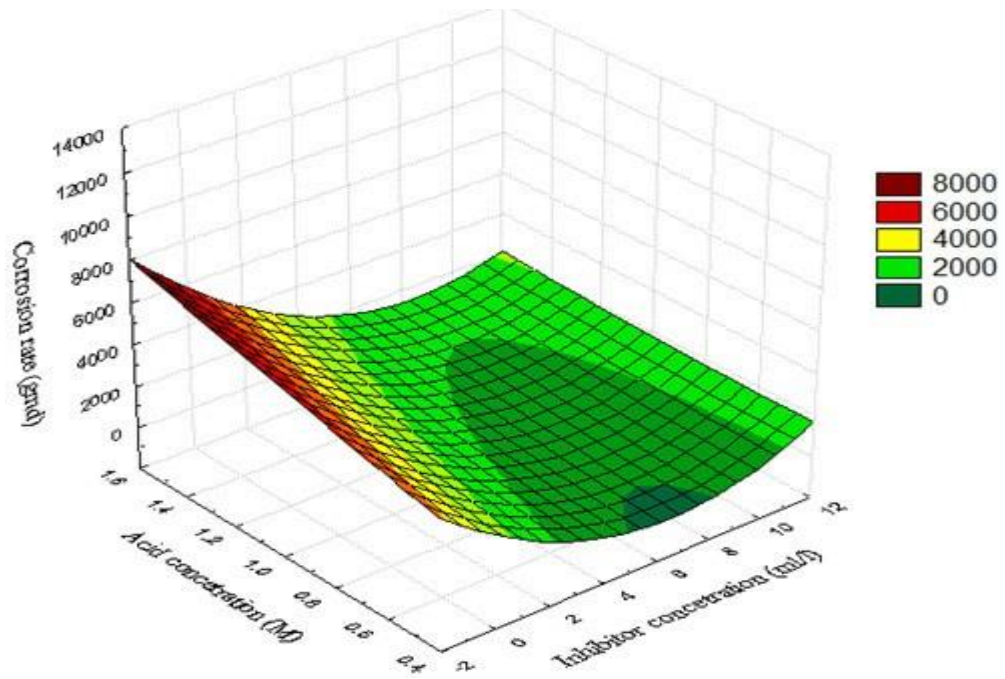


Fig.(3.42) 3D diagram of experimental corrosion rate against acid concentration and inhibitor concentration.

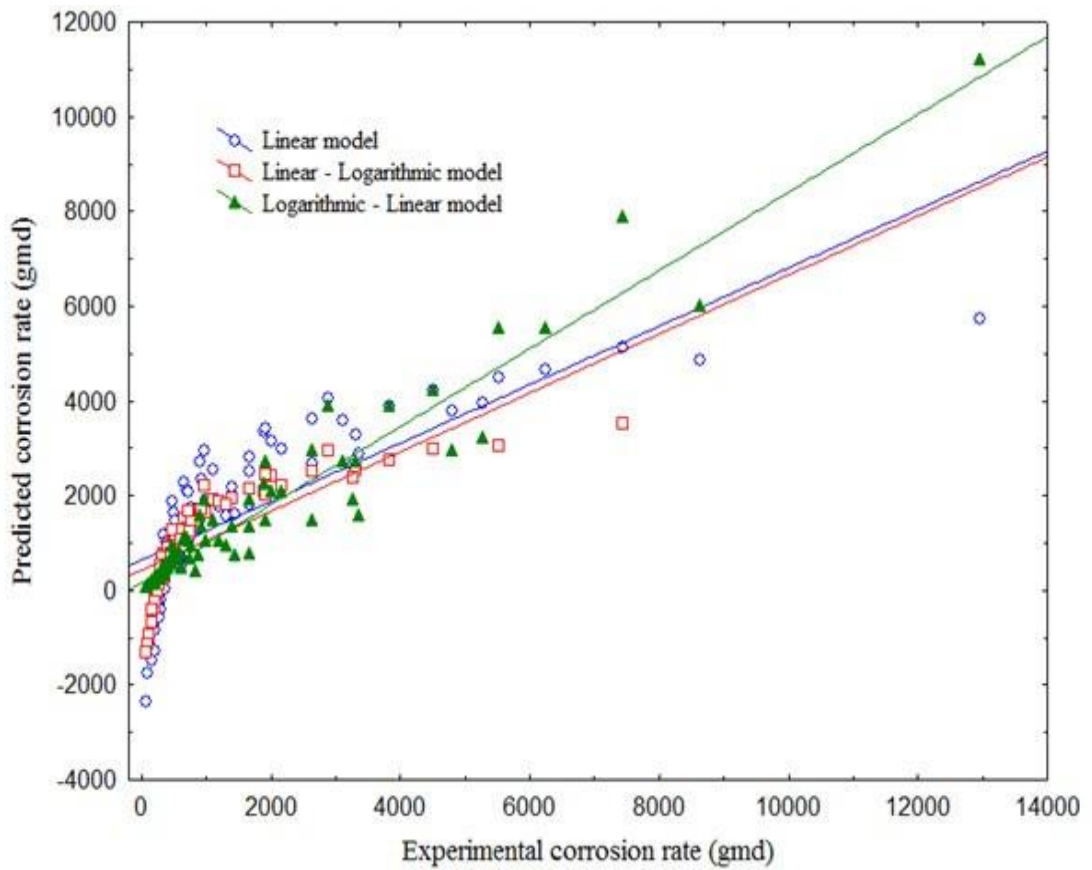


Fig.(3.43) Experimental corrosion rate against predicted corrosion rate for linear models.

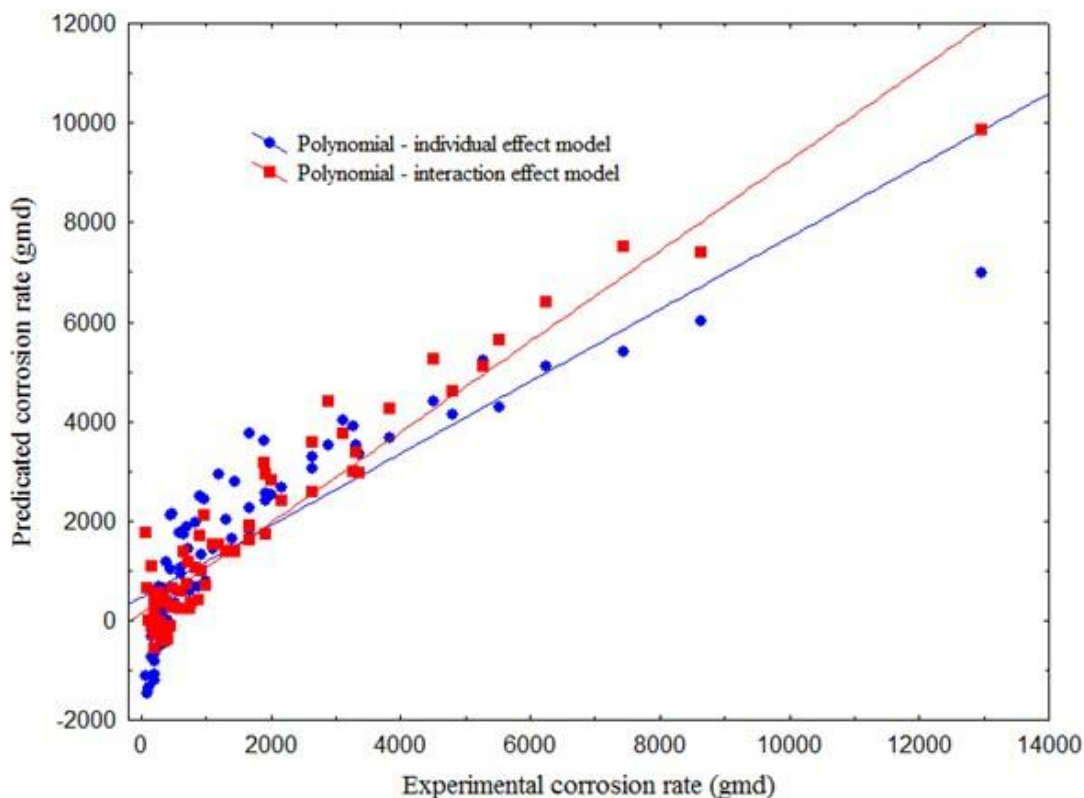


Fig.(3.44) Experimental corrosion rate against predicated corrosion rate for polynomials models.

3.10 Conclusions:

The following conclusions could be drawn from the present investigation:

1. The corrosion rate (CR) of carbon-steel in (0.5,1 and 1.5 M) H_2SO_4 solution is highly temperature dependent especially at higher temperatures.
2. Kinetic study shows that zero order is best fitting because the values of correlation coefficient is close to 1.0.
3. *Citrus aurantium leaves* extract proved to be an effective inhibitor of carbon-steel corrosion in 1 M sulfuric acid solution. Maximum inhibition efficiency obtained is 89 % at 40 °C and inhibitor concentration of 10 ml/L.
4. *Citrus aurantium leaves* extract is found to obey the Langmuir adsorption isotherm.

5. Activation energy is in general higher in the presence of the inhibitors than in absence and consequently the rate of corrosion decreases because the presence of inhibitor layer cause the reaction happening constrains.
6. The overall corrosion process is a function of the iron metal, corroding, inhibitor structure, temperature as well as concentration.
7. The negative sign of the free energy of adsorption ($\Delta G^{\circ}_{\text{ads}}$) indicates that the adsorption of the inhibitors on the carbon-steel surface was a spontaneous process and through to be physiosorption.
8. Quantum chemical calculations were also used as a theoretical tool to support the experimental results.
9. Several mathematical models were suggested and Logarithmic – Linear model was the best one with higher correlation coefficient and lowest standard error.
10. SEM confirm the corrosion of C-steel in 1 M H_2SO_4 and its inhibition by *Citrus aurantium leaves* extract.
11. The main constituent of *Citrus aurantium leaves* extract is alcohol groups such as (Linalool, $\text{C}_{10}\text{H}_{18}\text{O}$) It was analyzed by fourier transform infrared

3.11 Recommendation for Further Work:

1. Different types of plant extracts could be investigated and adopted as green inhibitors.
2. Plant extracts are found to be renewable, cheap inhibitors and non-toxic highly efficient, but less effort has been given towards the identification that which compound is active in the extract. This field needs more investigation.
3. Similar work can be repeated for other metals such as, copper, aluminum, etc.
4. Effect of velocity on corrosion rate can be recommended.
5. Electrochemical methods can be used to explain the effect of inhibitor on anodic and cathodic sites.
6. Similar work can be repeated in other acidic solutions, such as , H_3PO_4

References

- [1] Ahmed ,A.B. (2014). *Corrosion inhibition of low carbon steel in sulfuric acid by PVA and Piper Longum extracts*. University of Baghdad, Chemical Engineering Department (PhD).
- [2] Sathishkumar ,P., Kumaravelan, V. and Priya, D. D. (2015). **Comparative study of mild steel corrosion using hydrochloric acid and phosphoric acid medium with ocimum tenuiflorum (I) plant extract**. International Journal of Advanced Research, 3(4): 643-651.
- [3] Ajeel ,S.A., Waadulah, H.M. and Sultan, D.A. (2012). **Effects of H₂SO₄ and HCl concentration on the corrosion resistance of protected low carbon steel**. Al-Rafidain Engineering, 20(6): 70-76.
- [4] Uhlig, H.H., Revie, R.W. (2008). *Corrosion and corrosion control*.4th ed. John-Wiley & Sons, Inc.
- [5] Schweitzer, P.A. (2007). *Fundamentals of metallic corrosion*. 2nd ed. Taylor and Francis Group, LLC, United States of America.
- [6] Khadom ,A.A. (2000). *The influence of temperature on corrosion inhibition of carbon steel in phosphoric acid*. University of Baghdad, Chemical Engineering Department (M.Sc.).
- [7] Ismaeel ,H.K. (2014). *The effect of laser surface melting corrosion protection on alloys*. University of Technology, Chemical Engineering Department (M.Sc.).
- [8] Schweitzer, P.A. (2010). *Fundamentals of metallic corrosion*. 1ed. Taylor and Francis Group, LLC, United States of America..
- [9] Sheir, L.L., Jarman, R.A. and Burstein, G.T. (1994). *Corrosion Control*. 3rd ed. Jordan Hill.
- [10] Umoren ,S. A., Ogbobe, O., Igwe, I. O. and Ebenso, E. E. (2008). **Inhibition of mild steel corrosion in acidic medium using synthetic and naturally occurring polymers and synergistic halide additives**. Corrosion Science. 50(7): 1998-2006.
- [11] Karthikaiselvi ,R. and Subhashini, S. (2013). **Study of adsorption properties and inhibition of mild steel corrosion in hydrochloric acid media by water soluble**

References

composite (poly vinyl alcohol-o-methoxy aniline). Journal of the Association of Arab Universities for Basic and Applied Sciences, 16:74–82.

[12] Sharma ,A., Choudhary, G., Arpita, S. and Yadav, S. (2013). **Effect of temperature on inhibitory efficiency of azadirachta indica fruit on acid corrosion of aluminium.** International Journal of Innovative Research in Science, Engineering and Technology, 2(12): 2319-8753.

[13] Sarrou ,E., Chatzopoulou, P., Dimassi-Theriou, K. and Therios, I. (2013). **Volatile constituents and antioxidant activity of peel, flowers and leaf oils of Citrus aurantium leaves growing in greece.** Molecules, 18:1420-3049.

[14] Eddy ,N.O. and Odoemelam, S.A. (2009). **Inhibition of corrosion of mild steel in acidic medium using ethanol extract of Aloe vera.** Pigment and Resin Technology, 38(2): 111-115.

[15] Peme ,T., Olasunkanmi, L.O., Bahadur, I., Adekunle, A. S., Kabanda, M.M. and Ebenso, E.E. (2015). **Adsorption and corrosion inhibition studies of some selected dyes as corrosion inhibitors for mild steel in acidic medium: gravimetric, electrochemical, quantum chemical studies and synergistic effect with iodide ions.** Molecules, 20:16004-16029.

[16] Majnooni ,M-B., Mansouri, K., Gholivand, M-B., Mostafaie, A., Mohammadi-Motlagh, H-R., Afnanzade, N-S., Abolghasemi, M-M. and Piriyaiei, M. (2012). **Chemical composition, cytotoxicity and antioxidant activities of the essential oil from the leaves of Citrus aurantium leaves.** African Journal of Biotechnology, 11(2): 498-503.

[17] Abderrezak ,M. K., Abaza, I., Aburjai, T., Kabouche, A. and Kabouche, Z. (2014). **Comparative compositions of essential oils of Citrus aurantium growing in different soils.** Journal Mater Environ Sciences, 5(6): 1913-1918.

[18] Gece ,G. (2008). **The use of quantum chemical methods in corrosion inhibitor studies.** Corrosion Science, 50:2981-2992.

[19] Obot I.B. and Obi-Egbedi N.O., El-Khaiary, M.I., Umoren, S.A. and Ebenso, E.E. (2011). **Computational simulation and statistical analysis on the relationship between corrosion inhibition efficiency and molecular structure of some**

References

- phenanthroline derivatives on mild steel surface.** International Journal of Electrochemical Science, 6(11): 5649-5675.
- [20] Yaro ,A.S., Wael, R.K. and Khadom, A.A. (2010). **Reaction kinetics of corrosion of mild steel in phosphoric acid.** Journal of the University of Chemical Technology and Metallurgy, 45(4): 443-448.
- [21] Muthukrishnan, P., Prakash, P., Jeyaprabha, B. and Shankar, K. (2015). **Stigmasterol extracted from Ficus hispida leaves as a green inhibitor for the mild steel corrosion in 1 M HCl solution.** Arabian Journal of Chemistry, DOI.org/10.1016/j.arabjc.2015.09.005.
- [22] Musa ,A.Y., Khadom, A.A., Kadhum, A.H., Mohamad, A.B. and Takriff, M.S. (2010). **Kinetic behavior of mild steel corrosion inhibition by 4-amino-5-phenyl-4H-1,2,4-triazole-3-thiol.** Journal Taiwan Institute Chemical Engineering, 41:126-128.
- [23] Ozcan ,M., Dehri, I. and Erbil, M. (2004). **Organic sulphur containing compounds as corrosion inhibitors for mild steel in acidic media: Correlation between inhibition efficiency and chemical structure.** Applied Surface Science, 236:155-164.
- [24] Li ,W. H., He, Q., Pei, C. L. and Hou, B. R. (2008). **Some new triazole derivatives as inhibitors for mild steel corrosion in acidic medium.** Journal of Applied Electrochemistry, 38(3): 289-295.
- [25] Umoren, S.A., Eduok, U.M., Solomon, M.M. and Udoh A.P. (2011). **Corrosion inhibition by leaves and stem extracts of Sida acuta for mild steel in 1M H₂SO₄ solutions investigated by chemical and spectroscopic techniques** Arabian Journal of Chemistry, DOI:10.1016/j.arabjc.2011.03.00
- [26] Yaro ,A.S. and Khadom, A.A. (2008). **Evaluation of the performance of some chemical inhibitors on corrosion inhibition of copper in acid media.** Journal of Engineering, 14(2): 2350-2362.
- [27] Saratha ,R., Priya, S.V. and Thilagavathy, P. (2009). **Investigation of Citrus aurantiifolia leaves extract as corrosion inhibitor for mild steel in 1 M HCl.** E-Journal of Chemistry, 6(3): 785-795.

References

- [28] Adnan S.A-N. and Hanan M.A. (2009). **Corrosion inhibition of carbon steel on hydrochloric acid using Zizyphus Spina-Christisi extract.** Journal Basrah Researches Sciences, 35(1): 1817- 2695.
- [29] Dahmani ,M., Et-Touhami, A., Al-Deyab, S.S., Hammouti, B. and Bouyanzer, A. (2010). **Corrosion inhibition of C38 steel in 1 M HCl: A comparative study of Black Pepper extract and its isolated Piperine.** International Journal of Electrochemical Science, 5:1060 - 1069.
- [30] Yaro ,A.S., Khadom, A.A. and Ibraheem, H.F. (2011). **Peach juice as an anti-corrosion inhibitor of mild steel.** Anti-Corrosion Methods and Materials, 58(3): 116 - 124.
- [31] Iloamaeke ,I.M., Onuegbu, T.U., Ajiwe, V.I.E. and Umeobika, U.C. (2012).**Corrosion inhibition of mild steel by Pterocarpus Soyauxii leaves extract in HCl medium.** International Journal of plant, animal and environmental sciences, 2(3): 2231-4490.
- [32] Cang ,H., Fei, Z., Shao, J., Shi, W. and Xu, Q. (2013). **Corrosion inhibition of mild steel by Aloes extract in HCl solution medium.** International Journal Electrochemical Science, 8:720 - 734 .
- [33] Abdulkhaleq ,L.G. (2013). **The inhibitive effect of Eucalyptus Camaldulenis leaves extract on the corrosion of low carbon steel in hydrochloric acid.** Journal of Engineering and Development, 17(3): 1813- 7822.
- [34] Yaro ,A.S., Khadom, A.A. and Wael, R.K. (2013). **Apricot juice as green corrosion inhibitor of mild steel in phosphoric acid.** Alexandria Engineering Journal, 52:129-135.
- [35] Hamdy,A. and El-Gendy, N.S. (2013). **Thermodynamic, adsorption and electrochemical studies for corrosion inhibition of carbon steel by henna extract in acid medium.** Egyptian Journal of Petroleum, 22:17-25.
- [36] Aejitha ,S., Kasthuri, P.K. and Geethamani. (2014). **Inhibition effect of Antigonon Leptopus extract on mild steel in sulphuric acid medium.** Indian Journal of Applied Research, 4(12): 2249-5552.

References

- [37] Anbarasi ,K. and Vasudha, V.G. (2014). **Mild steel corrosion inhibition by Cucurbitamaxima plant extract in hydrochloric acid solution.** Journal Environ. Nanotechnol. 3(1): 16-22.
- [38] Fouda ,A.S., Elewady, G.Y., Shalabi, K. and Habouba, S. (2014). **Anise extract as green corrosion inhibitor for carbon steel in hydrochloric acid solutions.** International Journal of Innovative Research in Science, Engineering and Technology. 3(4): 2319-8753.
- [39] Thilagavathy ,P. and Saratha, R. (2015). **Mirabilis Jalapa flowers extract as corrosion inhibitor for the mild steel corrosion in 1M HCl.** IOSR Journal of Applied Chemistry, 8(1): 30-35.
- [40] Olasehinde ,E.F., Ogunjobi, J. K., Akinlosotu, O. M. and Omogbehin, S. A. (2015). **Investigation of the inhibitive properties of Alchornea laxiflora leaves on the corrosion of mild steel in HCl: Thermodynamics and kinetic study.** Journal of American Science, 11(1): 32-39.
- [41] Therese, K.S. and Vasudha, V. G. (2015). **Thermodynamic and adsorption studies for corrosion inhibition of mild steel using Millingtonia Hortensis.** International Journal of Information Research and Review, 2(1): 261-266.
- [42] Abdulrahman ,A. S., Kareem, A., Ganiyu, Kobe, H.I. and Caroline, A.I. (2015). **The corrosion inhibition of mild steel in sulphuric acid solution by adsorption of African Perquetina leaves extract.** International Journal of Innovative Research in Science, Engineering and Technology, 4(4): 2319 -8753.
- [43] Noor ,E.A., Aisha, Al-M., Aqlah, H. Al-Z. and Hubani, M.H. (2016). **Testing and the inhibitory action of red Onion seeds and peels extracts on the corrosion of steel in phosphoric acid.** International Journal of Electrochemical Science, 11:6523 - 6539.
- [44] Khadom ,A.A. (2014). **Dual function of benzotriazole as copper alloy corrosion inhibitor and hydrochloric acid flow improver.** Surface Engineering Applied Electrochem, 50(2): 57-70.
- [45] Begum ,A. (2011). **Evaluation of plants and weeds extract on the corrosion inhibition of mild steel in sulphuric acid.** E-Journal of Chemistry, 8(S1): S488-S494.

References

- [46] Quraishi ,M.A., Yadav, D.K. and Ahamad, I. (2009). **Green approach to corrosion inhibition by black pepper extract in hydrochloric acid solution.** The Open Corrosion Journal, 2: 56-60.
- [47] Wabanne ,J.T. and Okafor, V. (2001). **Inhibition of the corrosion of mild steel in acidic medium by Vernonia amygdalina: Adsorption and Thermodynamics Study.** Journal of Emerging Trends in Engineering and Applied Sciences, 2(4): 619-625.
- [48] Olasehinde ,E.F., Adesina, A.S., Fehintola, E.O., Badmus, B.M. and Aderibigbe, A.D. (2012). **Corrosion inhibition behaviour for mild steel by extracts of Musa sapientum peels in HCl solution: Kinetics and Thermodynamics Study.** IOSR Journal of Applied Chemistry, 2(6): 15-23.
- [49] Ismail ,M., Abdulrahman, A.S. and Hussain, M. S. (2011). **Solid waste as environmental benign corrosion inhibitors in acid medium.** International Journal of Engineering Science and Technology, 3(2): 1742-1748.
- [50] Vijayalakshmi ,P.R., Rajalakshmi, R. and Subhashini, S. (2011). **Corrosion inhibition of aqueous extract of Cocos nucifera-coconut palm - petiole extract from destructive distillation for the corrosion of mild steel in acidic medium.** Portugaliae Electrochimica Acta, 29(1): 9-21.
- [51] Zarrok ,H., Zarrouk, A., Salghi, R., Assouag, M., Hammouti, B., Oudda, H., Boukhris, S., Al Deyab, S. S. and Warad, I. (2013). **Inhibitive properties and thermodynamic characterization of quinoxaline derivative on carbon steel corrosion in acidic medium.** Der Pharmacia Lettre, 5 (2): 43-53.
- [52] Blaedel, W.J. and Meloche, V.W. (1963). *Elementary quantitative analysis.* 2nd ed. New York, 16: 684-698.
- [53] Ita ,B.I. (2004). **A study of corrosion inhibition of mild steel in 0.1 M hydrochloric acid by o-vanillin and o-vanillin hydrazine.** Bulletin of Electrochemistry, 20:(8) 363 – 370.
- [54] Kubba ,R.M., Ahlam, M.AL. and Hammud, K.K. (2016). **Theoretical study of new derivative of cefotaxime-amic acid as a corrosion inhibitor.** Iraqi Journal of Science, 57(2): 792-801.

References

- [55] Yadla ,S.V., Sridevi, V., Lakshmi, M.V.V.C. and Kumari, S.P.K. (2012). **A review on corrosion of metals and protection.** International Journal of Engineering Science and Advanced Technology, 2(3): 637 - 644.
- [56] Khadom ,A. A., Yaro, A.S., Kadum, A.A.H., Al Taie, A.S. and Musa, A.Y. (2009). **The effect of temperature and acid concentration on corrosion of low carbon steel in hydrochloric acid media.** American Journal of Applied Sciences, 6(7):1403-1409.
- [57] Obot, I.B. and Obi-Egbedi, N.O. (2010). **Adsorption properties and inhibition of mild steel corrosion in sulphuric acid solution by ketoconazole: Experimental and theoretical investigation.** Corrosion Science, 52:198-204.
- [58] Khadom, A. A., Ahmed, F. H. and Abod, B.M. (2015). **Evaluation of environmentally friendly inhibitor for galvanic corrosion of steel -copper couple in petroleum waste water.** Process Safety and Environmental Protection, 98:93-101.

الخلاصة

جرى في هذا العمل دراسة معدلات تآكل الفولاذ الكربوني الحاوي على نسبة قليلة من الكربون في حامض الكبريتيك (0.5-1.5 مولاري) عند درجات حرارة (30-60 م°) بوجود وعدم وجود المادة المانعة (مستخلص اوراق النارينج كمثبط عضوي) وبوجود المادة المانعة ضمن الحدود (2-10 مل/لتر) عند الزمن (3) ساعات. تم استخدام طريقة الفقدان بالوزن في هذا البحث. وان النتائج بينت ان معدل التآكل بوجود وعدم وجود المادة المانعة (مستخلص اوراق النارينج) تزداد مع زيادة درجة الحرارة عند اي تركيز لمانع التآكل. وان معدل التآكل يقل بزيادة تركيز المادة المانعة عند اي درجة حرارة. وقد تبين ان الحد الاعلى لكفاءة التثبيط في (0.5) مولاري هي (88,6%) عند درجة حرارة (50 م°) وتركيز المادة المانعة (10 مل/لتر) والزمن (3) ساعات ، اما في (1) مولاري فهي (89%) عند درجة حرارة (40 م°) وتركيز المادة المانعة (10 مل/لتر) والزمن (3) ساعات ، وفي (1.5) مولاري هي (83,3%) عند درجة حرارة (30 م°) وتركيز المادة المانعة (10 مل/لتر) والزمن (3) ساعات. اما عامل تغطية السطح فيمكن حسابه من معدلات التآكل والذي يتبع امتزاز ايزوثيرم لانكماير. ومن معادلة ارينيوس تم حساب طاقات التنشيط. وان قيمة الطاقة الحرة القياسية للامتزاز كانت حوالي -20 كيلو جول لكل مول مما يعني ان الامتزاز فيزيائي بين شحنة الجزيئات وشحنة المعدن. اما دراسة حركيات التفاعل بينت ان افضل مرتبة بالتفاعل هي المرتبة (صفر) وذلك من خلال قيم معامل الارتباط العالية الموجودة في المرتبة على خلاف المراتب الاخرى. وان دراسة طيف الاشعة تحت الحمراء لتحويلات فورير ومجهر المسح الالكتروني هي تقييم لفحص تركيب الجزيئة للمثبط وصورة السطح للمعدن على التوالي. وكذلك فان الدراسة النظرية تمت باستخدام كيمياء الكم والتي ايدت الدراسة العملية. وايضا تم دراسة الموديلات الرياضية التي من خلالها تم معرفة افضل موديل وهو (الموديل اللوغارتمي الخطي) وذلك من خلال معامل ارتباط عالي ونسبة خطأ قليلة.



وزارة التعليم العالي
والبحرث العلمي
جامعة ديالى
كلية العلوم

تثبيط تآكل الفولاذ الكربوني في وسط حامضي باستخدام مستخلص اوراق نبات النارج

رسالة مقدمة الى مجلس كلية العلوم / جامعة ديالى
وهي جزء من متطلبات نيل درجة الماجستير في علوم الكيمياء

من قبل

نور حاتم خورشيد

بكالوريوس. في الكيمياء 2014

جامعة ديالى- كلية العلوم

بأشراف

أ.د. كريم هنيكش حسن

أ.د. أنيس عبدالله كاظم

